Declassified in Part - Sanitized Copy Approved for Release 2011/12/13 : CIA-RDP80T00246A062100050001-6

50X1-HUM

Page Denied

Declassified in Part - Sanitized Copy Approved for Release 2011/12/13 : CIA-RDP80T00246A062100050001-6

Declassified in Part - Sanitized Copy Approved for Release 2011/12/13 : CIA-RDP80T00246A062100050001-6

50X1-HUM

AIRCRAFT, MODEL МиГ-19С

DESCRIPTION

Book I

AIRCRAFT FLIGHT PERFORMANCE

50X1-HUM

Declassified in Part - Sanitized Copy Approved for Release 2011/12/13 : CIA-RDP80T00246A062100050001-6

Declassified in Part - Sanitized Copy Approved for Release 2011/12/13 : CIA-RDP80T00246A062100050001-6

50X1-HUM

C O N T E N T S

Page

INTRODUCTION.....5
Chapter I. GENERAL.....7
Chapter II. BASIC DATA OF AIRCRAFT DESIGN.....11
Chapter III. AIRCRAFT GEOMETRICAL DATA.....17
Chapter IV. FLIGHT PERFORMANCES.....23
1. Level and Vertical Speeds. Climbing Time. Aircraft Ceiling.....23
2. Flight Range and Endurance.....30
3. Take-Off and Landing Characteristics.....32
4. Aircraft Control.....34
5. Aircraft Acceleration, Deceleration, Banked Turning and Diving Characteristics.....37
6. Possible Vertical Maximum Load Factors.....39
Chapter V. AERODYNAMIC CHARACTERISTICS.....41
1. Lift and Drag Coefficients.....41
2. Coefficients m_z, m_y, m_x and c_z of Moments and Lateral Forces.....43
3. Required and Available Thrusts.....45
Chapter VI. ENGINE CHARACTERISTICS AND FUEL CONSUMPTION.....47
Chapter VII. WEIGHT AND BALANCE DATA.....51
Appendix 1. Auxiliary Graphs and Formulas Used in Evaluation of MiG-15C Aircraft Flight Performance Characteristics.....75
Appendix 2. MiG-15C Levelling Diagram and Characteristics of Automatic Boost Units (Figs 154 and 155).....incort
Appendix 3. MiG-15C Aircraft Control Power Train Data.....89

50X1-HUM

Declassified in Part - Sanitized Copy Approved for Release 2011/12/13 : CIA-RDP80T00246A062100050001-6

Declassified in Part - Sanitized Copy Approved for Release 2011/12/13 : CIA-RDP80T00246A062100050001-6

50X1-HUM

INTRODUCTION

The present Description contains data on basic flight performances of the aircraft, type МиГ-19С.

The flight characteristics presented in the Book are based upon the results of State trials.

Aerodynamic data given in the Book are based on materials of wind tunnel trials. The Book also deals with geometry and weight of the aircraft as well as with the main characteristics of the РД-9Б engine taken into account in aerodynamic calculations.

The Book contains charts which can be used in estimation of aircraft flight performances.

50X1-HUM

Declassified in Part - Sanitized Copy Approved for Release 2011/12/13 : CIA-RDP80T00246A062100050001-6

Declassified in Part - Sanitized Copy Approved for Release 2011/12/13 : CIA-RDP80T00246A062100050001-6

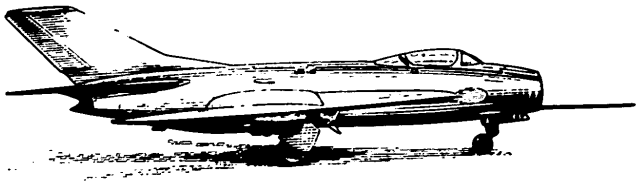

Fig. 1. Aircraft, Model МиГ-19С (side view)

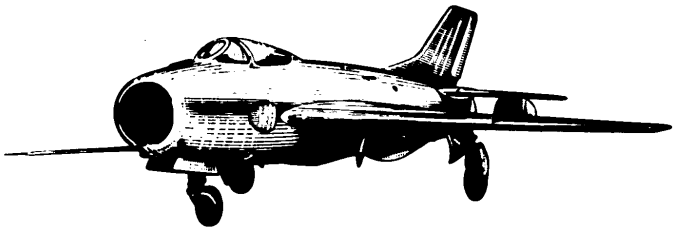

Fig. 2. Aircraft, Model Mul - 19C (3/4 front view)

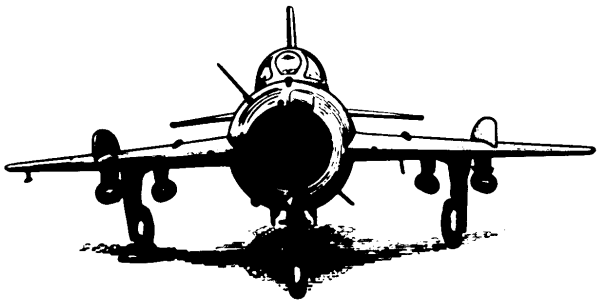

Fig. 3. Aircraft, Model "MiG"-19C (front view)

Declassified in Part - Sanitized Copy Approved for Release 2011/12/13 : CIA-RDP80T00246A062100050001-6

Declassified in Part - Sanitized Copy Approved for Release 2011/12/13 : CIA-RDP80T00246A062100050001-6

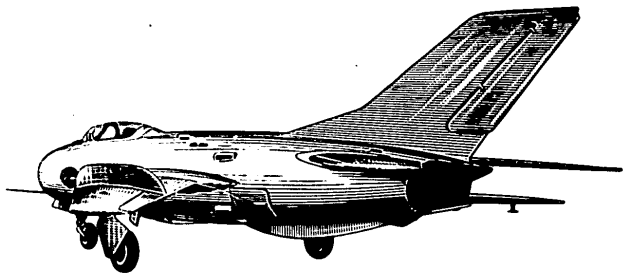

Fig. 4. Aircraft, Model MiG-19C (3/4 rear view)

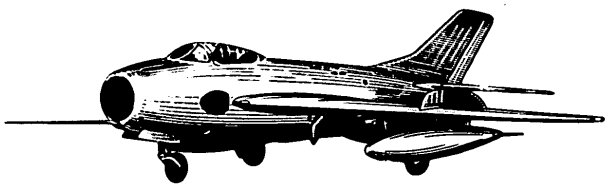

Fig. 5. Aircraft, Model MiG-19C with Drop Tanks 2x760 lit. (3/4 front view)

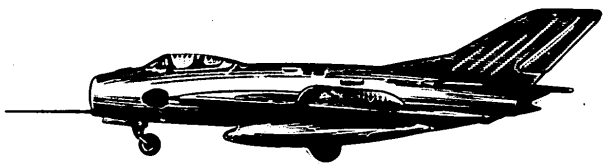

Fig. 6. Aircraft, Model MiG-19C with Drop Tanks 2x760 lit. (side view)

Chapter I

GENERAL

The jet aircraft, model МиГ-19С (Figs 1 and 6), is a multi-purpose supersonic fighter plane.

The МиГ-19С is a single-seat, twin-jet aircraft with a swept-back wing, controlled stabilizer, three cannon, pressurized cockpit and a landing gear with nose wheel (Figs 7 and 8).

The aircraft flight performances are presented in Table 1.

Table 1

Aircraft Flight Performances

Flight performances \ Flight conditions	Afterburner ON	Afterburner OFF
1	2	3
Maximum airspeed, km/hr	1452 (at 10,000-m. altitude)	1157 (at 1000-m. altitude)
Service ceiling, m.	17,500-17,900	15,600
Time of climb to 10,000-m. altitude, min.	1.1 2.2	2.1 3.4
Time of climb to 15,000-m. altitude, min.	2.6 3.7	7.1 8.2
Take-off run length, m.	-	690
Landing run length with use of automatic braking unit for three wheels, m.:		
- without drag parachute	-	690

Declassified in Part - Sanitized Copy Approved for Release 2011/12/13 : CIA-RDP80T00246A062100050001-6

Declassified in Part - Sanitized Copy Approved for Release 2011/12/13 : CIA-RDP80T00246A062100050001-6

- with drag parachute	-	610
Maximum flight range at H = 14,000 m., km.:		
- without drop tanks	-	1390
- with drop tanks, 2 x 760 lit.....	-	2200
Maximum flight endurance at H = 14,000 m., hr and minutes:		
- without drop tanks	-	1-43
- with drop tanks, 2 x 760 lit.	-	2-38

Notes: 1. The climbing time data put above the horizontal division line stand for time with no account for take-off run time and time of acceleration to V_{climb}, whereas the data below the line include the above time factors (take-off run and acceleration take 1.1 min.).
2. Climbing time with afterburner ON is given for conditions when the afterburner is started on the ground.
3. Flight range and endurance given above are for a single aircraft with 7 per cent fuel margin from the basic fuel reserve taking into account 7-minute engine ground operation before the take-off run and jettisoning of dry drop fuel tanks.
4. The drop tanks of 2 x 760 lit. capacity are filled with 600 lit. of fuel each at $\gamma = 0.83$ gr/cm^3.

For initial data for the MiG-19C aircraft strength calculations see Table 2.

Strength Characteristics of Aircraft without Drop Tanks (rated data)

Maximum operational load factor:	
- with air brakes closed	8
- with air brakes opened	8
Maximum IAS, km/hr	1200
Maximum Mach number	1.6
Maximum impact pressure, kg/m^2	7000

Important: When flying the aircraft, in all cases act as prescribed in the "MiG-19C Aircraft Operating and Piloting Instructions".

Strength of the drop tanks and their attachment units is characterized by the data given in Table 3.

Table 3

Strength Data of Drop Tanks and Their Attachment Units (tanks, 2 x 760 lit., on pylons or interchangeable tanks, 2 x 400 lit.)

1	Flight with fuelled or empty drop tanks:	
	(a) maximum permissible IAS, km/hr	1000
	(b) maximum permissible Mach number	1.3
	(c) maximum permissible impact pressure, kg/m^2	4830
2	Maximum operational load factor:	
	(a) with fuelled drop tanks	5
	(b) with empty tanks	6.5

For detailed presentation of specified limits of rated maximum airspeeds, Mach numbers and impact pressures for various flight altitudes see Table 7 and Figs 14 - 17.

Weight data of the aircraft, model MiG-19C, are given in Table 4.

Declassified in Part - Sanitized Copy Approved for Release 2011/12/13 : CIA-RDP80T00246A062100050001-6

Table 4

Declassified in Part - Sanitized Copy Approved for Release 2011/12/13 : CIA-RDP80T00246A062100050001-6

Weight data \ Version	Without drop tanks	With drop tanks, 2 x 760 lit.
All-up weight, kg	7560	8650
Landing weight (minimum, with 7 per cent fuel margin in main tanks and without ammunition), kg	5878	5984
Weight of fuel, kg	1800	2796
Capacity of tanks, lit.	2170	3370
Operational C.G. position range, per cent of MAC (without rockets)	38.5 - 44.0	39 - 44
Full C.G. position range, per cent of MAC:		
- without rockets	37.5 - 46.0	38.0 - 46.5
- with rockets	38.5 - 47.5	38.5 - 47.0

Notes: 1. Fuel specific weight equals 0.83 kg/lit.
2. Weight of aircraft with 2 x 760 lit. capacity tanks is given for conditions when the tanks are primed with 600 lit. of fuel each.

Complete list of weight and balancing data of the aircraft, model MiG-19C, is given in Chapter VII of the present Book.

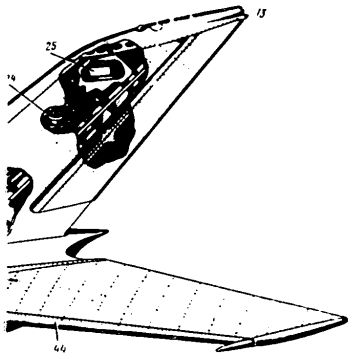

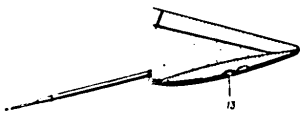

...mpass; 25 – receiver-amplifier ...taxiing lamp; 28 – L.G. nose ...ceiver of radio compass, type ... No. 9; 34 – air bottle; ... – cartridge belt; 39 – main ... – air brake; 42 – engine, type ...amic pressure emergency tube.

Declassified in Part - Sanitized Copy Approved for Release 2011/12/13 : CIA-RDP80T00246A062100050001-6

Declassified in Part - Sanitized Copy Approved for Release 2011/12/13 : CIA-RDP80T00246A062100050001-6

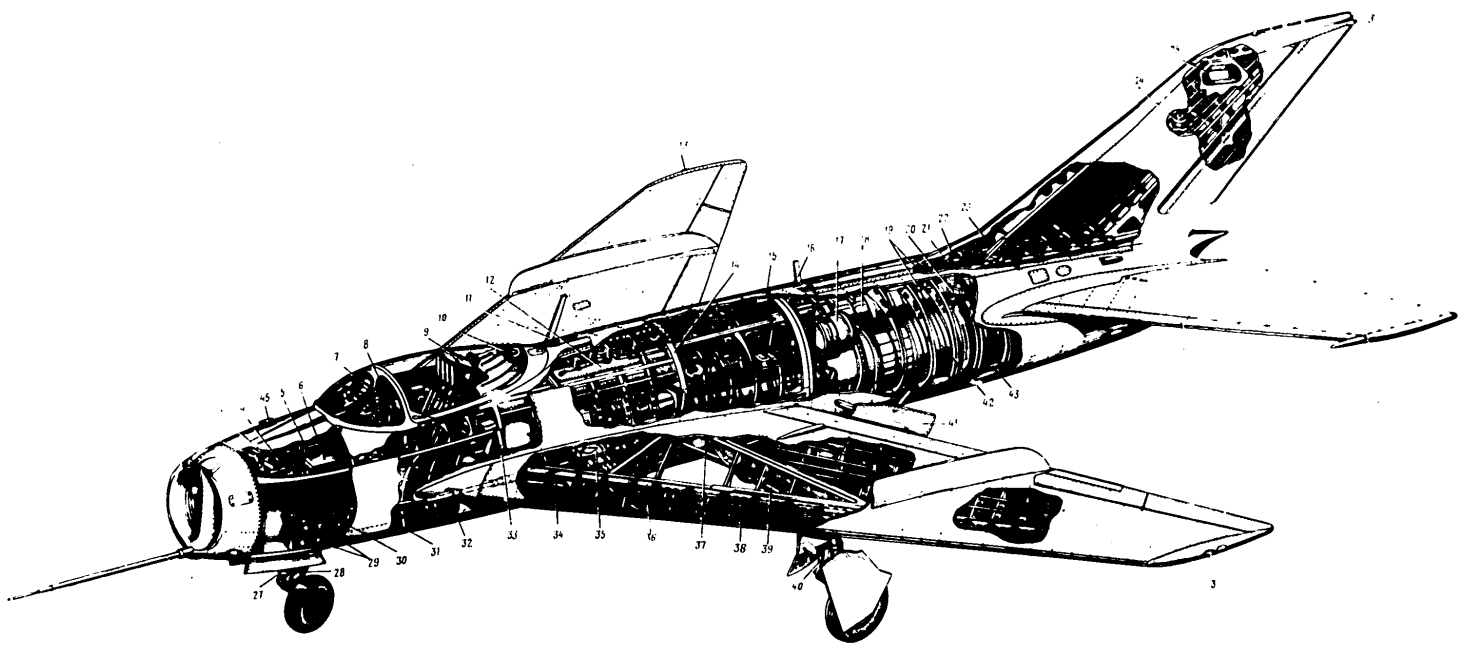

Fig. 7. Structure of Aircraft, Model МиГ-19С

1 – camera gun, type АКС-3М; 2 – РСИУ-4 command radio station transmitter; 3 – РСИУ-4 command radio station receiver; 4 – ФА-14А filter of СРО-1 IFF transponder station; 5 – 12-САМ-28 storage battery; 6 – receiver-transmitter of radio altimeter, type РВ-2; 7 – sighting head of АСП-5Н sight; 8 – АРК-5 radio compass control panel; 9 – ejection seat; 10 – canopy pressurization bottle; 11 – pin antenna of РСИУ-4 command radio station; 12 – fuel tank No. 1; 13 – navigating lights (АНО); 14 – frame No. 15; 15 – fuselage joint; 16 – antenna of СРО-1 IFF transponder station; 17 – oil tank (on engine); 18 – engine, type РД-9Б; 19 – automatic actuating mechanism (АРУ-2А); 20 – filler neck; 21 – mismatch transmitter, type ДР-5; 22 – spring-loaded artificial feel mechanism; 23 – electric actuator, type АИС-4; 24 – transmitter of ГИК-1 compass; 25 – receiver-amplifier unit of HOOTER-2 (СИРЕНА-2) station; 26 – airspeed tube; 27 – taxiing lamp; 28 – L.G. nose strut; 29 – oxygen bottles; 30 – converter, type РУ-11АМ; 31 – receiver of radio compass, type АРК-5; 32 – DME (distance measuring equipment) unit; 33 – frame No. 9; 34 – air bottle; 35 – НР-30 cannon; 36 – wing front spar; 37 – wing main beam; 38 – cartridge belt; 39 – main landing gear strut retraction jack; 40 – main landing gear strut; 41 – air brake; 42 – engine, type РД-9Б; 43 – fuel tank No. 4; 44 – controlled stabilizer; 45 – dynamic pressure emergency tube

Declassified in Part - Sanitized Copy Approved for Release 2011/12/13 : CIA-RDP80T00246A062100050001-6

Declassified in Part - Sanitized Copy Approved for Release 2011/12/13 : CIA-RDP80T00246A062100050001-6

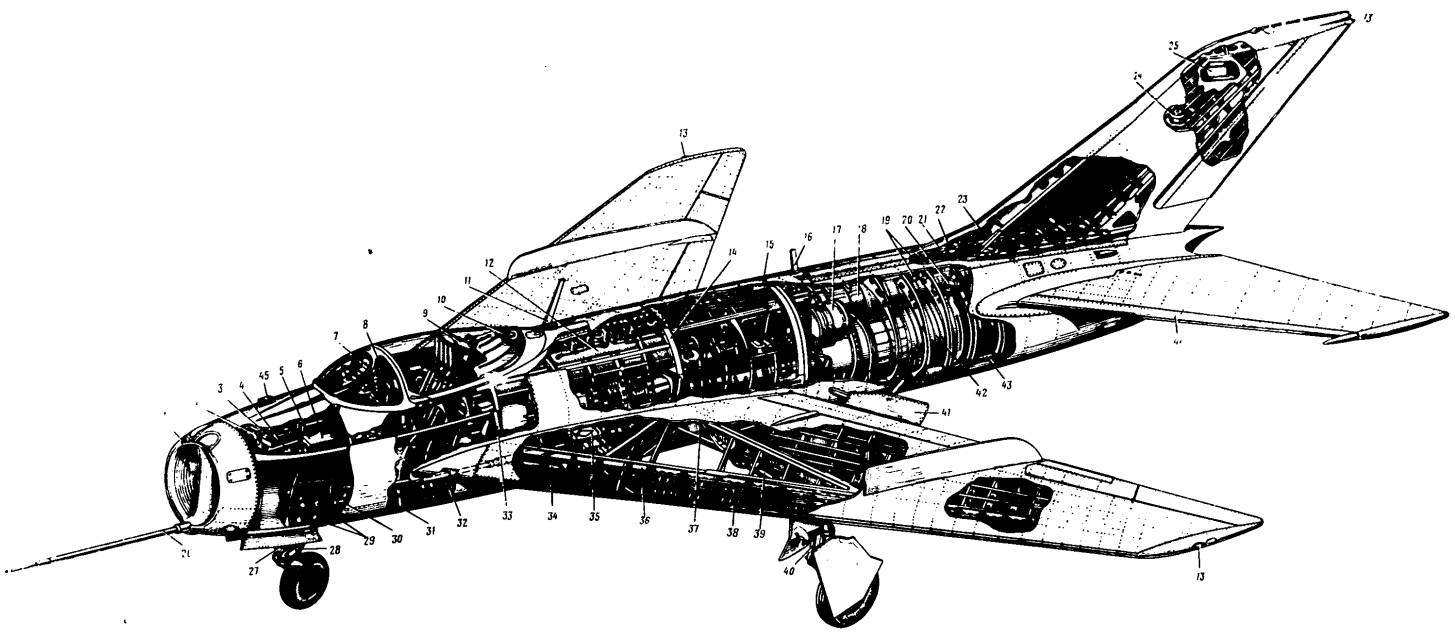

Fig. 7. Structure of Aircraft, Model МиГ-19С

1 – camera gun, type АКС-3М; 2 – РСИУ-4 command radio station transmitter; 3 – РСИУ-4 command radio station receiver; 4 – Ф-14А filter of СРО-1 IFF transponder station; 5 – 12-САМ-28 storage battery; 6 – receiver-transmitter of radio altimeter, type РВ-2; 7 – sighting head of АСП-5Н sight; 8 – АРК-5 radio compass control panel; 9 – ejection seat; 10 – canopy pressurization bottle; 11 – pin antenna of РСИУ-4 command radio station; 12 – fuel tank No. 1; 13 – navigating lights (АНО); 14 – frame No. 15; 15 – fuselage joint; 16 – antenna of СРО-1 IFF transponder station; 17 – oil tank (on engine); 18 – engine, type РД-9Б; 19 – automatic actuating mechanism (АРУ-2А); 20 – filler neck; 21 – mismatch transmitter, type ДР-5; 22 – spring-loaded artificial feel mechanism; 23 – electric actuator, type АПС-4; 24 – transmitter of ГИК-1 compass; 25 – receiver-amplifier unit of HOOTER-2 (СИРЕНА-2) station; 26 – airspeed tube; 27 – taxiing lamp; 28 – L.G. nose strut; 29 – oxygen bottles; 30 – converter, type РУ-11АМ; 31 – receiver of radio compass, type АРК-5; 32 – DME (distance measuring equipment) unit; 33 – frame No. 9; 34 – air bottle; 35 – НР-30 cannon; 36 – wing front spar; 37 – wing main beam; 38 – cartridge belt; 39 – main landing gear strut retraction jack; 40 – main landing gear strut; 41 – air brake; 42 – engine, type РД-9Б; 43 – fuel tank No. 4; 44 – controlled stabilizer; 45 – dynamic pressure emergency tube.

Declassified in Part - Sanitized Copy Approved for Release 2011/12/13 : CIA-RDP80T00246A062100050001-6

Declassified in Part - Sanitized Copy Approved for Release 2011/12/13 : CIA-RDP80T00246A062100050001-6

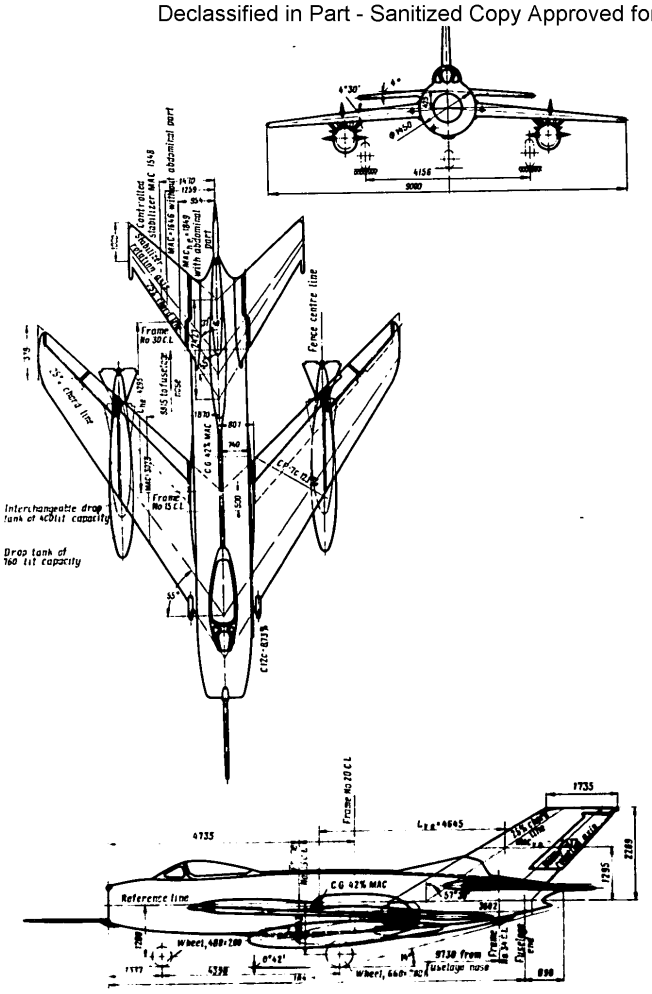

Fig. 8. Balance Diagram of Aircraft, Model МиГ-19С

Declassified in Part - Sanitized Copy Approved for Release 2011/12/13 : CIA-RDP80T00246A062100050001-6

Declassified in Part - Sanitized Copy Approved for Release 2011/12/13 : CIA-RDP80T00246A062100050001-6

Chapter II

BASIC DATA OF AIRCRAFT DESIGN

The МиГ-19С aircraft is a multi-purpose single-seat supersonic jet fighter plane.

The aircraft power plant consists of two engines, type РД-9Б (with afterburners), installed side by side in the fuselage.

As seen from the aircraft structural diagram (Fig.8), the aircraft is a midwing cantilever monoplane with swept-back wing and tail unit. The a/c is fitted out with a controlled stabilizer.

The aircraft is provided with a tricycle landing gear, the main wheels being retracted into the wing, and the nose wheel into the fuselage.

The aircraft L.G. wheels are braked automatically. The semi-monocoque fuselage has a production break line and maintenance split joint which divides the fuselage into two parts: nose and tail sections.

The quick-release joint of the fuselage provides good accessibility during mounting and dismounting of the engines.

The air for the engines is taken from the atmosphere and supplied through the intake ducts running from the aircraft nose to the engines. The bifurcated intake ducts pass at the sides of the pilot's cockpit located in the fuselage nose section. The pilot's cockpit is pressurized and is provided with air conditioning facilities. Air supply is provided to maintain normal working condition for the pilot. The cockpit may be supplied with hot or cooled air.

The cockpit air temperature is automatically maintained within the preset limits ($16\pm4^{\circ}C$) with the aid of the thermo-regulator and distribution valve. The cockpit is equipped

Declassified in Part - Sanitized Copy Approved for Release 2011/12/13 : CIA-RDP80T00246A062100050001-6

Declassified in Part - Sanitized Copy Approved for Release 2011/12/13 : CIA-RDP80T00246A062100050001-6

with a face-curtain-type ejection seat, an oxygen set, type KKO-1 , and with an anti-G suit, model BKK-2.

The cockpit canopy is glazed with a single glass panel and consists of a windshield and sliding section which can be jettisoned from any position in case of emergency.

For reliable removal of the canopy sliding section during emergency jettison procedure, the canopy is forced up by remover pneumatic guns.

Mounted on the canopy windshield is an armoured glass panel and sprayer tube of the fluid-type de-icer system.

The wing sweepback is 55° at the 25 per cent chord line; the wing is assembled of high speed superload airfoils with the mean thickness ratio of 8.2 per cent.

Installed on the wing are flaps with sliding hinge and pressure balanced ailerons; the left aileron carries a trim tab. To improve lateral stability control of the aircraft at high Mach numbers of flight the wings are provided, at their bottom surface in front of the flaps, with interceptors which are kinematically connected to the ailerons.

Mounted on the wing top surface are aerodynamic fences with h = 12 per cent b. The wing stresses skin is made of duralumin. The ailerons are provided with rod-type control.

Cut into the ailerons control system (non-reversible circuit) is booster, type BY-13M , supplied from the boost hydraulic system (with duplicating supply from the main hydraulic system).

The main hydraulic system supply is cut in automatically when the pressure in the boost hydraulic system drops below 65_{-5} kg/cm^2.

The control stick is loaded laterally with the aid of a spring-loaded artificial feel mechanism permanently cut into the system.

The horizontal empennage is swept back at 55° and has a controlled stabilizer without elevators.

The aircraft longitudinal control (stabilizer control) is effected through rigid control rods. It employs as the main driving unit a booster, type BY-14MC , cut into non-reversible circuit with supply from the boost hydraulic system (duplicating supply effected from the main hydraulic system); the supply from the main hydraulic system is cut in automatically

when the pressure before the booster drops below 65_{-5} kg/cm^2.

Besides the duplicating control from the main hydraulic system, the aircraft is additionally provided with stabilizer emergency control from the electric actuator, type AMC-4 , operated by the pilot through the electric follow-up system, by means of the stabilizer control handle. The electric system is selected for the longitudinal control automatically when the pressure before the booster drops below 50^{+5} kg/cm^2.

The control stick-to-stabilizer transmission ratio is the function of the impact pressure and flying altitude (i.e. Mach number included). The transmission ratio is changed with the aid of the variable ratio automatic boost unit, type APY-2A.

The stabilizer control handle is loaded longitudinally by the spring-loaded artificial feel mechanism through the actuating mechanism of the APY-2A boost unit (the stabilizer aerodynamic hinge moment is not imparted to the control handle).

Adjustment of pressures for different positions of the control handle is effected by changing the position of the feel mechanism with the aid of the trimming effect mechanism, type MI-100M, which is controlled by the pilot through shifting of the button on the control handle.

The APY-2A automatic boost unit practically ensures conventional piloting technique for the pilot independent of the value of the impact pressure and Mach number and allows to make best use of the aircraft maneuverability.

With the emergency control from the AMC-4 stabilizer automatic control unit (actuator) the pilot feels the same pressure on the control handle as when the control is effected from the booster; at this, the rate of the control handle movement, when actuated from the AMC-4 unit, will be slower.

The emergency control system is required due to the fact that more manual effort of the pilot is not sufficient to control the stabilizer (due to great change in the stabilizer hinge moment in flight).

The vertical empennage of the aircraft is swept back at the angle of $57^{\circ}30'$.

Serving as an additional vertical surface is the belly fin with a 0.54 m^2 area. The rudder control is of rod-type.

The aircraft is provided with three air brakes.

Two air brakes with a total area of 1.04 m^2 are installed

Declassified in Part - Sanitized Copy Approved for Release 2011/12/13 : CIA-RDP80T00246A062100050001-6

Declassified in Part - Sanitized Copy Approved for Release 2011/12/13 : CIA-RDP80T00246A062100050001-6

in the fuselage tail section (at the fuselage sides) and are deflected through 25° and the third air brake of 0.45 m^2 area is located on the fuselage centre section bottom and can be deflected through 45°.

Located at the bottom of the fuselage tail section is a compartment housing the container with the landing drag parachute, type ПТ-19.

The aircraft hydraulic system is divided into two systems: main hydraulic system and boost hydraulic system.

Each system is provided with a tank and pump group; pressures in both systems are equal. The main hydraulic system is operated by the pump from the right engine, whereas the boost system - by the pump from the left engine.

The main hydraulic system retracts and extends the landing gear, flaps and air brakes, controls the jet engine nozzle shutters and provides duplicating supply for the boosters in case of failure of the boost hydraulic system.

The aircraft pneumatic system actuates normal and emergency braking of the landing gear wheels, emergency release of the landing gear and flaps, release and firing and reloading of the a/c armament, separation (dropping) of the landing drag parachute, forcing up of the canopy sliding section during emergency jettison, canopy pressurization, closing of the shut-off fuel valves and the functioning of the de-icer system.

The aircraft fuel system incorporates four fuselage tanks of 2170-lit. total capacity and two drop tanks.

Instead of the drop tanks the aircraft can carry two bombs from 50 to 250 kg each.

The aircraft armament consists of three НР-30 cannon, two of which are mounted in the wings at the root ribs, the third being installed in the right bottom part of the fuselage nose section.

Used ammunition links of each cannon are accumulated, whereas the fired cartridge cases are ejected.

The aircraft is equipped with a rocket launching mount.

The aircraft armour consists of a bullet-proof glass panel (on canopy windshield), armour plate installed in front of the cockpit, armour head rest and armour back plate of the pilot's seat.

The aircraft radio equipment consists of U.S.U. receiving-transmitting command radio stations, type РСИУ-4, IFF transponder СРО-1, tail attack warning radar station СИРЕНА-2 (SIRENA-2), range-finding equipment, type СРД-1М, interconnected with АСП-5Н sight and equipment and instruments of the ОСП-48 Instrument Landing System which includes: automatic radio compass, type АРК-5, low range radio altimeter, type РВ-2, and marker receiver station, type МРП-48П.

Declassified in Part - Sanitized Copy Approved for Release 2011/12/13 : CIA-RDP80T00246A062100050001-6

Declassified in Part - Sanitized Copy Approved for Release 2011/12/13 : CIA-RDP80T00246A062100050001-6

Chapter III

AIRCRAFT GEOMETRICAL DATA

1. Wing (Fig.2)

Area (overall)	25 m^2
Span	9.0 m.
Mean aerodynamic chord (MAC)	3.023 m.
Sweepback angle	35°
Dihedral	-4°30'
Setting angle	0°
Aspect ratio	3.24
Taper ratio	3.04
Mean thickness ratio (relative to general direction of air stream - flight line)..	0.0824
Airfoil section at wing root (initial) ...	C-12C
Airfoil section at wing tip (initial) ...	CP-7C
Ground angle (with no L.G. strut compression)	-42'

2. Ailerons

Type	with balanced pressure
Area (of two ailerons) to hinge line	1.56 m^2
Span (of one aileron)	1.72 m.
Mean aerodynamic chord (to hinge line and perpendicular to it)	0.311 m.
Relative chord (relative to flight line, at aileron midspan, no balancing)	0.228
Balance area of two ailerons	0.6 m^2
Aileron trim tab area (left aileron, with plate)	0.053 m^2
Aileron maximum angular movement (normal to hinge line):	

Declassified in Part - Sanitized Copy Approved for Release 2011/12/13 : CIA-RDP80T00246A062100050001-6

Declassified in Part - Sanitized Copy Approved for Release 2011/12/13 : CIA-RDP80T00246A062100050001-6

down	+20°
up	-20°
Aileron trim tab maximum angular movement (normal to hinge line):	
down	+15°
up	-15°
Aileron control system booster	БУ-13М
Aileron-to-control stick transmission ratio $\left(\frac{P_{\text{handle booster off}}}{2\,M_{\text{hinge of one aileron}}}\right)$	$K_{\text{hinge}} = 2.53\ \frac{1}{m.}$

3. Flaps

Type	with sliding hinge
Area (of two flaps)	3.43 m^2
Span (of one flap)	1.781 m.
Flap relative chord (normal to aerodynamic centre line)	0.383
Take-off deflection angle (relative to flight line)	15°
Landing deflection angle (relative to flight line)	25°

4. Fuselage

Maximum diameter	1.45 m.
Engine air duct intake scoop diameter (by scoop leading edge)	0.8 m.
Overall length	10.428 m.
Fineness ratio $\lambda_f = \frac{l_f}{D_f}$	7.19
Nose section fineness ratio $\lambda_{n.s.} = \frac{l_{n.s.}}{D_f}$	3.27
Centre cylindrical section fineness ratio $\lambda_{c.s.} = \frac{l_{c.s.}}{D_f}$	0.95
Tail section fineness ratio $\lambda_{n.s.} = \frac{l_{t.s.}}{D_f}$	2.97
Middle section (without canopy)	1.65 m^2

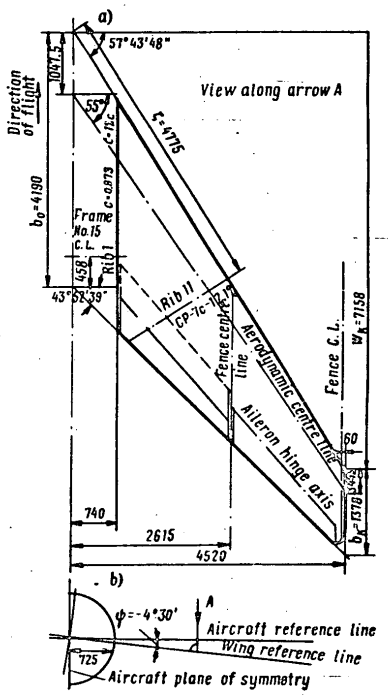

Fig. 9. Wing Theoretical Diagram
(a) separate wing; (b) wing with fuselage.

Declassified in Part - Sanitized Copy Approved for Release 2011/12/13 : CIA-RDP80T00246A062100050001-6

Declassified in Part - Sanitized Copy Approved for Release 2011/12/13 : CIA-RDP80T00246A062100050001-6

Middle section of canopy	0.2 m^2
Engine air duct intake scoop area (minimum)	0.411 m^2

5. Horizontal Empennage

Area of horizontal empennage with belly part	7.78 m^2
Area of horizontal empennage without belly part	5.0 m^2
Area of horizontal empennage adjustable control surfaces	4.4 m^2
Sweepback angle	55°
Aspect ratio	2.56
Taper ratio	2.49
Mean thickness ratio (relative to general direction of air stream-flight line)	7 per cent
Mean aerodynamic chord of horizontal empennage adjustable control surfaces	1.548 m.
Horizontal empennage arm (distance between 0.42 MAC of wing and 0.25 MAC of horizontal empennage adjustable control surfaces)	4.947 m.
Elevation of horizontal empennage MAC over wing root chord	0.415 m.
Horizontal empennage airfoil section (with respect to flight line)	NACA-M
Stabilizer angular movement (normal to rotation axis):	
down	11°30'
up	26°30'
Sweepback of rotation axis	52°20'
Booster in horizontal empennage control system	BU-14KC

Note: For additional data of MAC and horizontal empennage arms see Fig.8.

Declassified in Part - Sanitized Copy Approved for Release 2011/12/13 : CIA-RDP80T00246A062100050001-6

Declassified in Part - Sanitized Copy Approved for Release 2011/12/13 : CIA-RDP80T00246A062100050001-6

6. Vertical Empennage

Area	4.17 m^2
Sweepback angle	57°30'
Taper ratio	1.78
Constant thickness chord ratio of vertical empennage (relative to main direction of air stream - flight line)	8%
Vertical empennage arm (distance between 0.42 b_A wing to 0.25 b_A v.e.)	4.645 m.
Vertical empennage airfoil section	C-11C
Rudder area	0.93 m^2
Mean aerodynamic chord of vertical empennage	2.537
Mean aerodynamic chord of rudder (normal to hinge line)	0.454
Relative chord of rudder without balance (normal to hinge line)	0.274
Hinge balance area of rudder	0.24 m^2
Maximum angular movement of rudder (normal to hinge line)	±25°
Rudder-to-pedals transmission ratio $\left(\frac{P_{pedal}}{M_{hinge,rudder}}\right)$	$K_{hinge} = 6.59\ \frac{1}{m}$.
Area of belly fin	S = 0.54 m^2

7. Air Brakes

Total area of three air brakes	1.49 m^2
Maximum deflection of tail air brakes	25°
Maximum deflection of forward air brake	45°

8. General

Overall length of aircraft in flight position:	
without air-speed tube	12.54 m.
with air-speed tube	14.64 m.
Maximum height of aircraft on ground (shock absorbers are not compressed)	3.885 m.
Landing gear tread	4.156 m.
Wheel base-line	4.398 m.

Main landing gear wheels	660x200 mm
Nose landing gear wheel	480x200 mm

9. Drop Tanks

Type	underwing, on pylons	
Capacity lit.	2x760	2x400
Diameter, m.	0.58	0.526
Length (without stabilizer), m.	4.8	3.01
Length (diameter ratio - $\frac{l}{d}$)	8.27	5.7
Middle section, m^2	0.264	0.215

Declassified in Part - Sanitized Copy Approved for Release 2011/12/13 : CIA-RDP80T00246A062100050001-6

Declassified in Part - Sanitized Copy Approved for Release 2011/12/13 : CIA-RDP80T00246A062100050001-6

Chapter IV

FLIGHT PERFORMANCES[1]

For the sake of convenience, the aircraft flight performance data are given mainly in the form of tables and charts.

The most essential aircraft performance data reduced to the standard atmosphere conditions are presented in Figs 10 - 01 and Tables 5 - 14.

The characteristics are given for the aircraft without drop tanks.

If the aircraft is equipped with drop tanks the condition is stipulated in the text and diagrams by special notes.

1. Level and Vertical Speeds, Climbing Time, Aircraft Ceiling

Maximum level flight airspeeds of the aircraft and the corresponding Mach numbers, vertical speeds and climbing time data are given in Figs 10 - 19 and Tables 5 and 6.

Absolute maximum level airspeed of 1452 km/hr is attained by the aircraft at the 10,000-m. altitude with the afterburner ON.

Absolute maximum level airspeed of 1150 km/hr is attained by the aircraft with drop tanks at an altitude of 10,000 m. with the afterburner ON.

The aircraft maximum low altitude flight airspeed with the afterburner ON will be determined by the pilot in accordance with the Pilot's Instructions.

1/ Detailed information on the a/c flight performance data, essential for piloting the plane, will be found in the "MiG-19S Aircraft Operating and Piloting Instructions".

Declassified in Part - Sanitized Copy Approved for Release 2011/12/13 : CIA-RDP80T00246A062100050001-6

Declassified in Part - Sanitized Copy Approved for Release 2011/12/13 : CIA-RDP80T00246A062100050001-6

Maximum Mach number (Fig.12) of level flight with the afterburner ON is reached at an altitude of H = 11,000 m. and is equal to M = 1.355.

Maximum Mach number of level flight with the afterburner ON and with drop tanks, 2 x 760 lit., is reached at an altitude of 11,000 m. and is equal to 1.07.

Allowable rated maximum airspeeds of aircraft based on strength calculations (for aircraft with and without drop tanks), Mach numbers and impact pressures at different altitudes are given in Table 7 and in Figs 14 - 17; these also contain, for comparison, values of V and M corresponding to the level-flight at V_{max} with the use of afterburning.

The average best climb path airspeed of the aircraft without drop tanks at normal and maximum engine power settings practically does not depend on the flight altitude and is equal to 930 - 950 km/hr (by the airspeed indicator narrow pointer) up to the service ceiling at n = 11,150 r.p.m. (See Table 6), whereas with afterburning it corresponds to Mach 0.88 at altitudes above 5000 m.

The maximum rate of climb (See Fig.18 and Tables 5 and 6) decreases with the altitude increase; its peak value is obtained at ground level with the engines set at maximum power (n = 11,150 r.p.m.) and is equal to 115 m.p.s.; with afterburning, the rate of climb at the altitude of 5000 m. equals 180 m.p.s.

The unstick speed of the aircraft without drop tanks, with flaps 15° DOWN, equals 280 - 300 km/hr.

Climbing time data are presented in Tables 5 and 6 and in Fig.19.

Service ceiling with afterburning - 17,500 - 17,900 m.

Climb path airspeed from 5000-m. altitude and up corresponds to M = 0.90, indicated.

Notes: 1. Vertical speeds are given for conditions when afterburning is used on the ground level and off.

2. The climbing time data put above the horizontal division line stand for time with no account for take-off run time and time of acceleration to V_{climb}, whereas the data below the line include the above time factors (take-off run and acceleration take 1.1 min.).

3. When flying the ceiling the aircraft can attain greater-than-specified altitude by use of kinematic energy in a special climbing technique (zoom with deceleration from V_{max} condition).

Declassified in Part - Sanitized Copy Approved for Release 2011/12/13 : CIA-RDP80T00246A062100050001-6

Declassified in Part - Sanitized Copy Approved for Release 2011/12/13 : CIA-RDP80T00246A062100050001-6

Table 2

Level and Vertical Speeds and Climbing Time with Afterburning and Engines Speed of 11,150 r.p.m.

H, m.	0	1000	2000	3000	4000	5000	6000	7000	8000	9000	10,000	11,000	12,000	13,000	14,000	15,000	16,000	17,000
V_{max}, km/hr	-	-	-	-	-	-	1366	1405	1436	1454	1452	1440	1426	1402	1370	1322	-	-
$M_{V_{max}}$	-	-	-	-	-	-	1200	1251	1259	1330	1348	1355	1342	1321	1290	1245	-	-
V_y, m.p.s.	-	-	-	-	-	180	162	144	127	109	92	74	63	52	40	29	18	-
t, min.	0 / -	- / 1.0	0.1 / 1.2	0.2 / 1.3	0.3 / 1.4	0.4 / 1.5	0.6 / 1.7	0.7 / 1.8	0.8 / 1.9	0.9 / 2.0	1.1 / 2.2	1.3 / 2.4	1.5 / 2.6	1.8 / 2.9	2.2 / 3.3	2.6 / 3.7	3.4 / 4.5	4.9 / 6.0

Table 6

Level and Vertical Speeds and Climbing Time at Engines Maximum Power Setting, n = 11,150 r.p.m.

H, m.	0	1000	2000	3000	4000	5000	6000	7000	8000	9000	10,000	11,000	12,000	13,000	14,000	15,000
V_{max}, km/hr	1160	1157	1148	1140	1132	1124	1116	1108	1098	1087	1075	1058	1054	1047	1030	-
$M_{V_{max}}$	0.95	0.954	0.959	0.964	0.970	0.975	0.980	0.986	0.990	0.994	0.996	0.996	0.993	0.986	0.971	-
V_y, m.p.s.	115	107	100	93	86	78	71	64	56	49	42	34	27	19	12	4
t, min.	0 / -	0.1 / 1.2	0.3 / 1.4	0.5 / 1.6	0.7 / 1.8	0.9 / 2.0	1.1 / 2.2	1.3 / 2.4	1.6 / 2.7	1.9 / 3.0	2.3 / 3.4	2.7 / 3.8	3.3 / 4.4	4.0 / 5.1	5.0 / 6.1	7.1 / 8.2

Declassified in Part - Sanitized Copy Approved for Release 2011/12/13 : CIA-RDP80T00246A062100050001-6

Declassified in Part - Sanitized Copy Approved for Release 2011/12/13 : CIA-RDP80T00246A062100050001-6

Service ceiling at engines maximum power setting - 15,600 m.

Climb path airspeed for all altitudes V_{climb} = 930 km/hr by the airspeed indicator narrow pointer.

Notes: 1. Maximum level flight airspeeds at normal and maximum power settings of the engines are in practice equal up to the altitude of H = 13,000 m. From altitude H = 13,000 m. and up the airspeed values are given for engines maximum power setting.

2. The climbing time data put above the horizontal division line stand for time with no account for take-off run time and time of acceleration to V_{climb}, whereas the data below the line include the above time factors (take-off run and acceleration take 1.1 min.).

Table 7

Maximum Allowable Airspeeds, Mach Numbers and Impact Pressures (assumed for strength calculations)

(a) Without drop tanks

H, m.	0	2000	4000	6000	7500	8000	10,000	12,000	14,000	16,000
V, km/hr	1200	1330	1470	1640	1790	1770	1720	1700	1700	1700
$V_{i.}$ (w.p.), km/hr	1180	1230	1260	1290	1310	1275	1130	990	860	745
$V_{i.}$, km/hr	1200	1200	1200	1200	1200	1160	1000	855	732	625
Mach number	0.98	1.11	1.26	1.44	1.6	1.6	1.6	1.6	1.6	1.6
q, kg/m^2	7000	7000	7000	7000	7000	6500	4840	3530	2570	1830

(b) With drop tanks

H, m.	0	2000	4000	6000	7200	8000	10,000	12,000	14,000	16,000
V, km/hr	1000	1100	1225	1366	1450	1440	1400	1380	1380	1380
$V_{i.}$ (w.p.), km/hr	970	990	1050	1080	1090	1040	910	795	690	590
$V_{i.}$, km/hr	1000	1000	1000	1000	1000	914	813	695	594	507
Mach number	0.816	0.922	1.05	1.2	1.3	1.3	1.3	1.3	1.3	1.3
q, kg/m^2	4830	4830	4830	4830	4830	4290	3190	2330	1700	1240

Declassified in Part - Sanitized Copy Approved for Release 2011/12/13 : CIA-RDP80T00246A062100050001-6

Declassified in Part - Sanitized Copy Approved for Release 2011/12/13 : CIA-RDP80T00246A062100050001-6

Note: When flying the aircraft, in all cases act as prescribed in the "МиГ-19С Aircraft Operating and Piloting Instructions".

The landing glide path airspeed (before levelling out) with flaps 25° DOWN and at low throttle equals 300 – 310 km/hr.

The landing speed of the aircraft with the flaps 25° DOWN at low throttle power setting and aircraft landing weight of 5950 kg equals 235 km/hr.

The aircraft minimum airspeed (by the airspeed indicator wide pointer) at which the aircraft loses its stability and rolls is V = 220 – 230 km/hr (low throttle, flaps and landing gear retracted).

The pre-stalling airspeed of the aircraft as indicated by the airspeed indicator wide pointer is 350 km/hr. At this speed the aircraft is sufficiently stable and the control surfaces are effective.

Given in Fig.20 are some typical T.A.S. data of the aircraft.

2. Flight Range and Endurance

For long-range flights the aircraft may be used in two variants: without or with 2x760 or 2x400-lit. drop fuel tanks.

The maximum range and flight endurance data are given in Table 8 and in Figs 21 and 22[x/].

The total range L_{max} includes take-off and climb distances at maximum engine power setting plus gliding distance under low throttle conditions; the T_{max} value includes time data of the above flight components plus landing approach time.

The range and endurance values presented in Table 8 and in Figs 21 and 22 are given for a single aircraft with 7 per cent fuel margin (of the total fuel stock) with account for a 7-minute ground running of the engines before the take-off run and jettisoning of the drop fuel tanks when they are emptied.

All the data are given for fuel with a specific weight of γ = 0.83 kg/lit.

x/ Values L and T given in the Tables were obtained during trials of aircraft with fuel load of 1735 kg in the main tanks. Actual fuel stock equals 1800 kg.

During flight with drop tanks on a lighter fuel the decrease of the fuel specific weight may be compensated by fuelling the drop tanks to capacity (760 litres each).

The drop fuel tanks will be jettisoned as prescribed in the Pilot's Instructions. Capacities of the fuel tanks are given in Table 9.

Table 8

Maximum Flight Range and Endurance

H, m.	1000	5000	10,000	12,000	14,000	15,000
	Range L_{max}, km.					
Without drop tanks	500	760	1130	1300	1390	1310
With drop tanks, 2x760 lit.(primed with 600 lit.each)	840	1230	1830	2110	2200	-
	Endurance T_{max}, hrs and min.					
Without drop tanks	1-04	1-13	1-31	1-38	1-43	1-33
With drop tanks, 2x760 lit.(primed with 600 lit.each)	1-40	1-56	2-27	2-37	2-38	-

Table 9

Capacities of Aircraft Fuel Tanks and Corresponding Total Fuel Weight for γ = 0.83 kg/lit.

Tanks	Capacity, lit.	Fuel weight, kg
Main tanks	2170	1800
Drop tanks, 2x760 lit. (primed with 600 lit. each)	2x760	2x498
Drop tanks, 2x400 lit.	2x400	2x332

Declassified in Part - Sanitized Copy Approved for Release 2011/12/13 : CIA-RDP80T00246A062100050001-6

Declassified in Part - Sanitized Copy Approved for Release 2011/12/13 : CIA-RDP80T00246A062100050001-6

3. Take-Off and Landing Characteristics

The aircraft take-off and landing characteristics have been determined during operation on a dry concrete runway.

Take-off and landing characteristics of the aircraft are presented in Tables10, 11 and 12, and in Figs 23 and 24.

The take-off distance depends on the operating conditions of the engines, flaps deflection angle and aircraft all-up weight.

The flaps deflection angle considerably effects the speed of aircraft unsticking.

The aircraft will be taxied over the runway at low throttle r.p.m.

Table 10

Take-Off Distance at Engines Maximum Power Setting and with Afterburning, without Drop Tanks

	Engines operating conditions	
	Engines maximum power	Power augmentation (with afterburning)
Flaps deflection angle, δ_{3flap}	15°	0°
Engines speed, n	11,150 r.p.m.	11,150 r.p.m.
Take-off run distance on concrete runway, $l_{t.o.r.}$	650 m.	515 m.
Take-off run time, t	18 sec.	14 sec.
Holding off and clearing the obstruction (gaining H = 25 m.), $l_{holding\ off} + l_{cl.}$	875 m.	615 m.
Total take-off distance, $l_{t.o.}$	1525 m.	1130 m.
Unstick speed, $V_{unstick}$	284 km/hr	307 km/hr
Take-off weight, G	7400 kg	7310 kg

Table 11

Take-Off Distance at Engines Maximum Power Setting with Drop Tanks, 2x760 lit., and Take-Off Weight G = 8450 kg

Flaps deflection angle, δ_{3flap}	15°
Engines speed, n	11,150 r.p.m.
Take-off run distance on concrete runway, $l_{t.o.r.}$	900 m.
Take-off run time, t	21.9 sec.
Holding off and clearing the obstruction (gaining H = 25 m.), $l_{holding\ off} + l_{cl.}$	980 m.
Total take-off distance, $l_{t.o.}$	1880 m.
Unstick speed, $V_{unstick}$	305 km/hr

Table 12

Landing Distance at Landing Weight G = 5950 kg

	With drag parachute	Without drag parachute
Flaps deflection angle for landing, $\delta_{3\ flap}$	25°	25°
Glide from H = 25 m. and holding off, $l_{gl.} + l_{holding\ off}$	1090 m.	1090 m.
Landing run distance on concrete runway, $l_{l.r.}$	610 m.	890 m.
Total landing distance, l_l	1700 m.	1980 m.
Landing glide path airspeed (before levelling out) $V_{gl.}$	300-310 km/hr	300-310 km/hr
Touchdown speed, $V_{t.d.}$	235 km/hr	235 km/hr

Declassified in Part - Sanitized Copy Approved for Release 2011/12/13 : CIA-RDP80T00246A062100050001-6

Declassified in Part - Sanitized Copy Approved for Release 2011/12/13 : CIA-RDP80T00246A062100050001-6

The take-off of the aircraft may be executed with the engines at normal or maximum power settings, as well as with afterburning (power augmentation conditions).

Take-off with drop fuel tanks differs from the take-off procedure without drop tanks only in the length of the take-off run distance.

The landing run will be executed at the engine low throttl operation with application of all wheel brakes, with or witho employment of the drag parachute.

Extend the landing gear prior to landing at a speed of 500 - 550 km/hr. The landing gear extended, the landing approach is executed at level flight at an airspeed of 450 - 500 km/hr with the flaps extended.

The gliding to the levelling-off point will be started fro an altitude not lower than 200 m. The levelling-off will be started at an altitude of 8 - 7 m. and will be ended at an altitude not higher than 1 m.

By the holding-off moment the airspeed should be 300 - 310 km/hr.

Landing with empty drop fuel tanks is allowable; it is forbidden to land if more than 2500 lit. remain in the tanks (for details see the "МиГ-19С Aircraft Operating and Piloting Instructions").

4. Aircraft Control

All elements of pilotage can be performed on the МиГ-19С aircraft at all the allowable airspeeds of flight (See the "Pilot's Instructions").

Given below are characteristics used in evaluation of the aircraft control.

Note: During flight trials the stabilizer deflection angles were measured normal to the stabilizer rotation axis. Relation between the stabilizer deflectio angles in the plane normal to the rotation axis and relative to the flight line is expressed by the formula:

$$tg\varphi_{rel.to\ f.l.} = tg\varphi_{rot.ax.} \cos\chi_{rot.ax.} = 0.611\ tg\varphi_{rot.ax.}$$

Figs 25 - 43 present characteristics of longitudinal stability and control; Figs 25 - 27 deal with effect of Mach number on stabilizer deflection angle $\varphi_{st.}$ required to trim the aircraft in a level flight at different C.G. positions, flight altitudes and engine power settings.

Figs 28 - 32 present respective control stick travels "x" in mm and control handle pressures P in kg.

The figures show that the required stabilizer deflection angles and corresponding control stick travels "x" and control stick pressures P (at Mach number up to 0.9) change smoothly and steadily, whereas in the 0.9 - 0.98 Mach number range the curves go smoothly down which represents 5 - 10 mm of control stick travel and 2 - 3 kg pressures on the control stick.

At Mach numbers of 1 - 1.2 the required stabilizer deflection angle and the corresponding rate of pressure change will be considerable and the representing curve will go up; at Mach numbers over 1.2 the change of the required stabilizer deflection angle and control stick pressure increase will be slowed down; at Mach 1.3 - 1.4 the stabilizer angular movement and pressure change will be inconsiderable, their speed rate being almost neutral.

Maximum pressures on the control stick from the boost unit in a level flight are within the range of ±15 kg (with the trimming effect mechanism NEUTRAL).

From the above figures it can be seen that in a level flight a rearward travel of the C.G. position increases the required control stick travel and forward pressure and correspondingly decreases the backward pressure. The C.G. position of the aircraft without drop tanks and rockets changes in flight due to consumption of fuel and ammunition within the limits of 38.5 - 44 per cent MAC (in-flight aircraft C.G. shift data are given in Figs 139 - 142). Longitudinal trimming characteristics of the aircraft with the stabilizer booster ON are as follows:

The aircraft is trimmed by the trimming effect mechanism in a straight climb from H=0 to H=3000 m. at normal power setting of both engines at an airspeed of 750±30 km/hr by the airspeed indicator wide pointer, with landing gear, flaps and air brakes retracted and without drop tanks.

Declassified in Part - Sanitized Copy Approved for Release 2011/12/13 : CIA-RDP80T00246A062100050001-6

Declassified in Part - Sanitized Copy Approved for Release 2011/12/13 : CIA-RDP80T00246A062100050001-6

Figs 33 - 38 present trimming curves of the stabilizer deflection, control stick travel and pressure in a straight flight during take-off and landing procedures.

Figs 39 - 41 show changes of values $\frac{dP}{dn_y}$, $\frac{d\varphi}{dn_y}$ and $\frac{dx}{dn_y}$ which characterize maneuvrability and controllability of the aircraft in a flight under increase load factor conditions, i.e. change of: control stick pressure P, stabilizer deflection angle φ_{st} and control stick travel x, required to build up a load factor increase of $\Delta n_y = 1$ for altitudes of 5000 m. and 12,000 m.

These characteristics, as is seen from Figs 39 - 41, do not exceed the specified standard values; it should be noted that the above characteristics considerably change in their value at close-to-sonic speed values of Mach number.

With the increase of the flight altitude the required stabilizer deflection angles and stick travel for the present load factor increase considerably, whereas the character of the load factor pressure curves for different altitudes changes differently due to various stabilizer setting angles for load factor at low and high altitudes and due to the shape of the curves representing the control stick pressures from the boost unit (See the Levelling Diagram, Appendix 3).

Fig.42 shows the change of the stabilizer trimming angle (relative to the general direction of air stream - flight line) required to balance the increment of the pitching moment produced by the application of the air brakes.

Extension of the air brakes causes pitching of the aircraft which is more intensive at Mach numbers exceeding 1 and which is counteracted by forward movement of the control stick. It should be noted that extension of the air brakes facilitates pull-out of the aircraft from a dive. Fig.43 presents a record of time changes of the longitudinal control characteristics for load factor of 8.5 at the altitude of 3150 m. The presented material shows that the aircraft longitudinal control characteristics over the entire range of subsonic and supersonic speeds are sufficiently normal. Introduction of the controlled stabilizer (without elevators) and non-reversible booster control in the aircraft did not change the longitudinal control characteristics the pilot is accustomed to while the effectiveness of this type of control is much higher than that of the elevator control.

Figs 44 - 56 deal with aircraft lateral control characteristics; Figs 44 - 48 present trimming curves obtained in coordinated slip at flight altitudes of 6000 m. and 12,000 m.

$\delta^\circ_{aileron} = f(\gamma^\circ)$ - required ailerons deflection angle to create bank angle γ°;

$\delta^\circ_{rudder} = f(\gamma^\circ)$ - required rudder deflection angle to create bank angle γ°;

$P_{rudder} = f(\gamma^\circ)$ - pedal force required to create bank angle γ°.

Figs 49 - 50 show characteristics of coordinated slip with the landing gear extended, flaps 25° DOWN for engine low throttle operation at altitudes of 3400 m. and 4400 m., with the aircraft I.A.S. of 315 km/hr. Figs 51 - 53 show the same characteristics for flight with drop fuel tanks. Fig.54 gives the rolling rate of the aircraft bank and control stick pressure from the ailerons deflected through $\Delta\delta_{aileron} = \pm 6^\circ$ at the 12,000-m. flight altitude. The figures that follow present relative values characterizing the aircraft lateral controllability:

Fig.55 gives $\frac{d P_{aileron}}{d\omega_x}$, i.e. value of the required control stick pressure from the ailerons to create the rolling rate of turn of 1 rad/sec. (radian equals 57.3°); Fig 56 presents $\frac{dP_{rudder}}{d\gamma}$, i.e.value of the required pedal pressure to create a 1° bank.

Peculiar features of the aircraft controllability are dealt with in the "Pilot's Instructions".

5. Aircraft Acceleration, Deceleration, Banked Turning and Diving Characteristics

Characteristics of the aircraft acceleration and deceleration in level flight are given in Figs 57 - 73 and in Table 13.

Note: The characteristics of the aircraft without drop tanks are given for $G_{average} = 6500$ kg; those for the aircraft with drop tanks are given for $G_{average} = 7800$ kg.

Table 14 contains characteristics of best time steady turns.

Figs 74 and 75 present overload factors n_x in curvilinear manoeuvres with engines operating with afterburners ON.

Declassified in Part - Sanitized Copy Approved for Release 2011/12/13 : CIA-RDP80T00246A062100050001-6

Declassified in Part - Sanitized Copy Approved for Release 2011/12/13 : CIA-RDP80T00246A062100050001-6

Table 13

Altitude	10,000	12,000	15,000
Acceleration time with afterburning, min.:			
(a) from V_{climb} to 0.95 $V_{eng.max}$	1.3	1.75	3.0
(b) from V_{climb} to 0.99 $V_{eng.max}$	2.25	2.95	5.25
Acceleration time from V_{max} at engine maximum power setting to 0.99 V_{max} with power augmentation	2.5	5.2	5.0
Deceleration time from V_{max} to 0.7 V_{max} with deceleration through throttling down and extension of air brakes, seconds	27	-	60

Table 14

Characteristics of Best Time Steady Turns

Parameters	Engine operating conditions		
	Afterburning	Maximum power setting	
	H = 12,000 m.	H = 12,000 m.	H = 5000 m.
Airspeed, $V_{i.(w.p.)}$, km/hr	500 - 550	400 - 450	550 - 650
Time of turn, t_{turn}, sec.	85	120 - 130	40 - 45
Turn radius R_t, m.	3700	2600 - 4800	1200 - 1700
Bank angle γ, deg.	65	50 - 53	70 - 75
Overload factor, n ...	2.4	1.5 - 1.6	3.5 - 3.8

The turn execution procedure is standard. Execution of turns on the aircraft with drop fuel tanks in practice does not differ from the same procedure performed without drop fuel tanks.

Fig.76 shows characteristics of turns in the horizontal plane.

Fig.77 presents load factors during best time steady turns at the altitude of 12,000 m.

Fig.78 presents vertical dive characteristics.

6. Possible Vertical Maximum Load Factors

Figs 79 and 80 present maximum load factors as function of flight altitude and airspeed given by the beginning of vibration and at δ stabilizer max.

Maximum load factor value of n = 8 is reached at altitudes not lower than 9000 m.

Fig.81 presents C_y values for creation of maximum load factors.

Declassified in Part - Sanitized Copy Approved for Release 2011/12/13 : CIA-RDP80T00246A062100050001-6

Declassified in Part - Sanitized Copy Approved for Release 2011/12/13 : CIA-RDP80T00246A062100050001-6

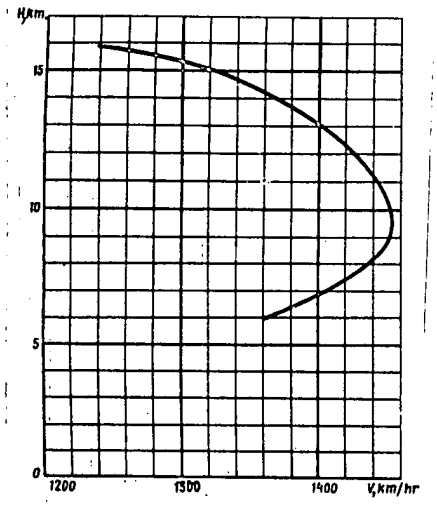

Fig. 10. Aircraft Maximum Level True Airspeeds with Afterburner ON
n = 11,150 r.p.m.

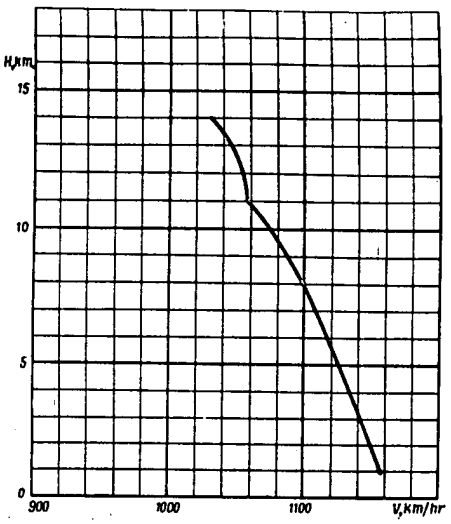

Fig. 11. Aircraft Maximum Level True Airspeeds at Engine Maximum Power Setting
n = 11,150 r.p.m.

Declassified in Part - Sanitized Copy Approved for Release 2011/12/13 : CIA-RDP80T00246A062100050001-6

Declassified in Part - Sanitized Copy Approved for Release 2011/12/13 : CIA-RDP80T00246A062100050001-6

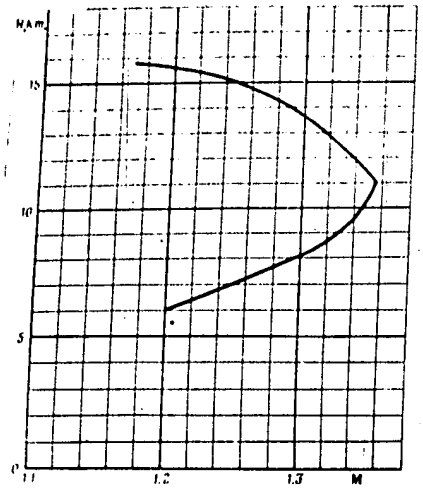

Fig. 12. Mach Number of Maximum Level Airspeed Flight (afterburner ON)

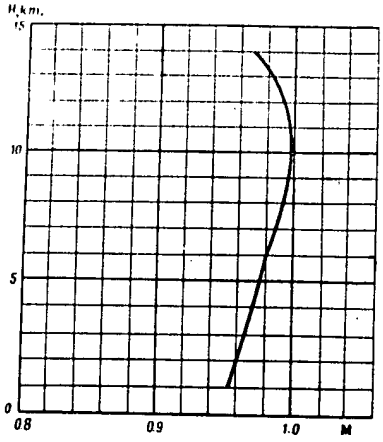

Fig. 13. Mach Number of Maximum Level Airspeed Flight (engine maximum power setting)

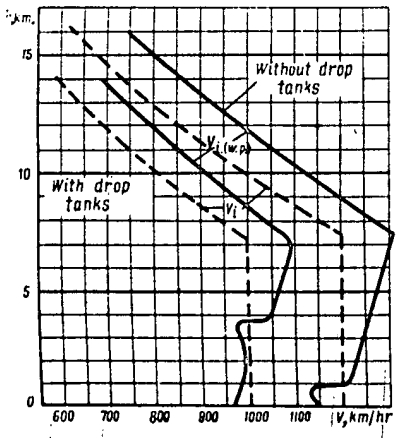

Fig. 14. Maximum Rated IAS and IAS (W.P.) (Calibrated)*

*) Indicated Air Speed, by Wide Pointer of Airspeed Indicator (calibrated)

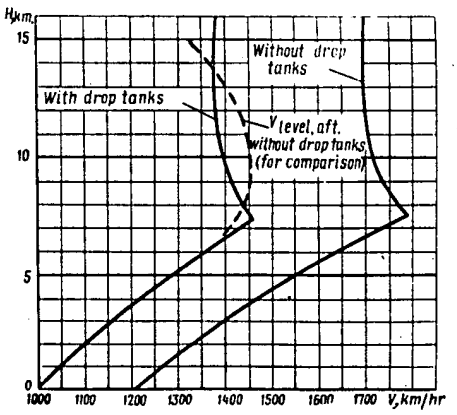

Fig. 15. Maximum Rated TAS

Declassified in Part - Sanitized Copy Approved for Release 2011/12/13 : CIA-RDP80T00246A062100050001-6

Declassified in Part - Sanitized Copy Approved for Release 2011/12/13 : CIA-RDP80T00246A062100050001-6

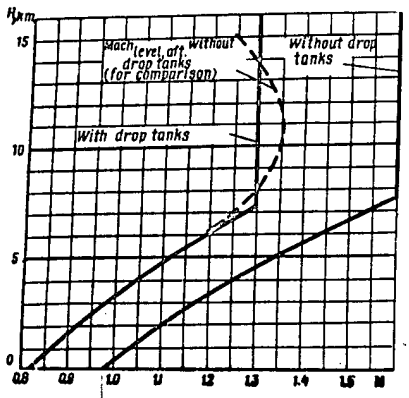

Fig. 16. Maximum Mach Numbers of Aircraft Flight

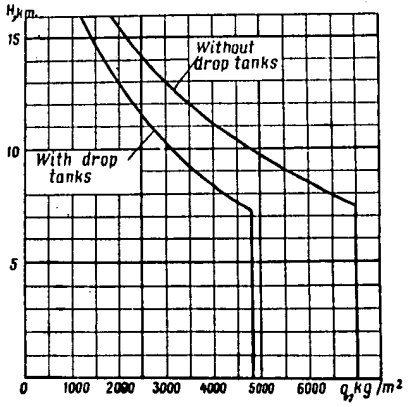

Fig. 17. Aircraft Maximum Rated Impact Pressures, $q_{max.max.}$ = 7000 kg/m²

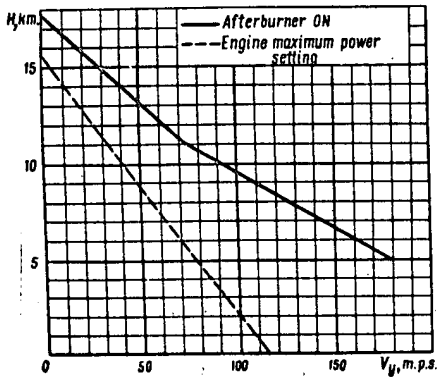

Fig. 18. Aircraft Maximum Vertical Speeds
n = 17 150 r.p.m.

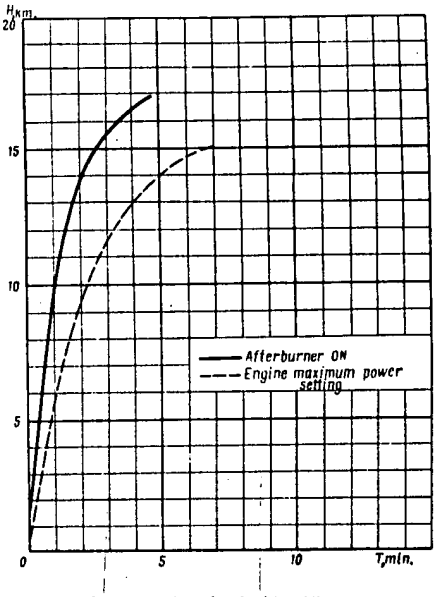

Fig. 19. Aircraft Climbing Time
n = 11.150 r.p.m.

Note: The climbing time presented in the Chart does not include take-off run time and acceleration time, the two factors taking 1.1 minutes.

Declassified in Part - Sanitized Copy Approved for Release 2011/12/13 : CIA-RDP80T00246A062100050001-6

Declassified in Part - Sanitized Copy Approved for Release 2011/12/13 : CIA-RDP80T00246A062100050001-6

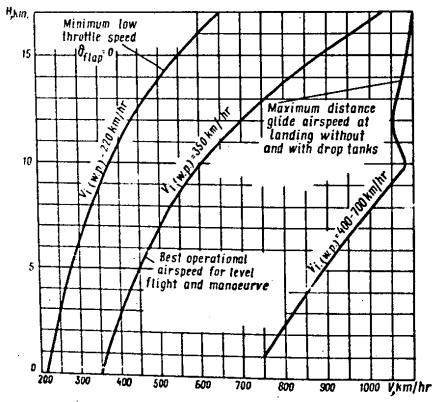

Fig. 20. Some Typical Aircraft TAS

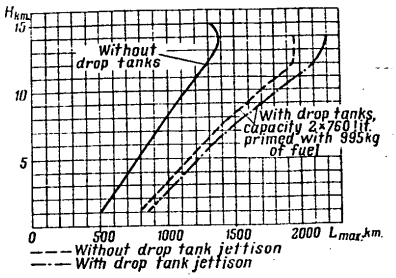

Fig. 21. Aircraft Maximum Flight Range (climb performed at engine maximum power setting)

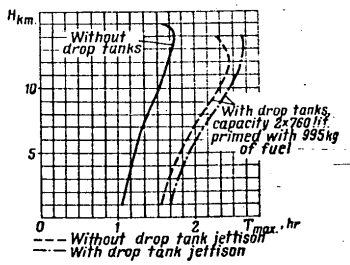

Fig. 22. Aircraft Maximum Flight Endurance (climb performed at engine maximum power setting)

Declassified in Part - Sanitized Copy Approved for Release 2011/12/13 : CIA-RDP80T00246A062100050001-6

Declassified in Part - Sanitized Copy Approved for Release 2011/12/13 : CIA-RDP80T00246A062100050001-6

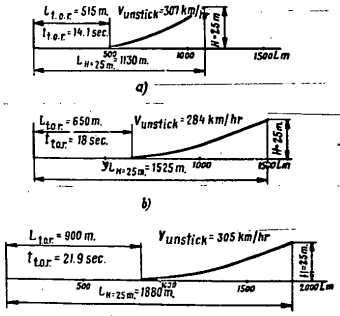

Fig. 23. Aircraft Take-Off Distance Data

a – with afterburner ON; $\delta_{flap} = 0°$; $G_{t.o.} = 7310$ kg; b – at engine maximum power setting, without drop tanks; $\delta_{flap} = 15°$; $G_{t.o.} = 7400$ kg; c – at engine maximum power setting, with drop tanks: $\delta_{flap} = 15°$; $G_{t.o.} = 8450$ kg.

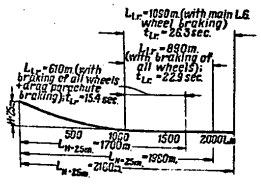
$L_{l.r.}$ = 1050 m. (with main L.G. wheel braking)
$t_{l.r.}$ = 26.5 sec.
$L_{l.r.}$ = 880 m. (with braking of all wheels);
$t_{l.r.}$ = 22.9 sec.
$L_{l.r.}$ = 610 m. (with braking of all wheels + drag parachute braking); $t_{l.r.}$ = 15.4 sec.
H=25m.
500
1000
1500
2000 Lm
$L_{H=25m.}$ = 1700 m.
$L_{H=25m.}$ = 1980 m.
$L_{H=25m.}$ = 2100 m.

Fig. 24. Aircraft Landing Distance Data

$\delta_{flap} = 25°$; $G_{landing} = 5950$ kg.

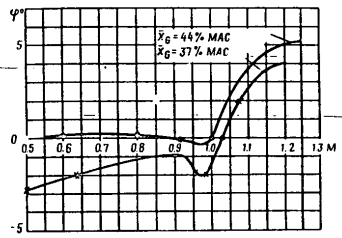

Fig. 25. Stabilizer Deflection Angles in Straight Flight

H=6 km.; afterburner ON (angles given in plane normal to rotation axis).

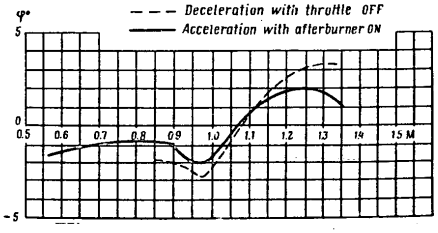

Fig. 26. Stabilizer Deflection Angles in Straight Flight

$H_{average}$ = 10 km.; $\bar{x}_G$ = 38.5% MAC (angles given in plane normal to rotation axis).

Declassified in Part - Sanitized Copy Approved for Release 2011/12/13 : CIA-RDP80T00246A062100050001-6

Declassified in Part - Sanitized Copy Approved for Release 2011/12/13 : CIA-RDP80T00246A062100050001-6

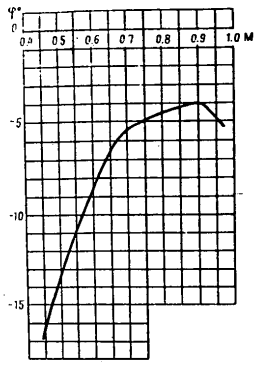

Fig. 27. Stabilizer Deflection Angles in Straight Flight

$H_{average}$ = 11.5 km.; $\bar{x}_G$ = 37.5% MAC; low throttle setting (angles given in plane normal to rotation axis).

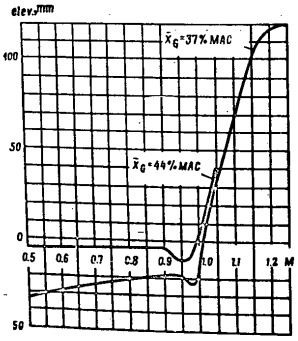

Fig. 28. Control Stick Travel in Straight Flight

$H_{average}$ = 6 km.; afterburner ON.

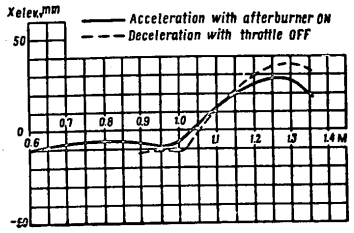

Fig. 29. Control Stick Travel in Straight Flight

$H_{average}$ = 10 km.; $\bar{x}_G$ = 38.5% MAC.

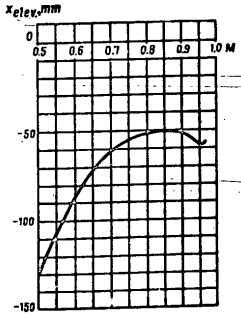

Fig. 30. Control Stick Travel in Straight Flight

$H_{average}$ = 11.5 km.; $\bar{x}_G$ = 37% MAC; low throttle setting.

Declassified in Part - Sanitized Copy Approved for Release 2011/12/13 : CIA-RDP80T00246A062100050001-6

Declassified in Part - Sanitized Copy Approved for Release 2011/12/13 : CIA-RDP80T00246A062100050001-6

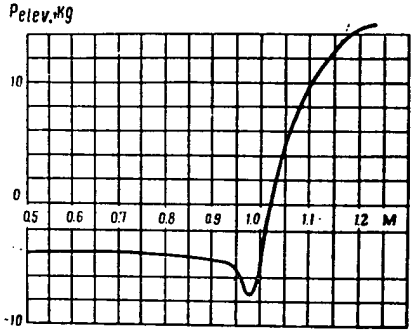

Fig. 31. Control Stick Pressures in Straight Flight

$H_{average}$ = 6 km.; $\bar{x}_G$ = 37 – 39% MAC; afterburner ON.

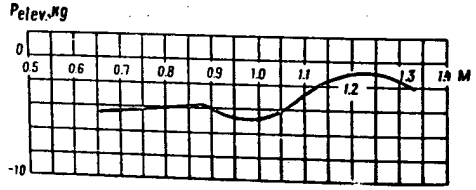

Fig. 32. Control Stick Pressures in Straight Flight

H=10 km.; $\bar{x}_G$ = 38% MAC; afterburner ON.

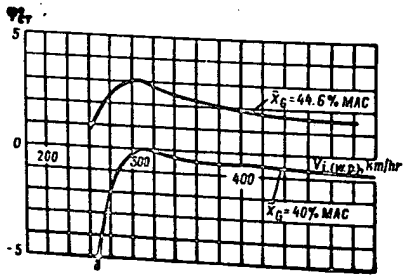

Fig. 33. Stabilizer Deflection Angles at Aircraft Take-Off (normal power setting, landing gear extended, flaps in take-off position)

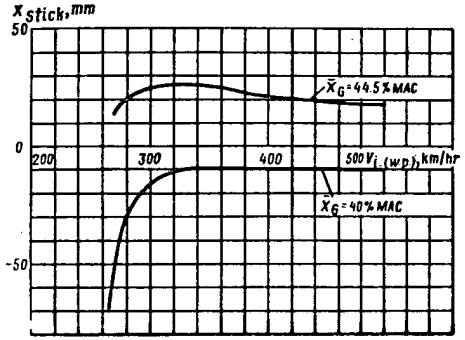

Fig. 34. Control Stick Travel at Aircraft Take Off (normal power setting, landing gear extended, flaps in take-off position)

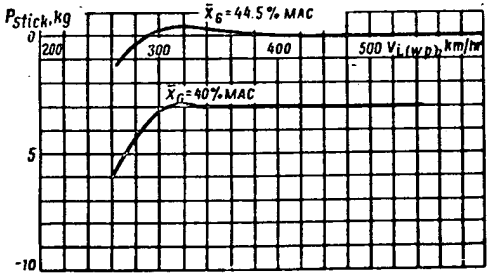

Fig. 35. Control Stick Pressures at Aircraft Take-Off (normal power setting, landing gear extended, flaps in take-off position)

Declassified in Part - Sanitized Copy Approved for Release 2011/12/13 : CIA-RDP80T00246A062100050001-6

Declassified in Part - Sanitized Copy Approved for Release 2011/12/13 : CIA-RDP80T00246A062100050001-6

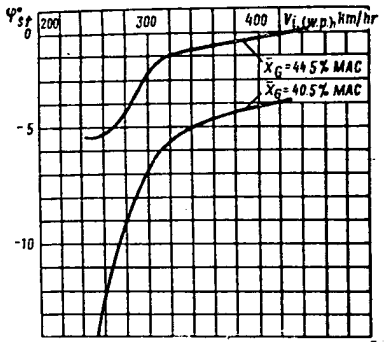

Fig. 36. Stabilizer Deflection Angles at Landing (low throttle, landing gear extended, flaps for landing)

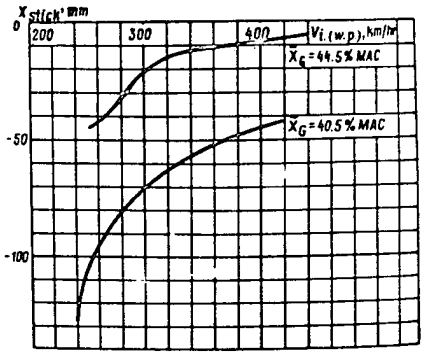

Fig. 37. Control Stick Travel at Aircraft Landing (low throttle, landing gear extended, flaps for landing)

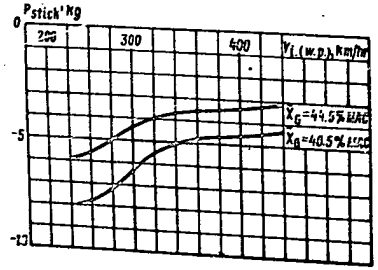

Fig. 38. Control Stick Pressures at Landing (low throttle, landing gear extended, flaps for landing)

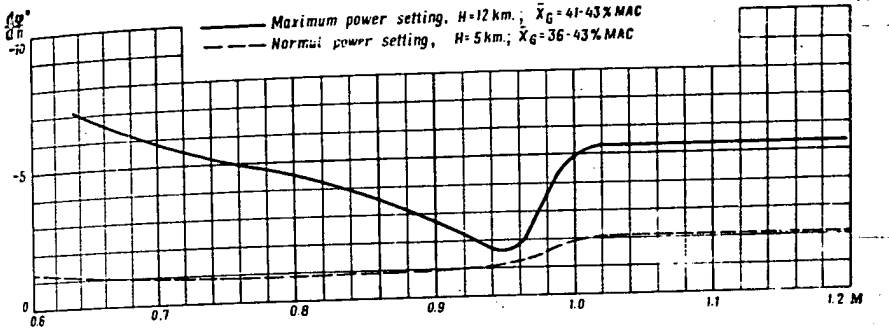

Fig. 39. Stabilizer Deflection Angles Required to Create Instantaneous Load Factor (angles are given in plane normal to rotation axis)

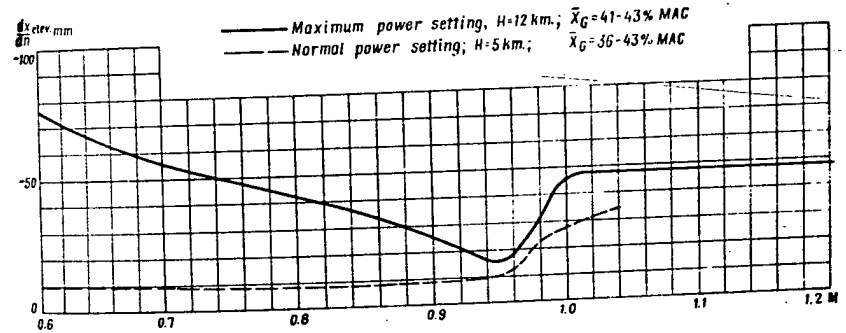

Fig. 40. Control Stick Travel Required to Create Instantaneous Load Factor

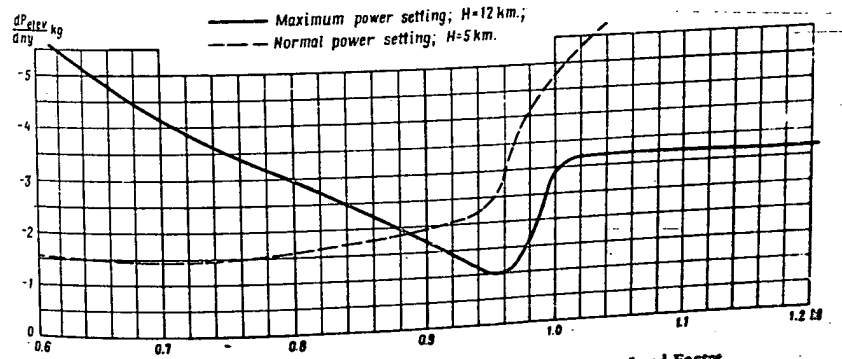

Fig. 41. Control Stick Pressures Required to Create Instantaneous Load Factor

Declassified in Part - Sanitized Copy Approved for Release 2011/12/13 : CIA-RDP80T00246A062100050001-6

Declassified in Part - Sanitized Copy Approved for Release 2011/12/13 : CIA-RDP80T00246A062100050001-6

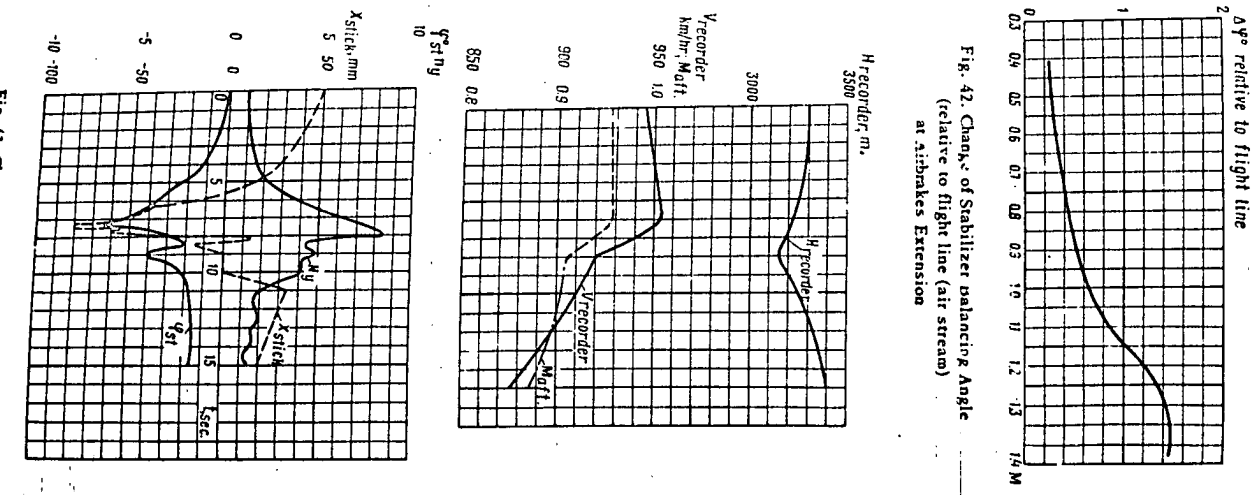

Fig. 42. Change of Stabilizer Balancing Angle (relative to flight line (air stream) at Airbrakes Extension

Fig. 43. Change of Aircraft Controllability Characteristics when Load Factor n_y = 8.5 is Reached

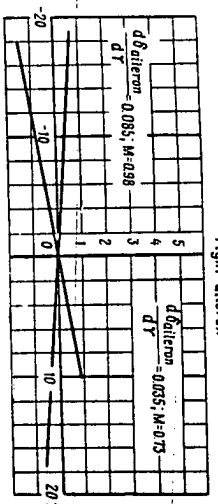

Fig. 44. Trimming Curves of Aileron Deflections by Bank Angle at Coordinated Slip

$H_{average}$ = 6000 m.

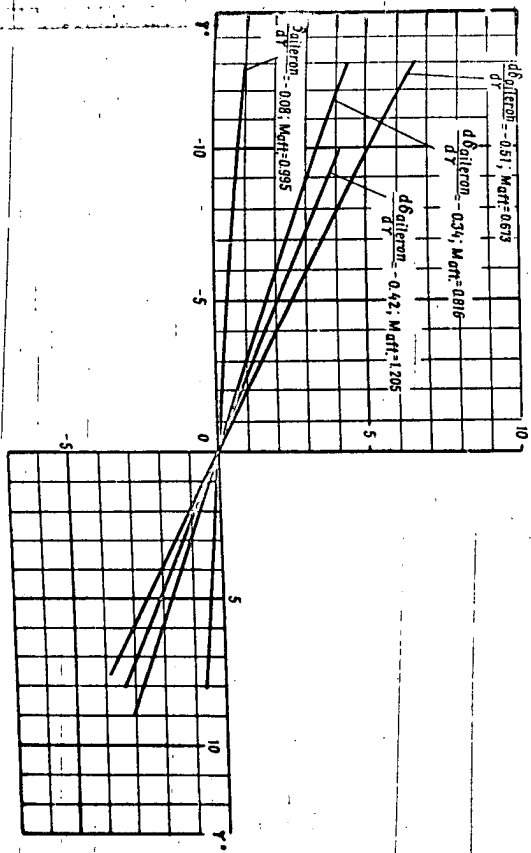

Fig. 45. Trimming Curves of Aileron Deflections by Bank Angle at Coordinated Slip

H=11,000 m.

Declassified in Part - Sanitized Copy Approved for Release 2011/12/13 : CIA-RDP80T00246A062100050001-6

Declassified in Part - Sanitized Copy Approved for Release 2011/12/13 : CIA-RDP80T00246A062100050001-6

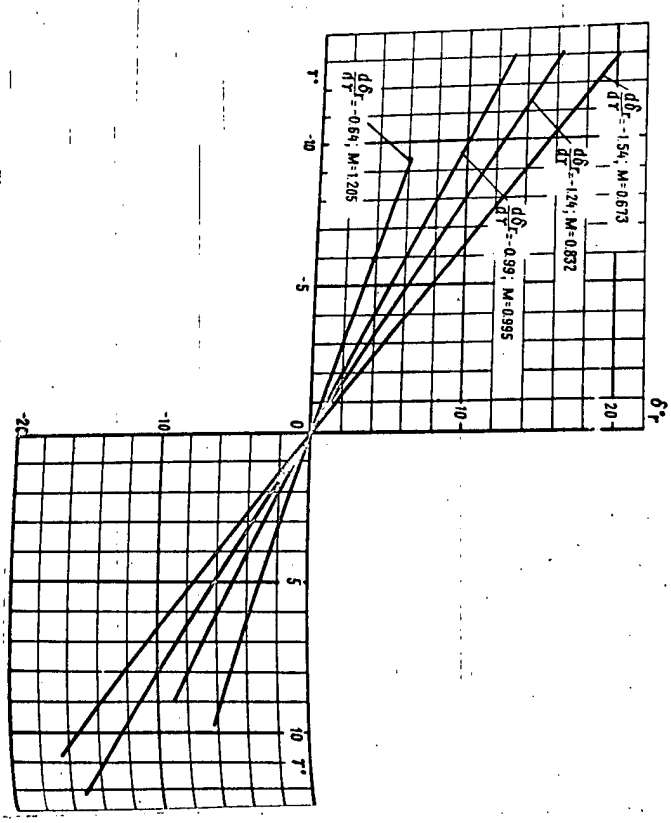

Fig. 47. Trimming Curves of Rudder Deflections by Bank Angle at Coordinated Slip
$H_{average}$ = 12,000 m.

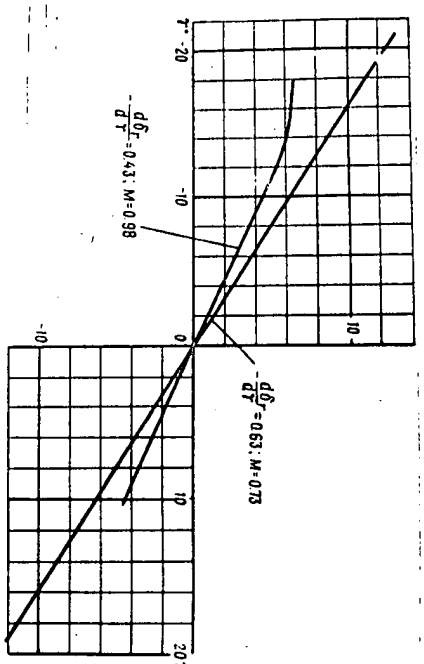

Fig. 46. Trimming Curves of Rudder Deflections by Bank Angle at Coordinated Slip
$H_{average}$ = 6000 m.

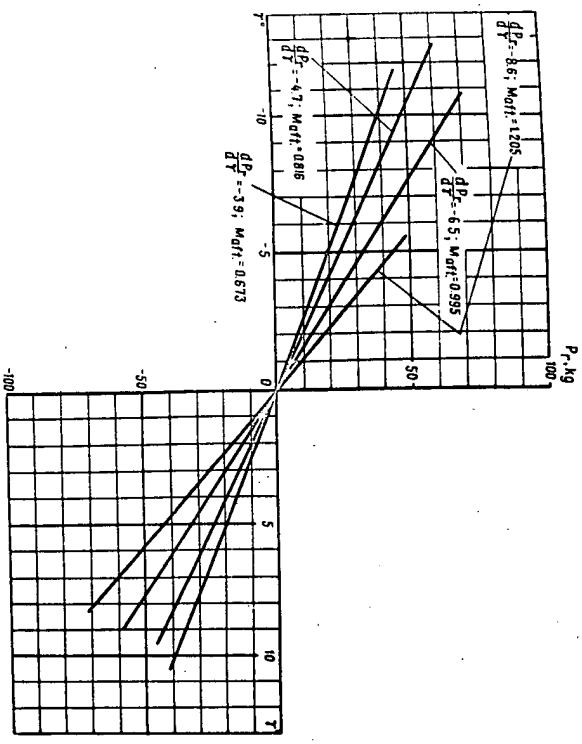

Fig. 48. Trimming Curves of Rudder Deflections by Bank Angle at Coordinated Slip
H=12,000 m.

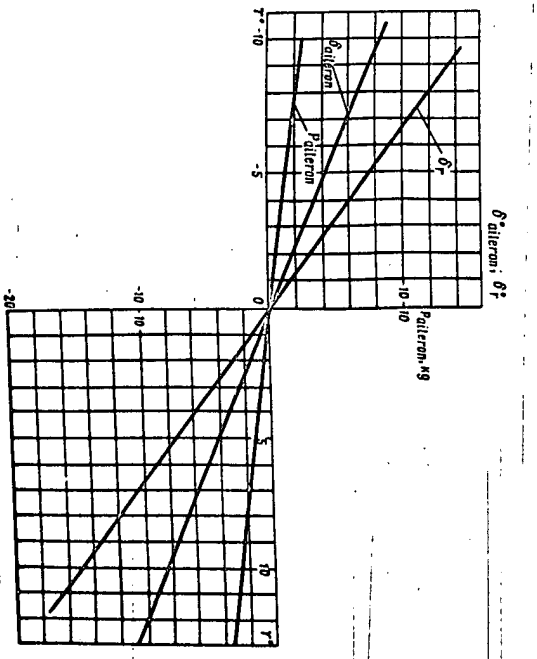

Fig. 49. Trimming Curves of Rudder and Ailerons Deflections and Ailerons Pressure Curves at Coordinated Slip
Landing Gear Extended; Flaps 25° DOWN; Low Throttle; V_i(e.p.)= 315 km/hr; H=4400 m.

Declassified in Part - Sanitized Copy Approved for Release 2011/12/13 : CIA-RDP80T00246A062100050001-6

Declassified in Part - Sanitized Copy Approved for Release 2011/12/13 : CIA-RDP80T00246A062100050001-6

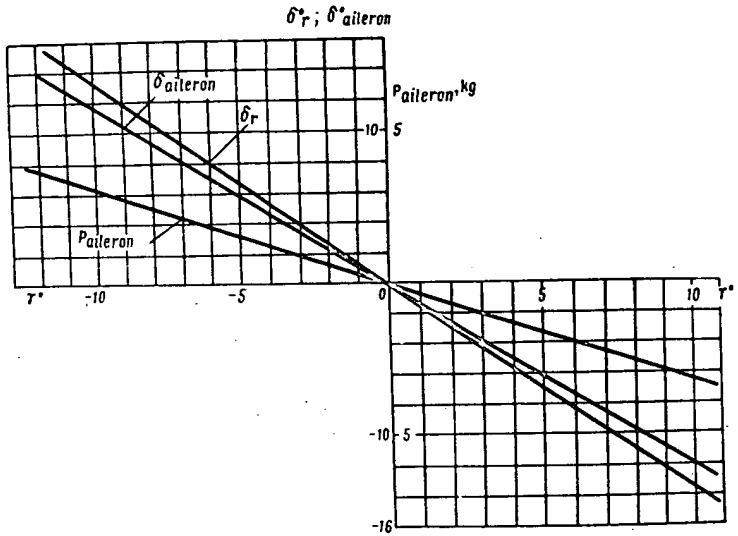

Fig. 50. Trimming Curves of Rudder and Ailerons Deflections and Ailerons Pressure Curves during Coordinated Slip of Aircraft with Drop Tanks

Landing Gear Extended; Flaps 25° DOWN; Low Throttle;
$V_{i.(w.p.)}$ = 315 km/hr; H=3400 m.

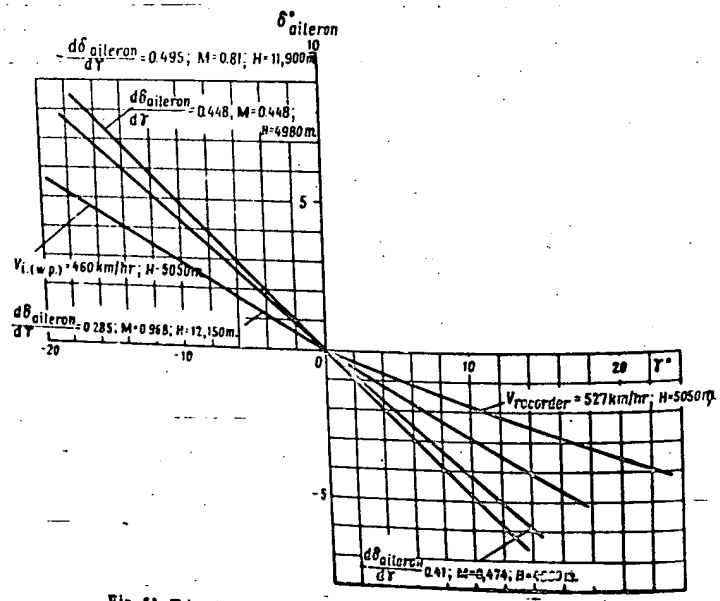

Fig. 51. Trimming Curves of Ailerons Deflections by Bank Angle at Coordinated Slip of Aircraft with Drop Tanks

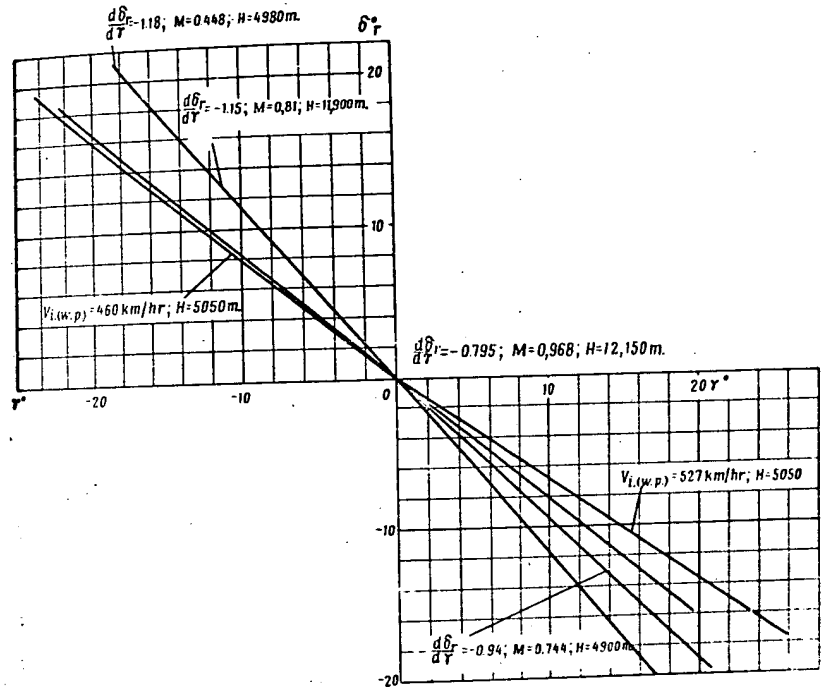

Fig. 52. Trimming Curves of Rudder Deflections by Bank Angle at Coordinated Slip of Aircraft with Drop Tanks

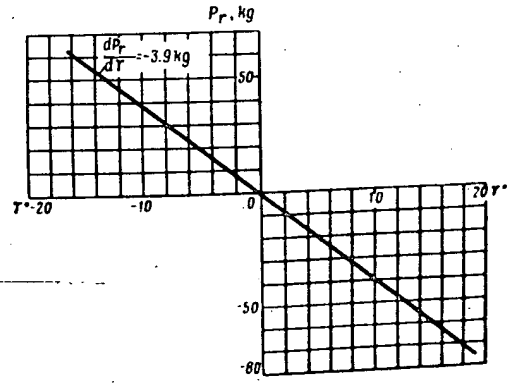

Fig. 53. Trimming Curve of Rudder Pressure by Bank Angle at Coordinated Slip of Aircraft with Drop Tanks

H = 12.000 m.
$V_{i.(w.p.)}$ = 470 – 540 km/hr.

Declassified in Part - Sanitized Copy Approved for Release 2011/12/13 : CIA-RDP80T00246A062100050001-6

Declassified in Part - Sanitized Copy Approved for Release 2011/12/13 : CIA-RDP80T00246A062100050001-6

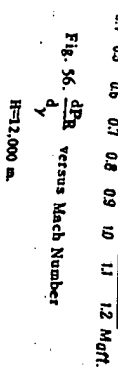

Fig. 56. $\frac{dP_R}{d_y}$ versus Mach Number
H=12,000 m.

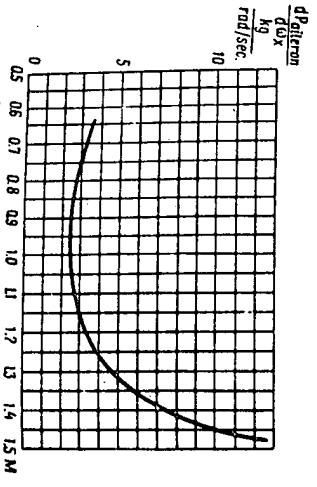

Fig. 55. Control Stick Pressure Required to Build Up 1 rad/sec. Rolling Rate of Turn
H=12,000 m.

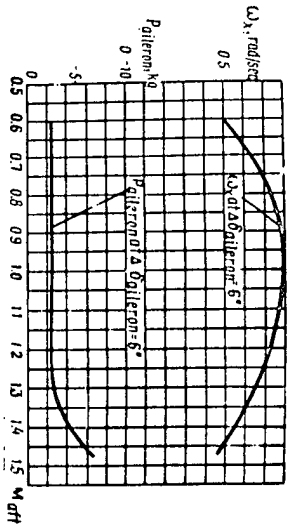

Fig. 54. ω_x and $P_{aileron}$ versus Mach Number
$\delta_{aileron} = \pm 6°$; H=12,000 m.

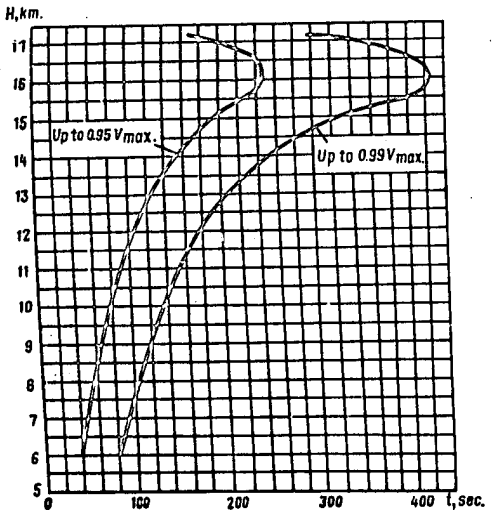

Fig. 57. Acceleration Time from V_{climb} to 0.95 $V_{max.}$ and to 0.99 $V_{max.}$ with Afterburner ON

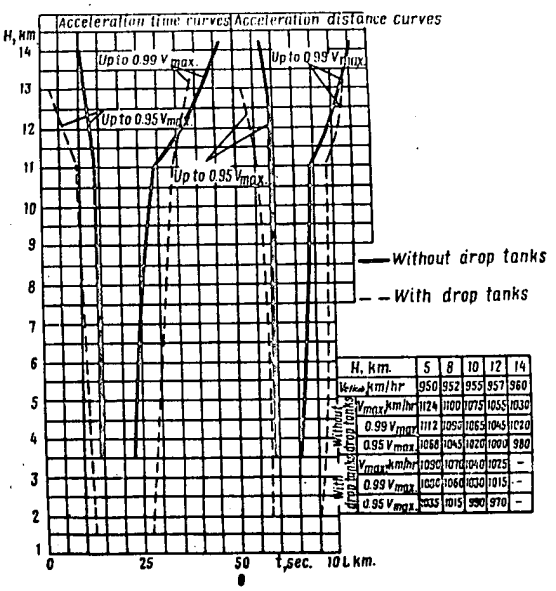

H, km.	5	8	10	12	14
V_{climb} km/hr	950	952	955	957	960
V_{max} km/hr	1124	1100	1075	1055	1030
0.99 V_{max}	1112	1055	1065	1045	1020
0.95 V_{max}	1068	1045	1020	1000	980
V_{max} km/hr	1090	1070	1045	1025	-
0.99 V_{max}	1030	1060	1030	1015	-
0.95 V_{max}	1035	1015	990	970	-

Fig. 58. Aircraft Time and Distance Characteristics during Acceleration from V_{climb} to 0.95 $V_{max.}$ and to 0.99 $V_{max.}$ at Engine Maximum Power Setting

Declassified in Part - Sanitized Copy Approved for Release 2011/12/13 : CIA-RDP80T00246A062100050001-6

Declassified in Part - Sanitized Copy Approved for Release 2011/12/13 : CIA-RDP80T00246A062100050001-6

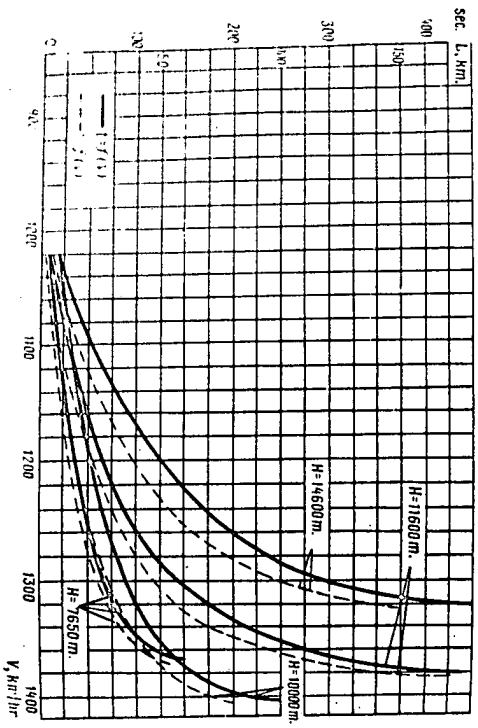

Fig. 59. Acceleration Characteristics with Engines Operating with Afterburner ON (without drop tanks)

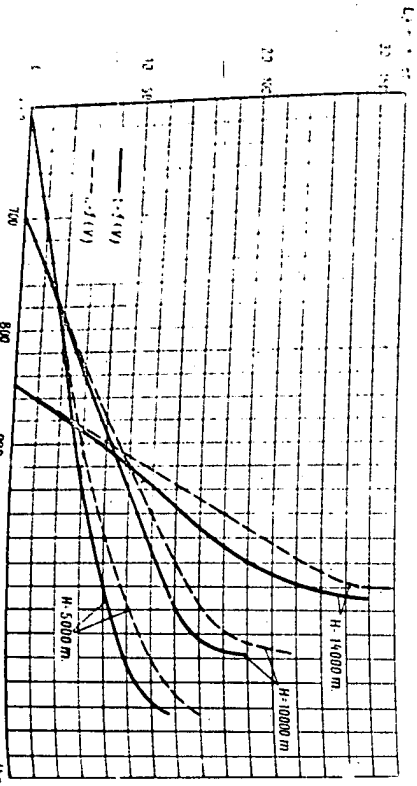

Fig. [illegible] Acceleration Characteristics with Engines at Maximum Power Setting (without drop tanks)

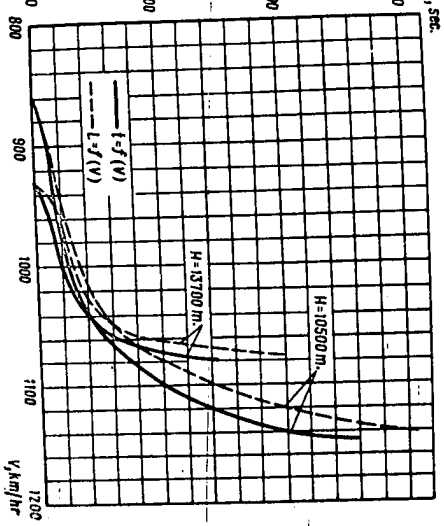

Fig. 61. Acceleration Characteristics with Engines Operating with Afterburner ON (with drop tanks)

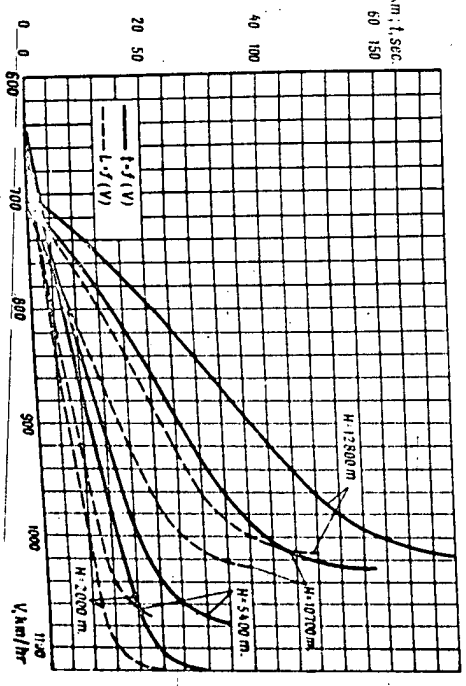

Fig. 62. Acceleration Characteristics with Engines at Maximum Power Setting (with drop tanks)

Declassified in Part - Sanitized Copy Approved for Release 2011/12/13 : CIA-RDP80T00246A062100050001-6

Declassified in Part - Sanitized Copy Approved for Release 2011/12/13 : CIA-RDP80T00246A062100050001-6

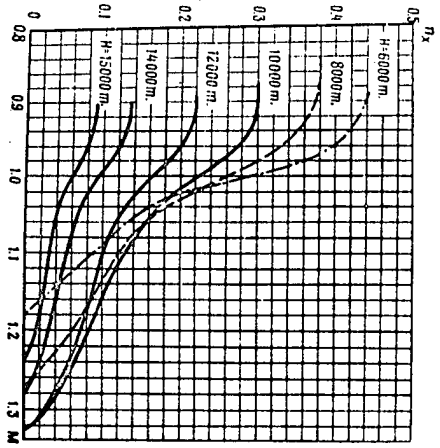

Fig. 63. Load Factor n_x during Acceleration, Engines Operating with Afterburner ON
$G_{average}$ = 6700 kg.

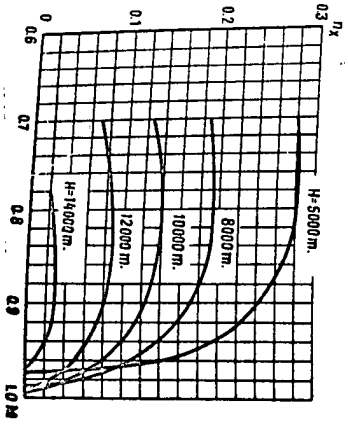

Fig. 64. Load Factor n_x during Acceleration with Engines at Maximum Power Setting
$G_{average}$ = 6700 kg.

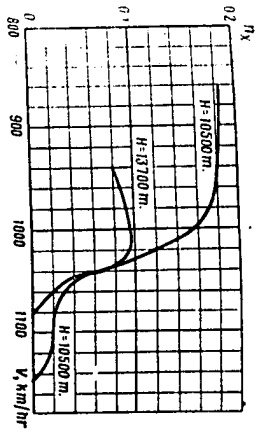

Fig. 65. Load Factor n_x during Acceleration. Engines Operating with Afterburner ON (with drop tanks)

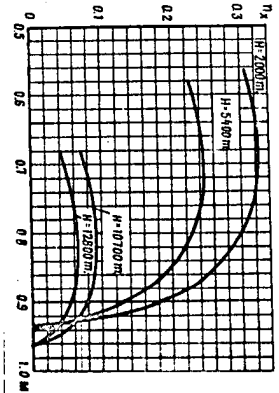

Fig. 66. Load Factor n_x during Acceleration with Engines at Maximum Power Setting (with drop tanks)

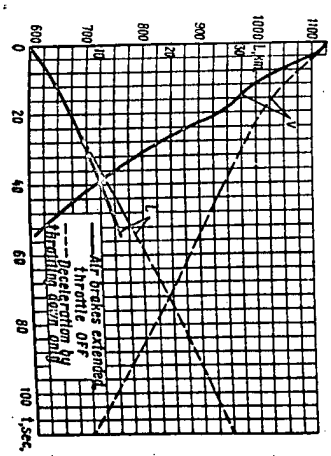
V, km/hr
600 700 800 900 1000 1100
0 20 40 60 80 100 t, sec.
L, km
10 20 30
Deceleration by throttle down only
Air brakes extended, throttle OFF

Fig. 67. Deceleration Characteristics
H=5300 m.

Declassified in Part - Sanitized Copy Approved for Release 2011/12/13 : CIA-RDP80T00246A062100050001-6

Declassified in Part - Sanitized Copy Approved for Release 2011/12/13 : CIA-RDP80T00246A062100050001-6

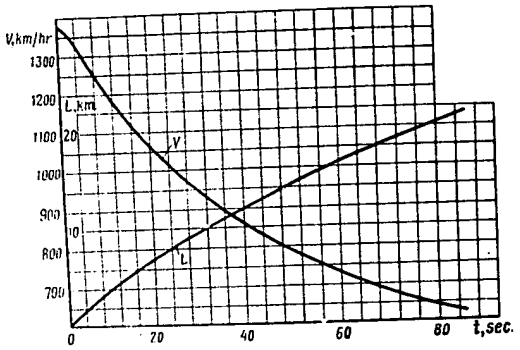

Fig. 68. Deceleration Characteristics
H=10,500 m.; Throttle Down; Air Brakes Extended.

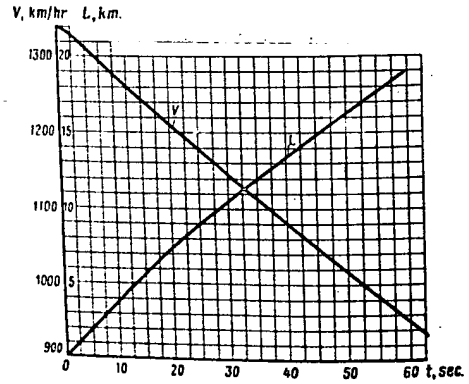

Fig. 69. Deceleration Characteristics
H=15,000 m.; Throttle OFF; Air Brakes Extended.

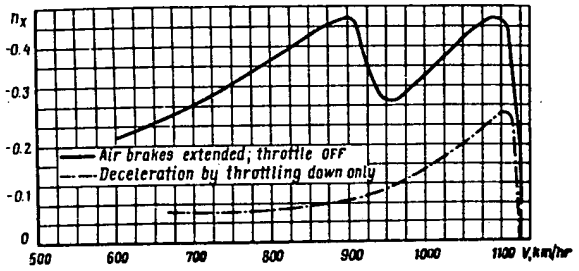

Fig. 70. Load Factor n_x during Deceleration in Level Flight at H = 5300 m.

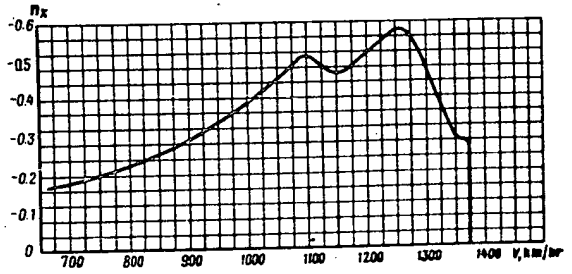

Fig. 71. Load Factor n_x during Deceleration in Level Flight at H=10,500 m.
Throttle OFF. Air Brakes Extended.

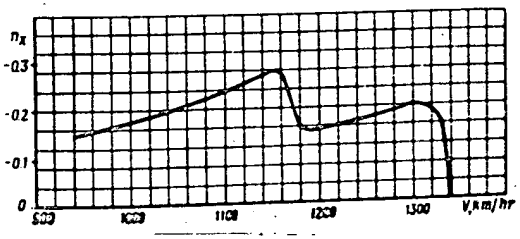

Fig. 72. Load Factor n_x during Deceleration in Level Flight at H=15,000 m.
Throttle OFF. Air Brakes Extended.

Declassified in Part - Sanitized Copy Approved for Release 2011/12/13 : CIA-RDP80T00246A062100050001-6

Declassified in Part - Sanitized Copy Approved for Release 2011/12/13 : CIA-RDP80T00246A062100050001-6

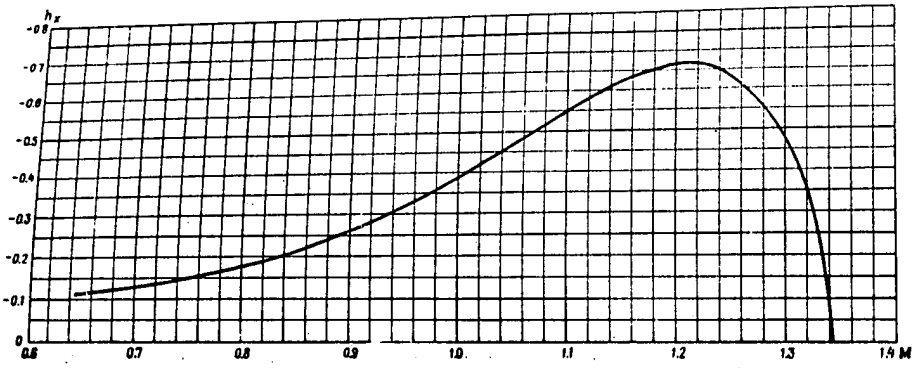

Fig. 73. Load Factor n_x during Deceleration at H=10.000 m.
Throttle OFF, Air Brakes Extended.

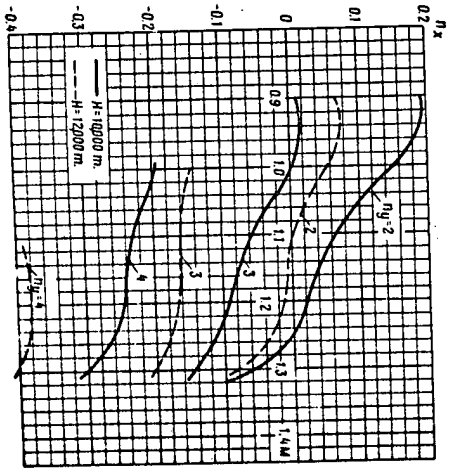

Fig. 74. Load Factor n_x in Curvilinear Manoeuvres, Engines Operating with Afterburner ON
$G_{average}$ = 6700 kg.

Declassified in Part - Sanitized Copy Approved for Release 2011/12/13 : CIA-RDP80T00246A062100050001-6

Declassified in Part - Sanitized Copy Approved for Release 2011/12/13 : CIA-RDP80T00246A062100050001-6

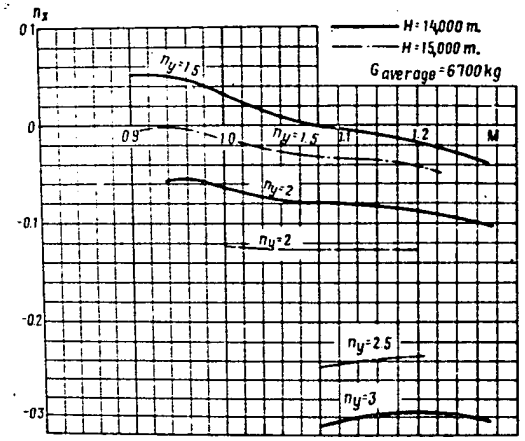

Fig. 75. Load Factor n_x in Curvilinear Manoeuvres, Engines Operating with Afterburner ON

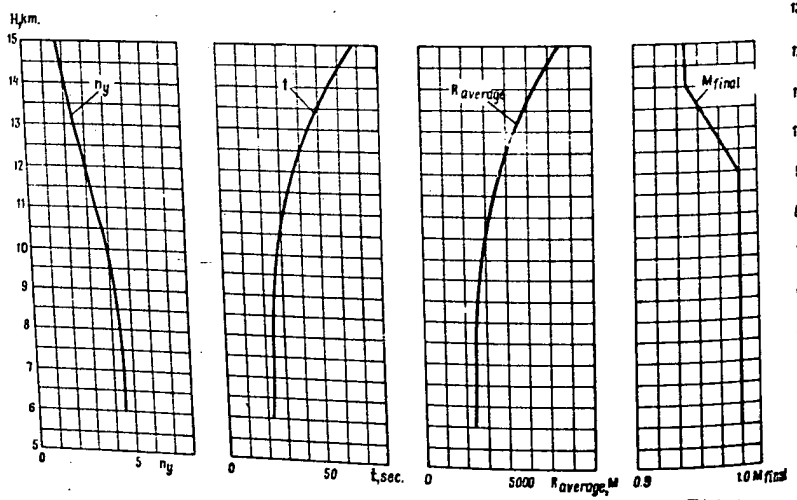

Fig. 76. Characteristics of Unsteady 180° Turns in Horizontal Plane, Engines Operating with Afterburner ON

$V_{initial} = 0.9\ V_{max.}$

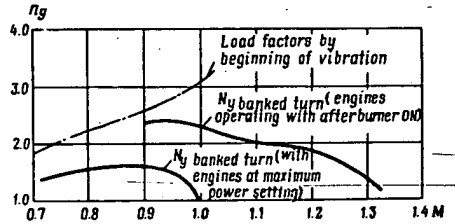

Fig. 77. Load Factors of Steady, Banked Turns

H=12.000 m.

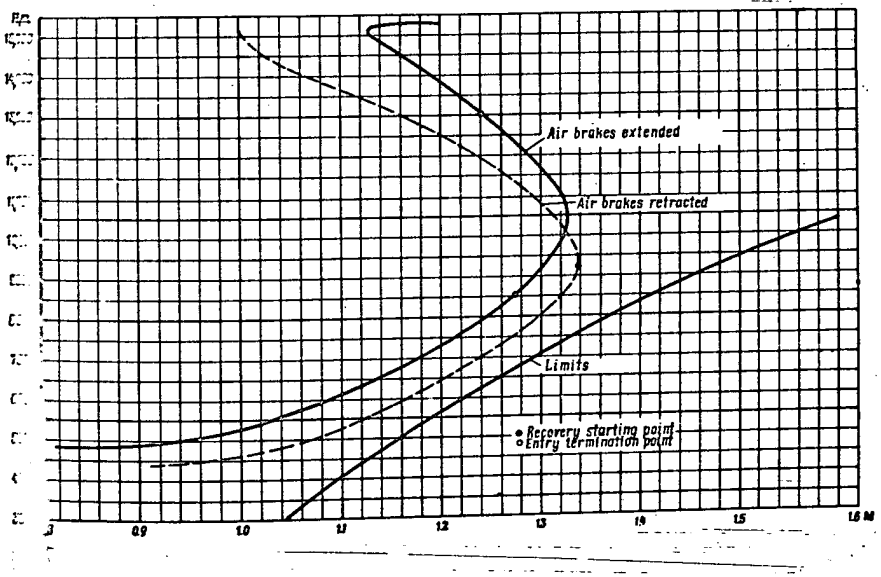

Fig. 78. Vertical Dives with Throttle OFF, Air Brakes Extended or Retracted

Declassified in Part - Sanitized Copy Approved for Release 2011/12/13 : CIA-RDP80T00246A062100050001-6

Declassified in Part - Sanitized Copy Approved for Release 2011/12/13 : CIA-RDP80T00246A062100050001-6

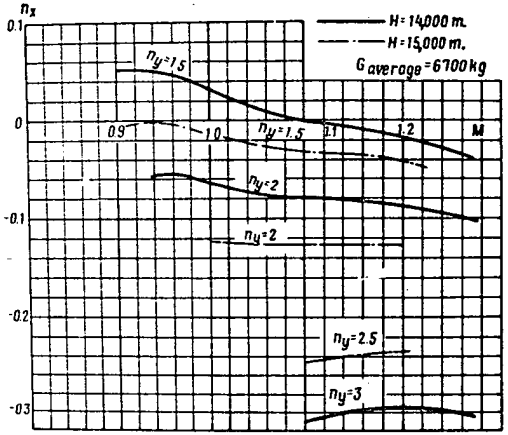

Fig. 75. Load Factor n_x in Curvilinear Manoeuvres, Engines Operating with Afterburner ON

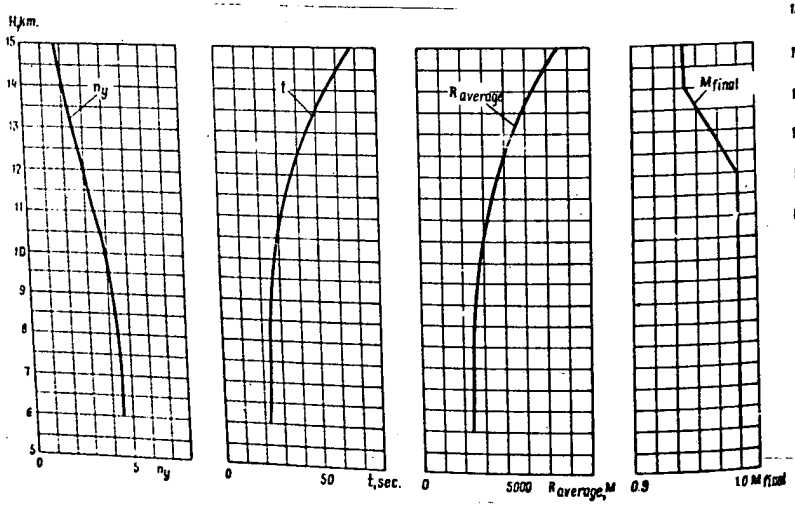

Fig. 76. Characteristics of Unsteady 180° Turns in Horizontal Plane, Engines Operating with Afterburner ON

$V_{initial} = 0.9\ V_{max.}$

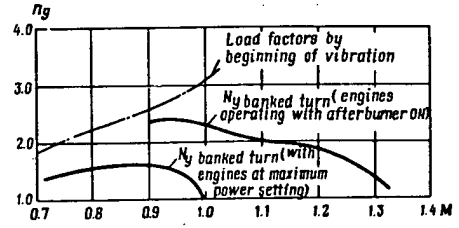

Fig. 77. Load Factors of Steady, Banked Turns

H=12.000 m.

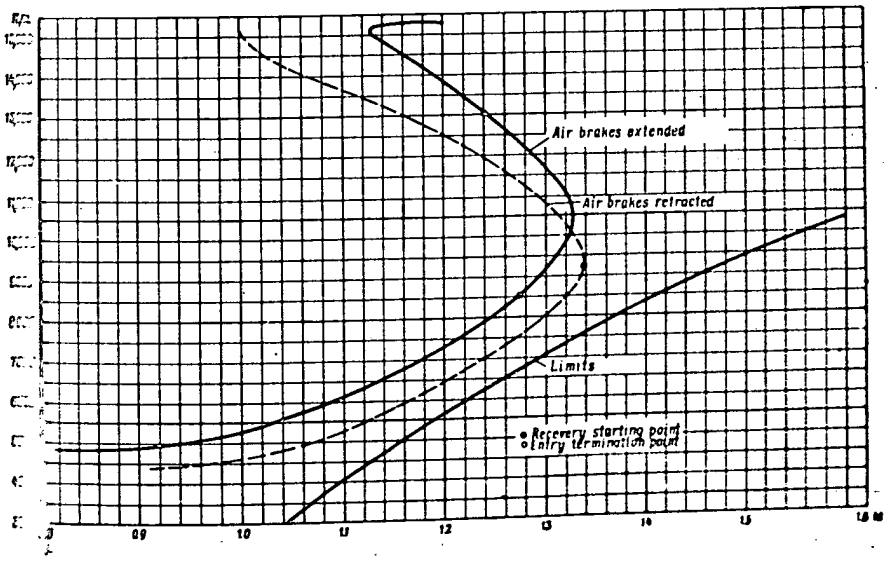

Fig. 78. Vertical Dives with Throttle OFF, Air Brakes Extended or Retracted

Declassified in Part - Sanitized Copy Approved for Release 2011/12/13 : CIA-RDP80T00246A062100050001-6

Declassified in Part - Sanitized Copy Approved for Release 2011/12/13 : CIA-RDP80T00246A062100050001-6

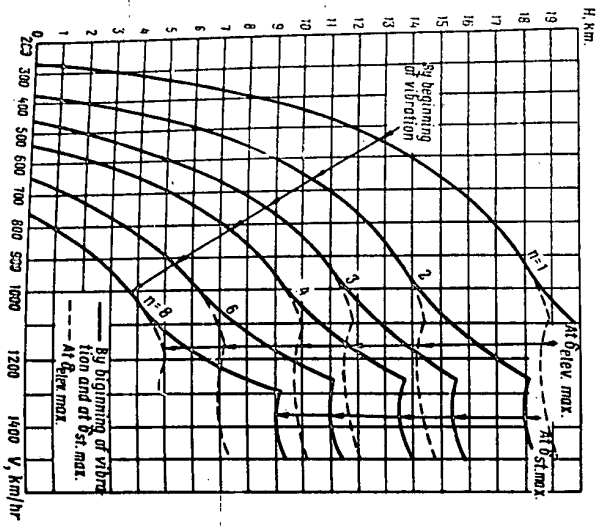

Fig. 79. Maximum Load Factors versus Flight Altitude and Airspeed (by beginning of vibration and at $\delta_{st,\ max.}$; $G_{average}$ = 6700 kg).

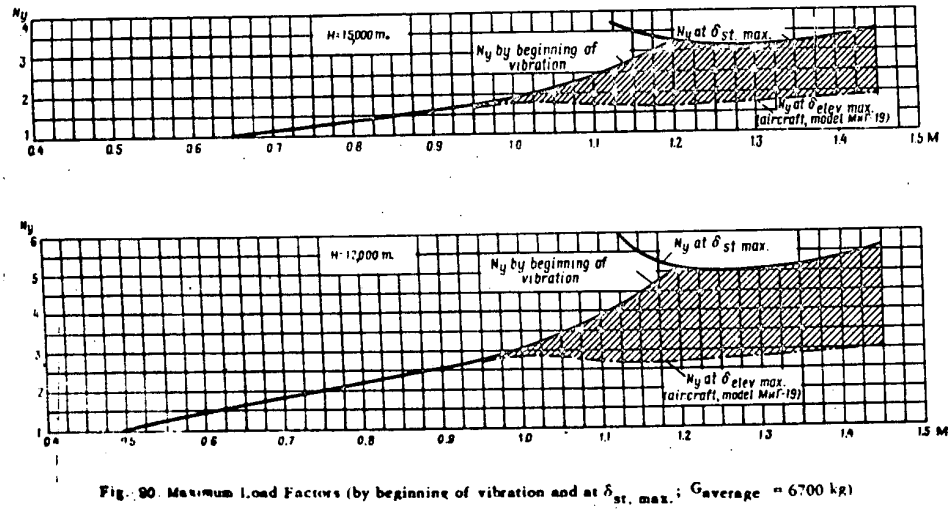
Ny
H=15,000 m.
Ny by beginning of vibration
Ny at δst. max.
Ny at δelev. max. (aircraft, model MwF-19)
H=12,000 m.
Ny by beginning of vibration
Ny at δst max.
Ny at δelev max. (aircraft, model MwF-19)

Fig. 80. Maximum Load Factors (by beginning of vibration and at $\delta_{st,\ max.}$; $G_{average}$ = 6700 kg)

Declassified in Part - Sanitized Copy Approved for Release 2011/12/13 : CIA-RDP80T00246A062100050001-6

Declassified in Part - Sanitized Copy Approved for Release 2011/12/13 : CIA-RDP80T00246A062100050001-6

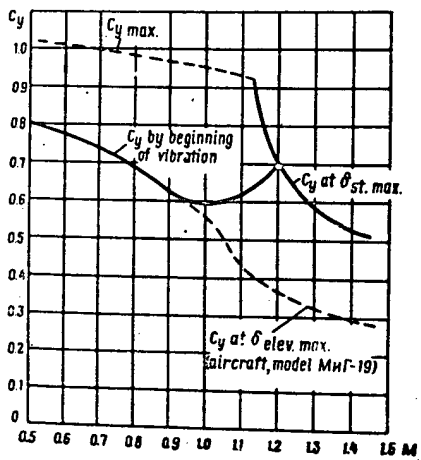

Fig. 81. Aircraft Lift Coefficient

Chapter V

AERODYNAMIC CHARACTERISTICS

The aircraft aerodynamic characteristics described below (Figs 82 - 94) are obtained by calculations based on the results of wind tunnel tests.

Note: The charts given in the figures correspond to the semidependent axes system (See Fig.154). Coefficient c_y is presented both in the charts and tables in its absolute value (the "-" sign has been dropped for convenience's sake).

1. Lift and Drag Coefficients

The aircraft lift and drag coefficients: curves $C_y = f(\alpha)$ and aircraft representative polar curves, i.e. $C_x = f(C_y)$ for different angles of flap deflection, with retracted and extended landing gear at H=0 and low airspeeds of flight (Mach number = 0.2) are presented in Figs 82 and 83.

The increase of the sweepback angle to $\chi = 55^\circ$ and decreased aspect ratio to $\lambda = 3.04$ in the МиГ-19С aircraft as compared with the МиГ-17 aircraft ($\chi = 45^\circ$ and $\lambda = 4.08$) to a certain extent changed the shape of the upper portion of lift $C_y = f(\alpha)$ curve (See Fig.83). Value $C_{y\ max}$ will not be obtained in practice with the МиГ-19С aircraft (at the tested angles of attack). Up to $\alpha = 12 - 15^\circ$ the dependence of $C_y = f(\alpha)$ is totally linear; with further increase of α in the range of 18 - 22° the increase of C_y is slowed down without reaching the maximum.

The increase of the wing sweepback angle shifts the maximum values of derivative C_y^α to the region of great Mach numbers and smoothes the derivative C_y^α curve passage through Mach numbers.

Dependence of aircraft coefficient $C_x = f(C_y)$ upon various Mach numbers (both engines operate, landing gear and flaps

Declassified in Part - Sanitized Copy Approved for Release 2011/12/13 : CIA-RDP80T00246A062100050001-6

Declassified in Part - Sanitized Copy Approved for Release 2011/12/13 : CIA-RDP80T00246A062100050001-6

retracted, flight altitude H = 5000 m.) is presented in Figs 84-86.

Value of C_x for altitudes other than 5000 m. may be determined from the formula:

$$C_{x_H} = C_{x_{H=5}} + \Delta C_{x_H}$$

For altitudes H = 0 - 10 km.:

$$\Delta C_{x_H} = k_H (H_{km} - 5);$$

for altitudes H = 10 -15 km.:

$$\Delta C_{x_H} = 0.00065 + k_H (H_{km} - 10)$$

H, km.	0-5	5-10	10-15
K_H	0.00011	0.00013	0.00025

Coefficient k_H is a correction to C_x value for every 1 km. altitude change.

Fig.85 shows that the noticeable increase of coefficient c_x begins from Mach number = 0.94.

Indicated in the chart by ΔC_x is an increase of the fuselage tail unit drag which is produced by decreased area of the jet nozzle(shutters are brought closer together)when the engines operate without afterburning.

Figs 87 and 88 show drag coefficients and thrust coefficient in level flight.

Aircraft lift-drag ratio $K_{l-d} = \frac{C_y}{C_x}$ is presented in Figs 89 and 90.

Maximum aircraft lift-drag ratio $K_{l-d\ max}$ with flaps retracted is equal to 11.4; this value, obtained at C_y = 0.3; Mach number = 0.3 and H=0 varies slightly within the zero-to-10,000 altitude range at Mach number = 0.4 - 0.6.

In level flight maximum lift-drag ratio $K_{l-d\ max}$ equals 10.7; the value is obtained at C_y = 0.3; Mach number $\approx$ 0.6 and H=0 and varies slightly within the zero-to-10,000 m. altitude range.

Influence of landing gear extension on the lift-drag ratio is shown in Fig.89.

Minimum aircraft drag coefficient $C_{x\ min.}$ equals 0.0152 at Mach number = 0.6 and C_y =0 at H=0.

Fig.91 presents the drag coefficient of the aircraft air brakes (related to the wing area) as function of Mach number.

Fig.92 presents the increment of the aircraft C_x as a result of attachment of two drop fuel tanks of 760-lit. capacity each.

At Mach numbers lower than 0.8 the drop fuel tanks increase aircraft coefficient C_x by ΔC_x = 0.0028; at Mach numbers higher than 0.8 the C_x value increases considerably.

Complete stoppage of the engines (autorotation condition of engines) increases the aircraft drag coefficient by ΔC_x = 2xC.0037.

Figs 93 and 94 show aircraft lift coefficient C_y as function of angles of attack at different Mach numbers.

2. Coefficients m_z, m_y, m_x and c_z [x/] of Moments and Lateral Forces

Fig.95 presents aircraft pitching moment coefficient m_z as function of the wing angle of attack with the flaps extended and retracted. Extension of the flaps causes the aircraft pitching.

Fig.96 shows aircraft pitching moment coefficient m_z as function of lift coefficient C_y at different Mach numbers.

With Mach number increase the aircraft stability considerably increases. Figs 97 and 98 present coefficient m_z as function of air brakes application and drop tanks attachment.

The air brakes and drop tanks produce an additional pitching moment. Fig.99 shows change of coefficient m_z versus 1° change of stabilizer setting angle at different Mach numbers, i.e. $m_z = f(M)$.

Note: The stabilizer setting angle is given parallel to the flight line; during the flight trials the angle was measured in the plane normal to the stabilizer rotation axis. Relation between these angles is expressed by the formula:

$$tg\varphi_{rel.to.flight\ line} = tg\varphi_{1\ rot.ax.} \cos\pi_{rot.ax.} = 0.611\ tg\varphi_{1\ rot.ax.}$$

x/ Graphs m_z, m_x, m_y and c_z are drawn up for dead engines conditions. With the engines operating, corrections should be introduced according to the formulas given in the text.

Declassified in Part - Sanitized Copy Approved for Release 2011/12/13 : CIA-RDP80T00246A062100050001-6

The graphs show that for all aircraft flight procedures and flight attitudes in the entire range of the operational angles of attack, stabilizer deflection angles, and Mach numbers the aircraft is stable and the stabilizer is effective.

Note: Some features of the aircraft attitude are dealt with in Chapter IV, Article 4 (Aircraft Controllability) and in the "Pilot's Instructions". The normal character of the pitching moments change (by α wing and Mach number) of the МиГ-19С aircraft wing flying in a wide range of Mach numbers (at subsonic, close-to-sonic and supersonic speeds) is ensured by the construction and configuration of the wing and horizontal empennage and, in particular, through provision of aerodynamic fences on the wing and specific elevation of the horizontal empennage relative to the wing.

Operation of the engines at n = 11,150 r.p.m. changes aircraft pitching moment coefficient m_z by the following rated value:

$$\Delta m_{z_{eng.}} = 2k \frac{P_{eng.}(1-\Delta\bar{P})}{\rho V_s^2} + 0.17 \frac{\alpha^\circ}{V_s} + 1.2 \times 10^{-6} V_s \alpha^\circ;$$

where: K = - 0.000873 with the landing gear down;
K = + 0.000053 with the landing gear up;
P - engine thrust, kg, according to Figs 114 and 115;
$\Delta\bar{P}$ - engine thrust losses, kg, according to Fig.117;
V_s - speed, m.p.s.;
ρ - air density;
α - angle of attack, in degrees.

Recalculation of pitching moment coefficient m_z for other aircraft C.G. position is done by the formula:

$$m_{z_2} = m_{z_1} + (\bar{X}_{C.G.2} - \bar{X}_{C.G.1}) C_y - (\bar{Y}_{C.G.2} - \bar{Y}_{C.G.1}) \times (C_x - C_y \frac{\alpha^\circ}{57.3});$$

$$\bar{y}_{C.G.} = \frac{y}{b_A}$$

Index "1" corresponds to the initial C.G. position given in the Graphs, and index "2" corresponds to the new aircraft C.G. position; this formula is sufficiently accurate for recalculation at angles of attack not greater than 15°.

Figs 100 - 108 present aircraft rolling and yawing moments coefficients m_x and m_y as functions of the angles of attack, slip angles, Mach numbers and amounts of ailerons application with the flaps retracted and extended. The graphs also show that the aircraft maintains its lateral stability and the ailerons and rudder are effective in the entire range of the angles of attack, control surfaces deflection and Mach numbers.

Operation of the engines at n = 11, 150 r.p.m. changes aircraft coefficient m_y by the following rated value:

$$\Delta m_{y\ eng.} = 0.058 \frac{\beta^\circ}{V_s} + 0.4 \times 10^{-6} V_s - \beta^\circ,$$

where: β is the aircraft slip angle in degrees.

Figs 109 and 110 present the coefficient of the aircraft lateral force and its derivative. Operation of the engines with n = 11,150 r.p.m. changes aircraft coefficient C_z by the following rated value:

$$\Delta C_{z\ eng.} = -0.1 \frac{\beta^\circ}{V_s} - 0.71 \times 10^{-6} V_s \beta^\circ.$$

Fig.111 shows the curve representing the aircraft Re number value as function of Mach numbers at H = 5000 m.

3. Required and Available Thrusts

Figs 112 and 113 show required and available thrusts of the aircraft, the data being obtained by aerodynamic calculation for the engines operating in the maximum power and afterburning conditions.

$$P_{required} = \frac{1}{2} C_x \rho S V_s^2; \quad P_{available} = 2 (P_{eng.} - P_{loss}),$$

where $P_{eng.}$ is the engine thrust;
P_{loss} is the engine power loss in the inlet and outlet ducts (See Fig.117).

The minimum thrust required for the level flight is about 650 kg at all altitudes.

Declassified in Part - Sanitized Copy Approved for Release 2011/12/13 : CIA-RDP80T00246A062100050001-6
Declassified in Part - Sanitized Copy Approved for Release 2011/12/13 : CIA-RDP80T00246A062100050001-6

Declassified in Part - Sanitized Copy Approved for Release 2011/12/13 : CIA-RDP80T00246A062100050001-6

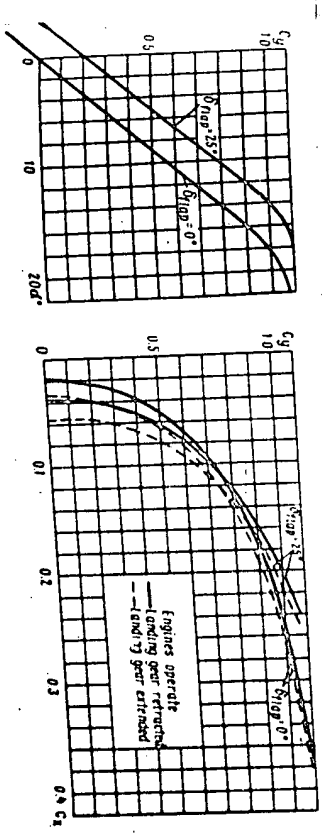

Fig. 83. Aircraft Representative Polar Curves
δ_{flap} = 15°; M=0.2; H=0.

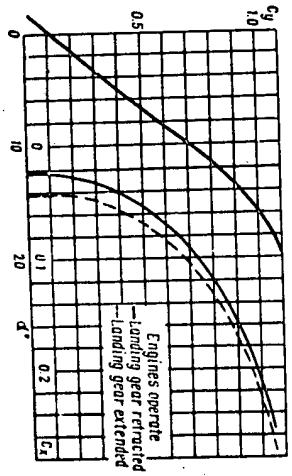

Fig. 82. Aircraft Representative Polar Curves
M=0.2; H=0.

Declassified in Part - Sanitized Copy Approved for Release 2011/12/13 : CIA-RDP80T00246A062100050001-6

Declassified in Part - Sanitized Copy Approved for Release 2011/12/13 : CIA-RDP80T00246A062100050001-6

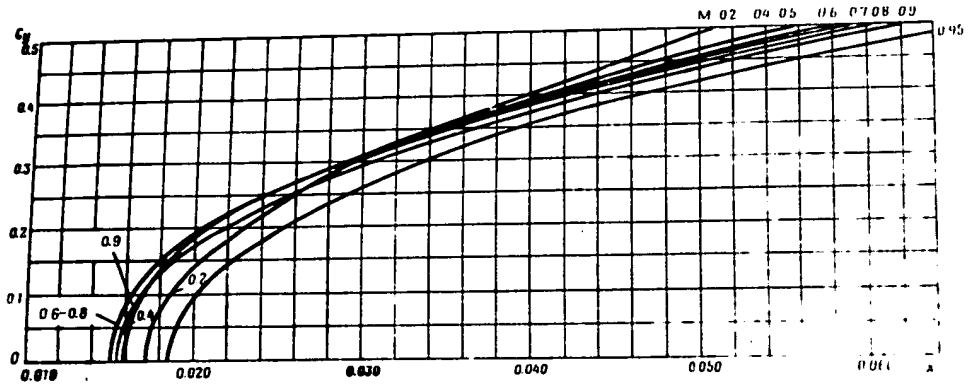

Fig. 84. Aircraft Representative Polar Curves
M≤ 0.95, H=5000 m.; $c_x = c_{x5} + \Delta c_{xH}$.

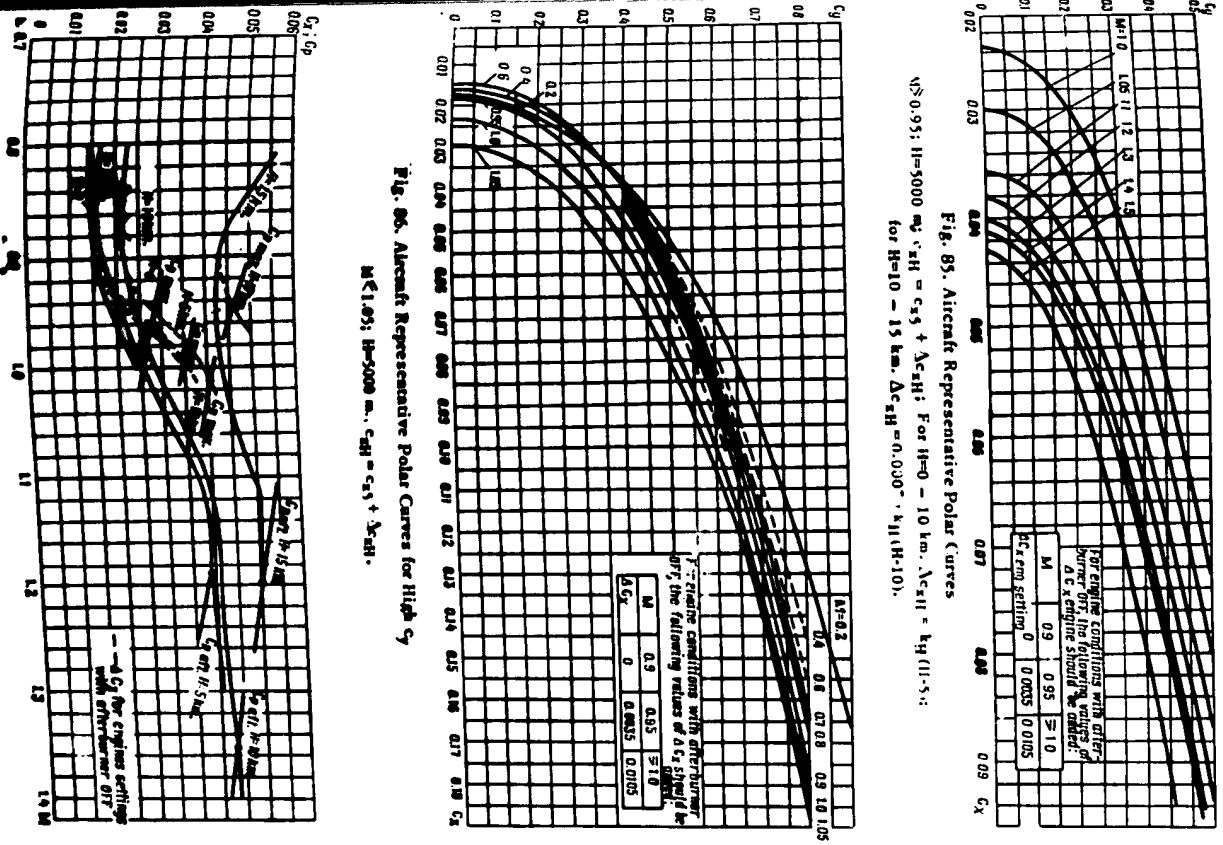

Fig. 85. Aircraft Representative Polar Curves
M≤0.95; H=5000 m; $c_{xH} = c_{x5} + \Delta c_{xH}$; For H=0 – 10 km. $\Delta c_{xH} = k_H(11-x_i)$;
for H=10 – 15 km. $\Delta c_{xH} = 0.0030 \cdot k_H(H-10)$.

Fig. 86. Aircraft Representative Polar Curves for High c_y
M≤1.05; H=5000 m.; $c_{xH} = c_{x5} + \Delta c_{xH}$.

Fig. 87. Drag and Trust Conditions in Level Flight

Declassified in Part - Sanitized Copy Approved for Release 2011/12/13 : CIA-RDP80T00246A062100050001-6

Declassified in Part - Sanitized Copy Approved for Release 2011/12/13 : CIA-RDP80T00246A062100050001-6

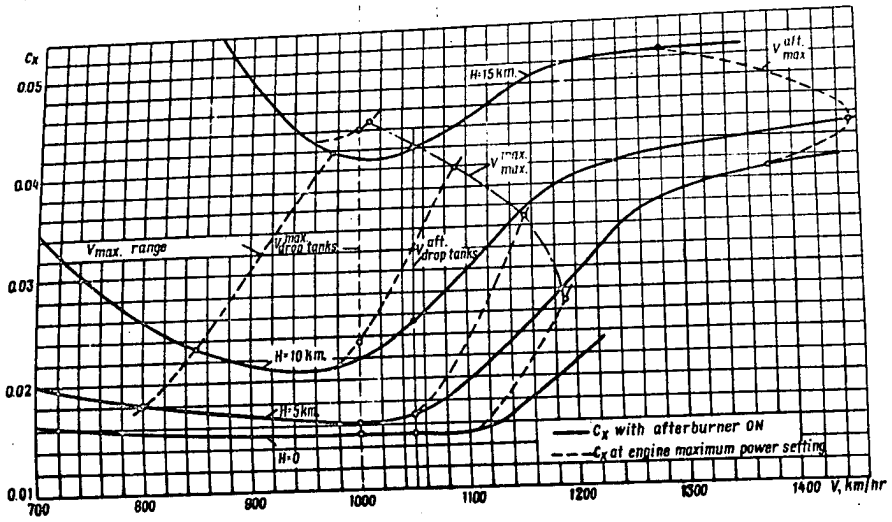

Fig. 88. Aircraft Rated Drag Coefficient in Level Flight

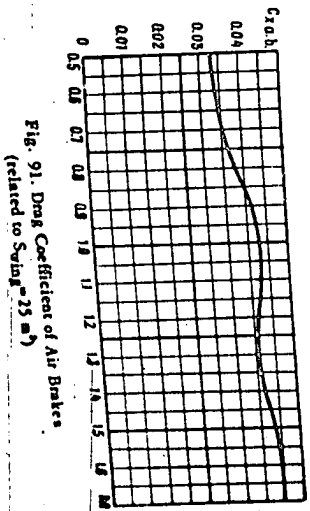

Fig. 91. Drag Coefficient of Air Brakes (related to Swing = 25 m²)

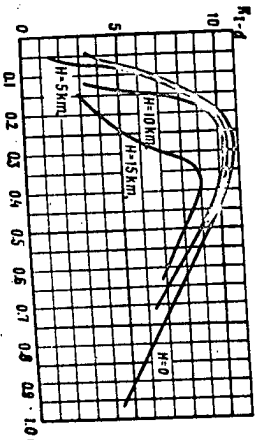

Fig. 90. Aircraft Lift-Drag Ratio in Level Flight

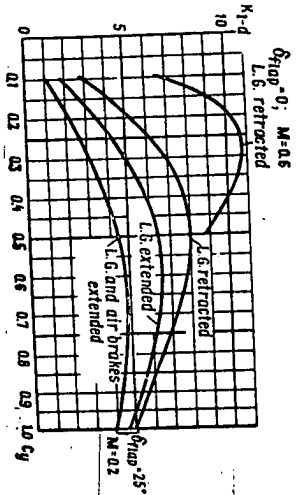

Fig. 89. Aircraft Lift-Drag Ratio at H=0

Declassified in Part - Sanitized Copy Approved for Release 2011/12/13 : CIA-RDP80T00246A062100050001-6

Declassified in Part - Sanitized Copy Approved for Release 2011/12/13 : CIA-RDP80T00246A062100050001-6

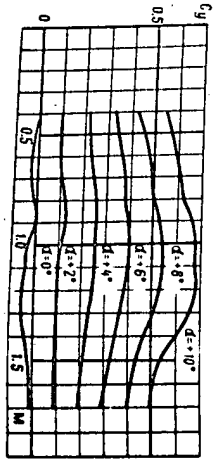

Fig. 93. Aircraft Lift Coefficient

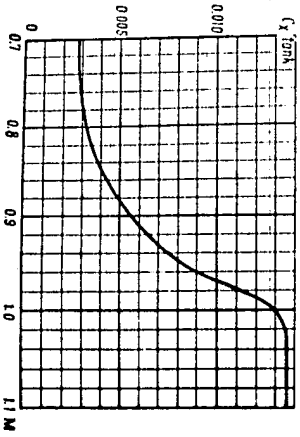

Fig. 92. Drag Coefficient of Drop Tanks, τ=2x760 lit. (related to S_{wing}= 25 m²)

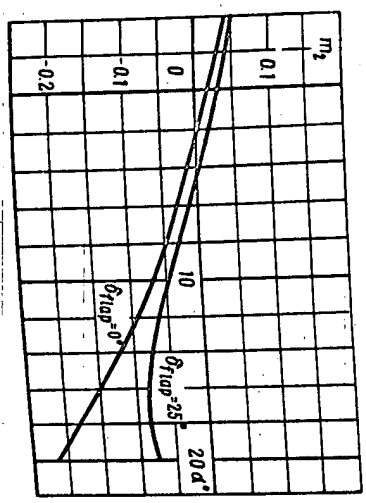

Fig. 95. Aircraft Pitching Moment Coefficient
C. G. position: $\bar{x}_G$ = 38% MAC; $\bar{z}_G$ =0; M=0.2;
Re = 13.55x10⁶; ϕ_{st} = 0°.

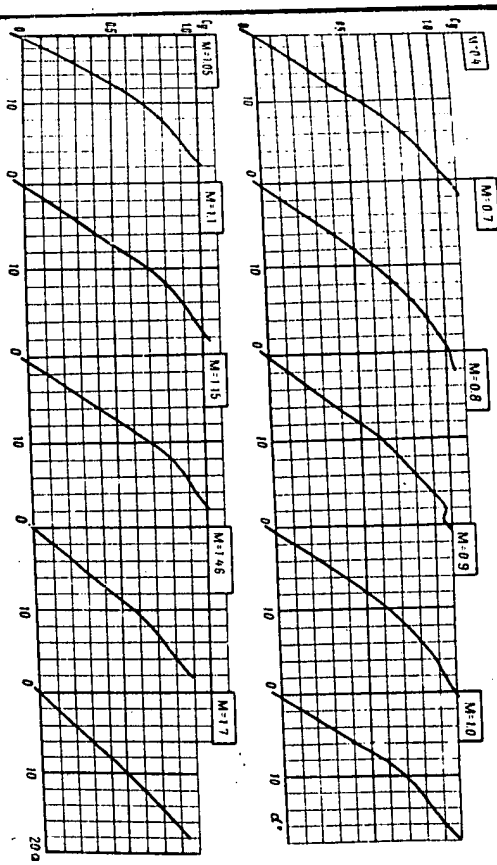

Fig. 94. Aircraft Lift Coefficient

Declassified in Part - Sanitized Copy Approved for Release 2011/12/13 : CIA-RDP80T00246A062100050001-6

Declassified in Part - Sanitized Copy Approved for Release 2011/12/13 : CIA-RDP80T00246A062100050001-6

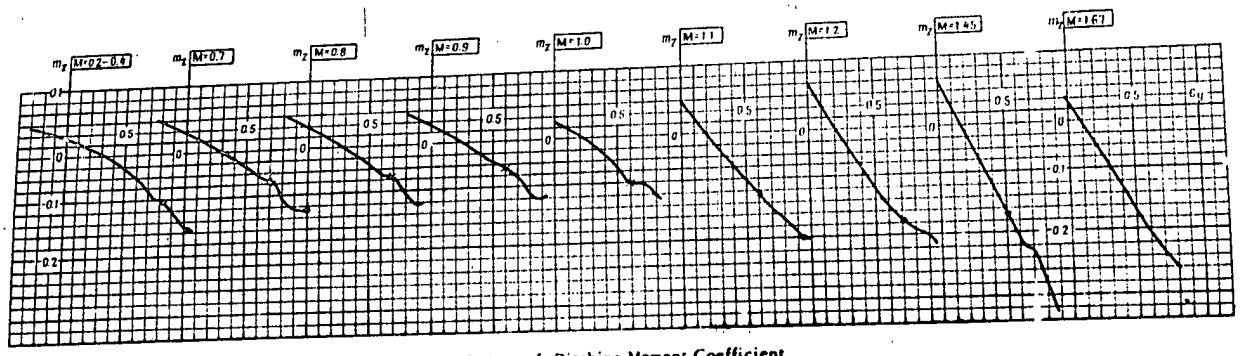

Fig. 96. Aircraft Pitching Moment Coefficient

$\delta_{flap} = 0°$; $\phi_{st} = 0°$; $\bar{x}_G = 48\%$ MAC

Note: Marks on the curves indicate c_y of typical conditions obtained in trials; mark × represents c_y of the beginning of warning vibration; mark 0 – c_y max. (uncontrolled roll); mark □ – c_y at stabilizer maximum deflection angle.

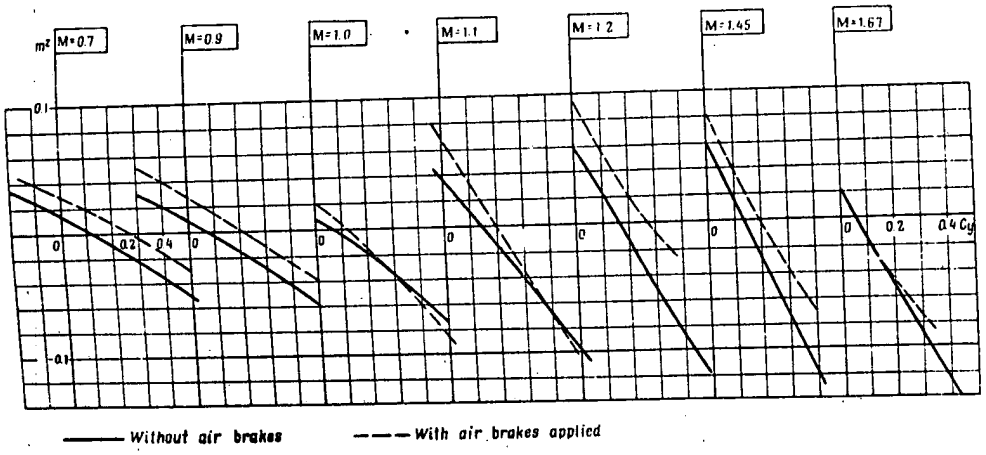

Fig. 97. Aircraft Pitching Moments as Function of Air Brakes Application

$2S_{a.b.} = 1.04\ m^2$ and $S_{a.b.} = 0.45\ m^2$; $\delta_{flap} = 0°$; $\phi_{st} = 0°$; $\bar{x}_G = 0.38$.

Declassified in Part - Sanitized Copy Approved for Release 2011/12/13 : CIA-RDP80T00246A062100050001-6

Declassified in Part - Sanitized Copy Approved for Release 2011/12/13 : CIA-RDP80T00246A062100050001-6

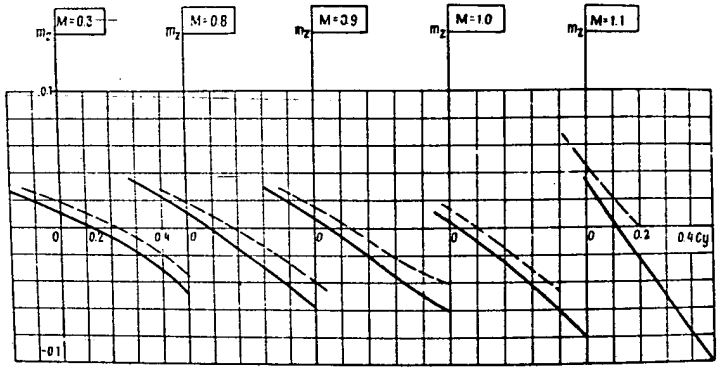

Fig. 98. Aircraft Pitching Moments as Function of Drop Tanks Attachment
$\delta_{flap} = 0°$; $\varphi_{st} = 0°$; $\bar{x}_G = 0.38$ MAC.

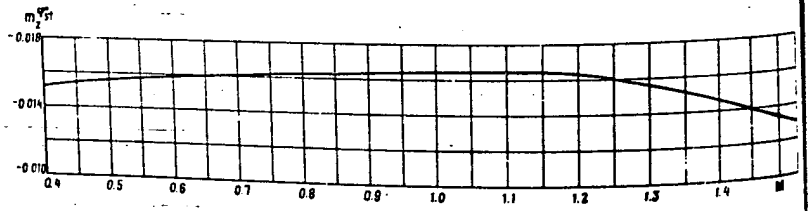

Fig. 99. Values of Aircraft Derivative $m_z^{\varphi_{st}}$
$\bar{x}_G = 38\%$ MAC; $\bar{y}_G = 0$; $\varphi = 0°$ (stabilizer angle relative to the line of flight).

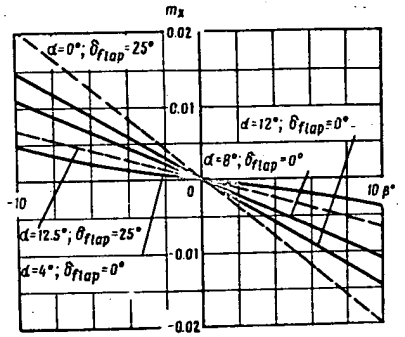

Fig. 100. Aircraft Rolling Moment Coefficients
Wing anhedral $\psi = -4°30'$; M = 0.2; Re = 2.0×10^6;
$\bar{x}_G = 38\%$ MAC; $\bar{y}_G = 0$; $\beta°$ – side slip angle.

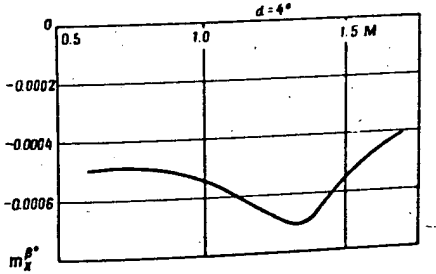

Fig. 101. Aircraft Rolling Moment Coefficient Derivative
$\bar{x}_G = 38\%$ MAC; $\bar{y}_G = 0$; $\varphi_{st} = -0°30'$; $\delta_R = 0°$;
$\delta_{flap} = 0°$; wing anhedral $\psi = -4°30'$.

Declassified in Part - Sanitized Copy Approved for Release 2011/12/13 : CIA-RDP80T00246A062100050001-6

Declassified in Part - Sanitized Copy Approved for Release 2011/12/13 : CIA-RDP80T00246A062100050001-6

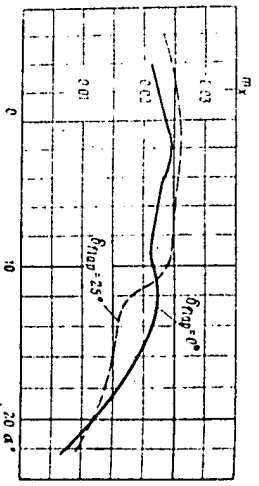

Fig. 102. Aircraft Rolling Moment Coefficient at Full Ailerons Deflection
$\delta_{aileron,\ left} = +20°$; $\delta_{aileron,\ right} = -20°$; $\bar{x}_G = 38\%$ MAC; $\bar{z}_G = 0$; M = 0.2; Re = 2.0×10^6

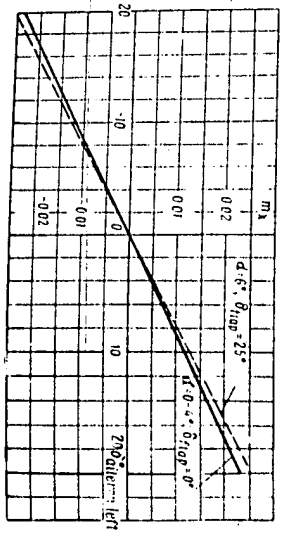

Fig. 103. Aircraft Rolling Moment Coefficient with Both Ailerons Applied
$\bar{x}_G = 38\%$ MAC; $\bar{z}_G = 0$; M=0; Re = 2.0×10^6.

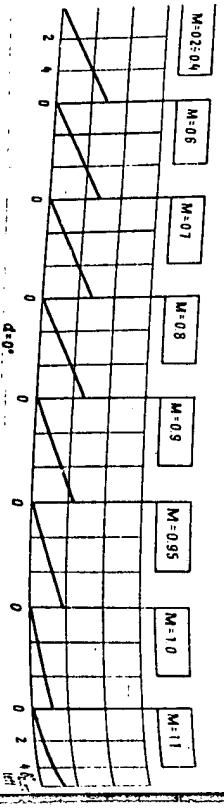

Fig. 104. Rolling Moment Coefficient with Ailerons Applied
$\bar{x}_G = 38\%$ MAC; $\bar{z}_G = 0$ (both ailerons applied).

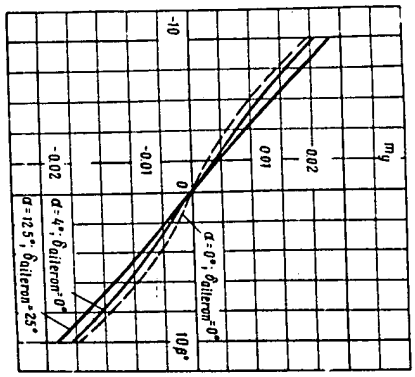

Fig. 105. Aircraft Yawing Moment Coefficient
$\bar{x}_G = 38\%$ MAC; $\bar{z}_G = 0$; M=0.2; Re=2.0×10^6;
$\beta°$ side slip angle.

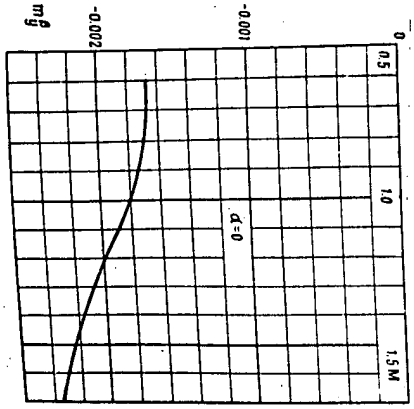

Fig. 106. Aircraft Yawing Moment Coefficient Derivative
$\bar{x}_G = 38\%$ MAC; $\bar{z}_G = 0$; $\delta_{flap} = 0°$; $\phi_{st} = 0°$.

Declassified in Part - Sanitized Copy Approved for Release 2011/12/13 : CIA-RDP80T00246A062100050001-6

Declassified in Part - Sanitized Copy Approved for Release 2011/12/13 : CIA-RDP80T00246A062100050001-6

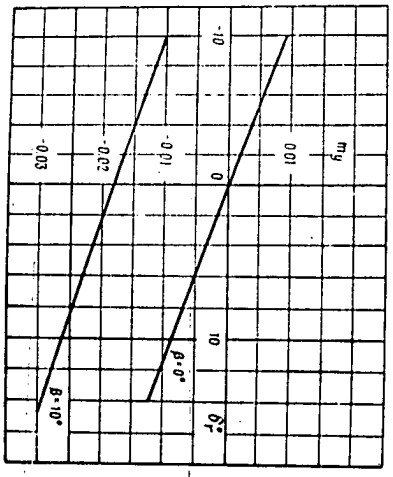

Fig. 107. Aircraft Yawing Moment Coefficient
$\bar{x}_G$ = 38% MAC; $\bar{y}_G$ = 0; M = 0.2; Re = 2.0×10^6; α = 8°; δ_{flap} = 0°.

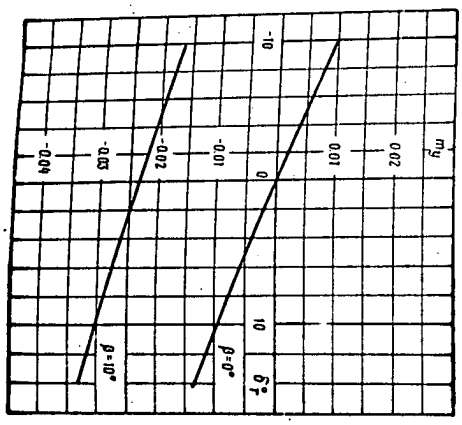

Fig. 108. Aircraft Yawing Moment Coefficient
$\bar{x}_G$ = 38% MAC; $\bar{y}_G$ = 0; M = 0.2; Re = 2.0×10^6; α = 12.5°; δ_{flap} = 25°.

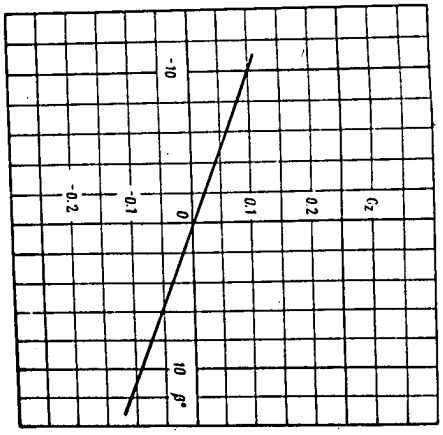

Fig. 109. Aircraft Lateral Force Coefficient
$\bar{x}_G$ = 38% MAC; δ_{flap} = 0°; M = 0.2; Re = 2.0×10^6;
α = 0–12°; δ_r = 0°; β° – side slip angle.

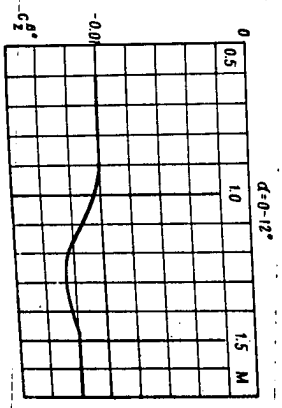

Fig. 110. Aircraft Lateral Force Coefficient Derivative
$\bar{x}_G$ = 38% MAC; $\bar{y}_G$ = 0; ϕ_{st} = 0°30'; δ_{flap} = 0°;
δ_r = 0°; β° – side slip angle.

Declassified in Part - Sanitized Copy Approved for Release 2011/12/13 : CIA-RDP80T00246A062100050001-6

Declassified in Part - Sanitized Copy Approved for Release 2011/12/13 : CIA-RDP80T00246A062100050001-6

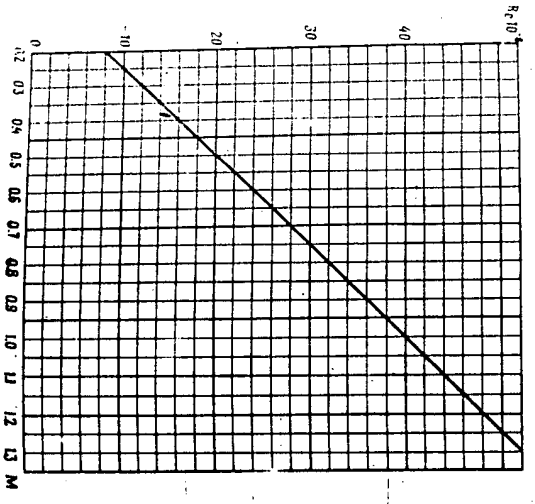

Fig. 111. Re Numbers of Flying Aircraft (H=5000 m.)

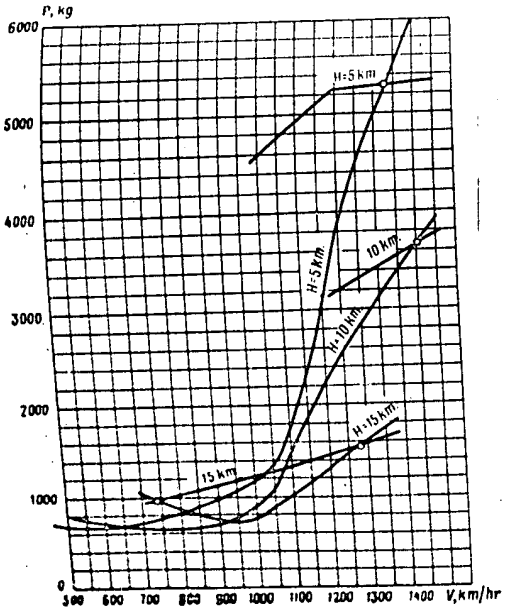

Fig. 112. Rated Available and Required Aircraft Thrust, Engines Operating with Afterburner ON

G_5 = 6880 kg; G_{10} = 6800 kg; G_{15} = 6660 kg.

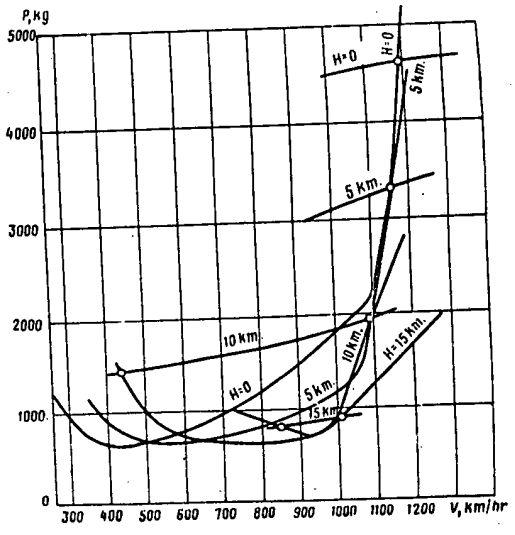

Fig. 113. Rated Available and Required Aircraft Thrust at Engine Maximum Power Setting

G_o = 6950 kg; G_5 = 6880 kg; G_{10} = 6800 kg; G_{15} = 6660 kg.

Declassified in Part - Sanitized Copy Approved for Release 2011/12/13 : CIA-RDP80T00246A062100050001-6

Declassified in Part - Sanitized Copy Approved for Release 2011/12/13 : CIA-RDP80T00246A062100050001-6

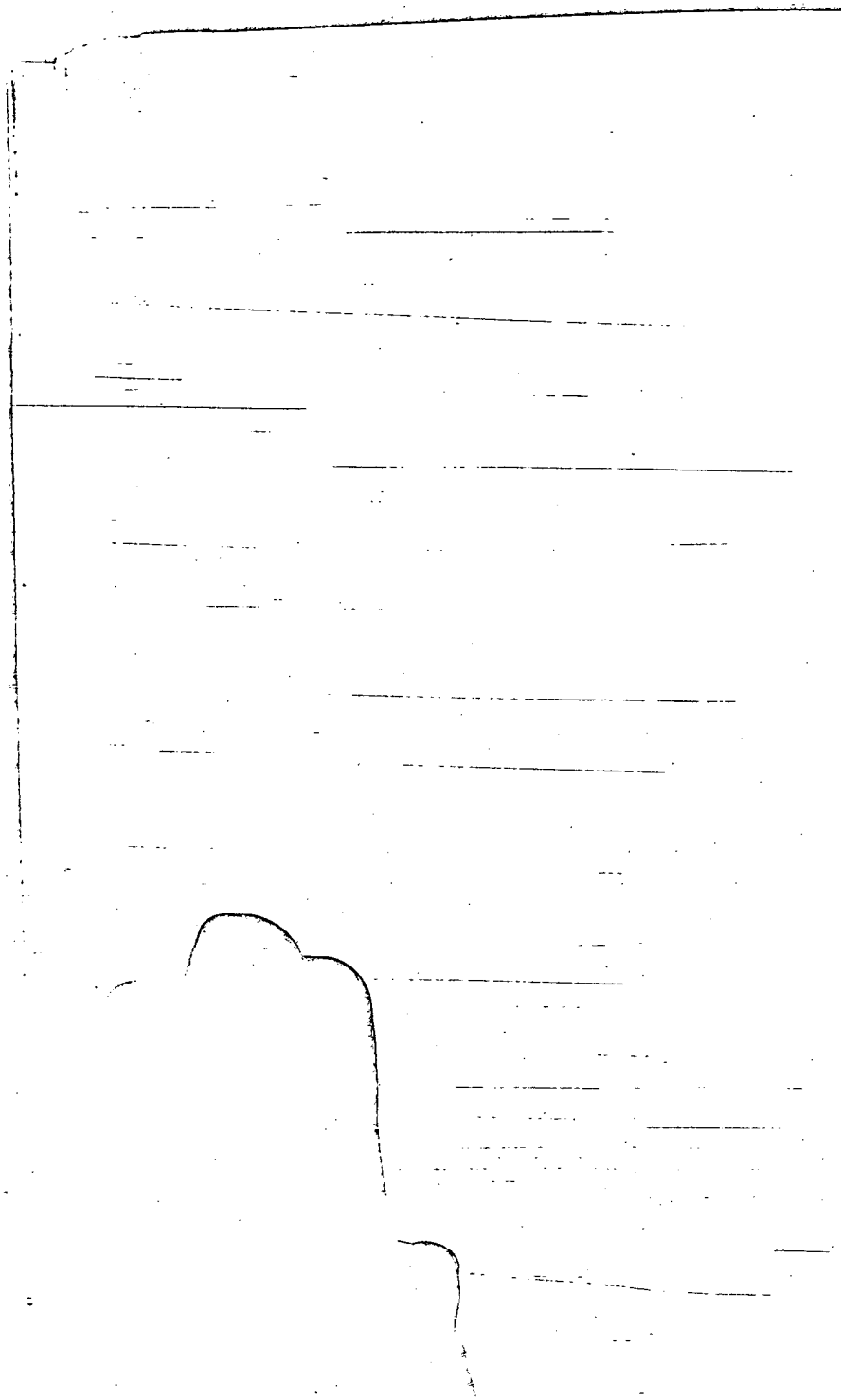

Chapter VI

ENGINE CHARACTERISTICS AND FUEL CONSUMPTION

Figs 114 - 116 and Table 15 present characteristics of the jet engine, type РД-9Б , assumed for aerodynamic calculations.

The engine maximum thrust is reached on the ground at V=0, and equals 2x2600 kg at the engine maximum power setting (at n = 11,150 r.p.m.) and 2x3250 kg with the afterburner ON (at n = 11,150 r.p.m.).

With the altitude increase the thrust sharply reduces, for instance, at the 10,000-m. altitude, at an airspeed of 700 km/hr it equals 2x1150 kg with afterburning and 2x900 kg at the engine maximum power setting.

The aircraft thrust also reduces with the decrease of the engine speed. The minimum engine thrust for 4100 r.p.m. at zero altitude equals 100 kg; with the altitude gain the engine minimum r.p.m. considerably increases.

Fig.117 presents thrust losses in the engine ducts.

Figs 118 - 121 show the engine r.p.m. as function of the level flight speed and altitude with/without drop fuel tanks (2x760 lit.) based on the endurance trials results.

The engine per hour fuel consumption (Figs 122 - 123) changes depending on the altitude, airspeed and r.p.m. (the consumption decreases with altitude increase and with the reduction of airspeed and r.p.m.).

Figs 124 - 129 present per hour throttle fuel flow in level flight without/with drop fuel tanks.

Specific fuel consumption at constant r.p.m. (Figs 130 - 131) also decreases with the altitude gain and airspeed reduction. Beginning with altitudes higher than 11,000 m. the specific fuel consumption is constant.

Absolute minimum specific fuel consumption ($C_{e.min}$) is obtai-

Declassified in Part - Sanitized Copy Approved for Release 2011/12/13 : CIA-RDP80T00246A062100050001-6

Declassified in Part - Sanitized Copy Approved for Release 2011/12/13 : CIA-RDP80T00246A062100050001-6

ed on the ground at n = 10,400 r.p.m. and is equal to 0.86 kg/kg of thrust per hour (See Fig.116). At 9600 - 9700 r.p.m. and lower the by-pass band opens the ports. With the by-pass band opened the engine parameters are somewhat reduced: specific fuel consumption is increased and thrust is decreased.

The aggregate time of the engines continuous operation at maximum Power setting and with afterburning should not exceed 6 minutes at altitudes up to 6000 m. and 10 minutes at altitudes over 6000 m.

After continuous operation of the engines at the maximum power setting or with afterburning during the time periods specified in Table 15 these operating conditions may be set up repeatedly only after the engine was cooled down at the normal or any lower power setting during not less than 1 minute.

Figs 132 - 134 present specific fuel consumption at different altitudes as function of Mach number and thrust.

The graphs given in the figures are used to determine the aircraft engine fuel consumption during flight range calculation before flight trials.

To determine fuel consumption at predetermined flight altitude and speed, it is necessary to estimate the required thrust and to add engine ducts thrust losses to the obtained value. The obtained sum is the throttle thrust of the engines. Half the value is the throttle thrust of one engine. By the thrust obtained from Figs 132 - 134 for the given flight altitude and speed, determine specific throttle fuel consumption C_e throttle.

From the obtained thrust and specific consumption, the required per hour throttle fuel flow(for both engines)will be:

$$2G_{throttle} = 2P_{throttle} \cdot C_e$$

Figs 135 - 140 present the level flight per km. fuel consumption as function of flight speed and altitude.

Characteristics of РД-9Б Engine in Standard Conditions
(State Trials Data)

Oporation conditions	r.p.m.	Stand thrust, kg	Per hour fuel consumption (on stand), kg	Specific fuel consumption on stand, kg/kg of thrust per hour	Allowable operation time, min.
Afterburning	11,150±50	3250	5200	1.6	6 min. at altitudes up to 6000 m.; 10 min. at altitudes above 6000 m.
Maximum power setting	11,150±50	2600	2420	0.93	6 min. at altitudes up to 6000 m.; 10 min. at altitudes over 6000 m.
Normal power setting	11,150±50	2150	1910	0.89	Unlimited
Low throttle on ground	4100^{+200}	Not over 100	Not over 300	-	10

Declassified in Part - Sanitized Copy Approved for Release 2011/12/13 : CIA-RDP80T00246A062100050001-6

Declassified in Part - Sanitized Copy Approved for Release 2011/12/13 : CIA-RDP80T00246A062100050001-6

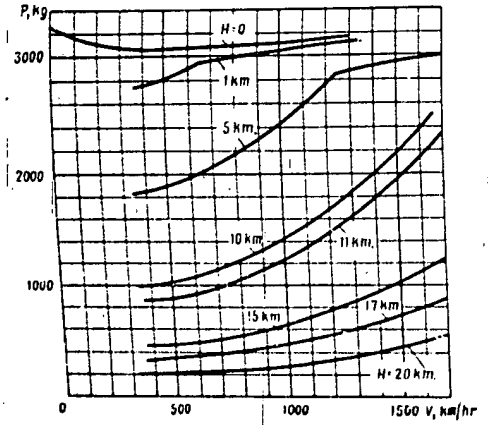

Fig. 114. Thrust of Engine, Type РД-9Б
(afterburner ON, n=11,150 r.p.m.)

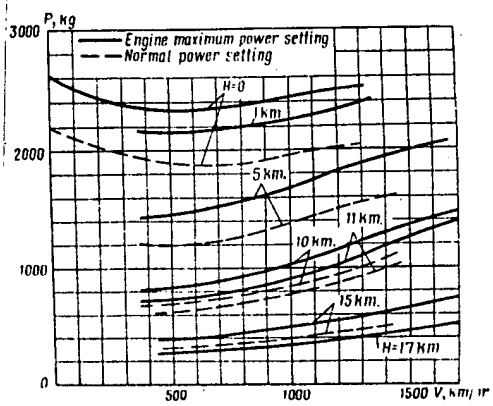

Fig. 115. Thrust of Engine, Type РД-9Б

Declassified in Part - Sanitized Copy Approved for Release 2011/12/13 : CIA-RDP80T00246A062100050001-6

Declassified in Part - Sanitized Copy Approved for Release 2011/12/13 : CIA-RDP80T00246A062100050001-6

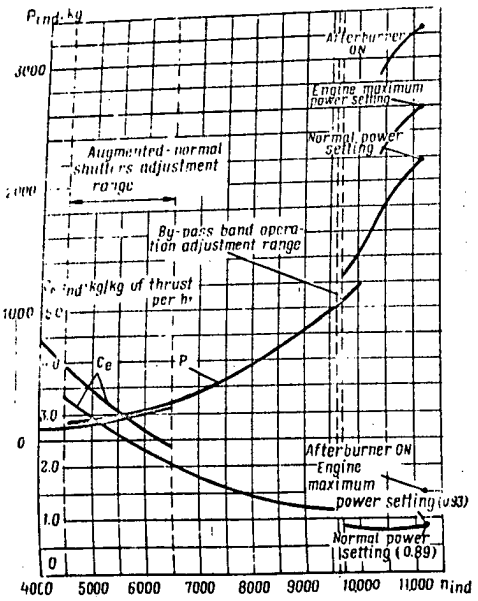

Fig. 116. РД-9Б Engine Stand Trials Characteristics

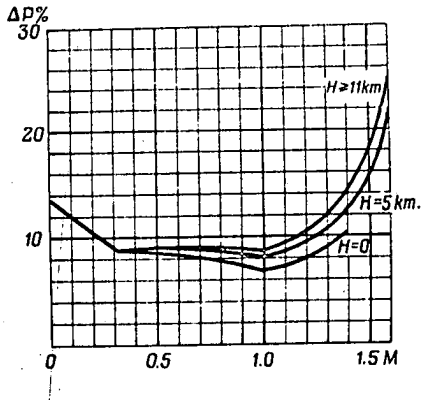

Fig. 117. Thrust Losses in РД-9Б Engine Ducts

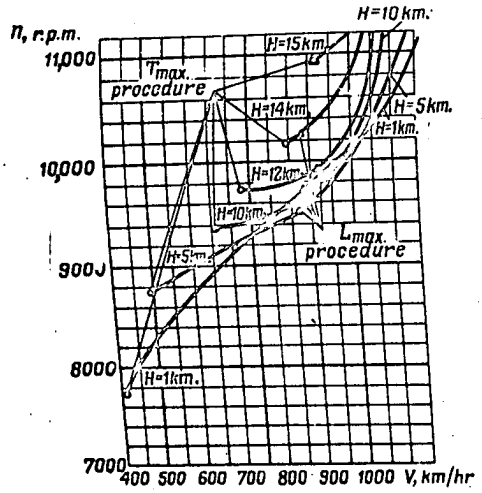

Fig. 118. Engine R.P.M. in Level Flight during Maximum Range Trials (for TAS)

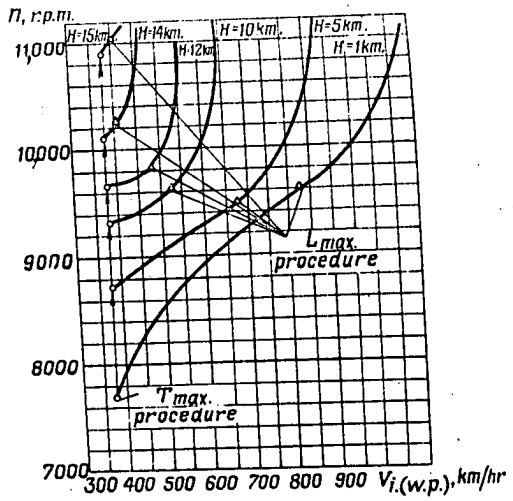

Fig. 119. Engine R.P.M. in Level Flight during Maximum Range Trials

Declassified in Part - Sanitized Copy Approved for Release 2011/12/13 : CIA-RDP80T00246A062100050001-6

Declassified in Part - Sanitized Copy Approved for Release 2011/12/13 : CIA-RDP80T00246A062100050001-6

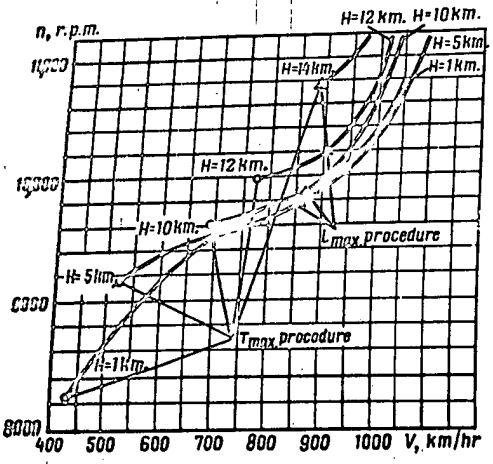

Fig. 120. Engine R.P.M. in Level Flight with Drop Tanks of 2x760 lit. Capacity, Fuelled with 995 kg (during maximum range trials)

1) n, r.p.m.; 2) L_{max} procedure; 3) T_{max} procedure; 4) V, km/hr.

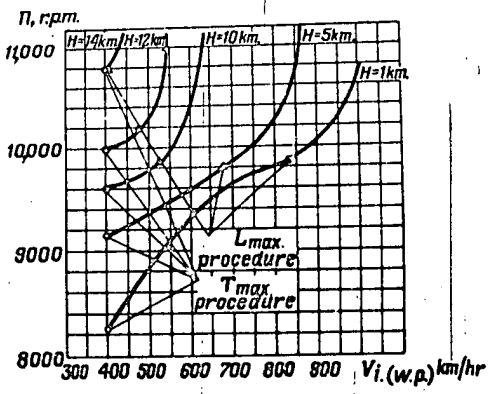

Fig. 121. Engine R.P.M. in Level Flight with Drop Tanks of 2x760 lit. Capacity, Fuelled with 995 kg (during maximum range trials)

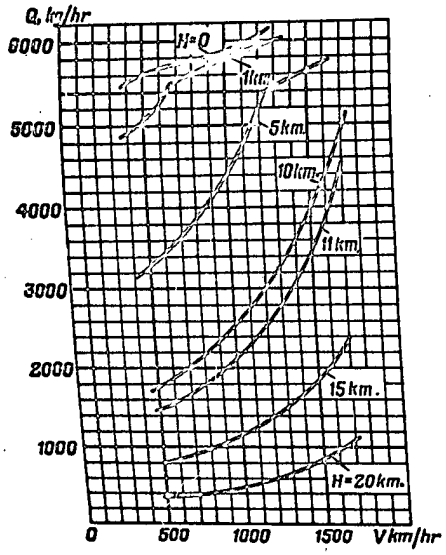

Fig. 122. Per Hour Fuel Consumptions of Engine, Type РД-9Б (with Afterburner ON)

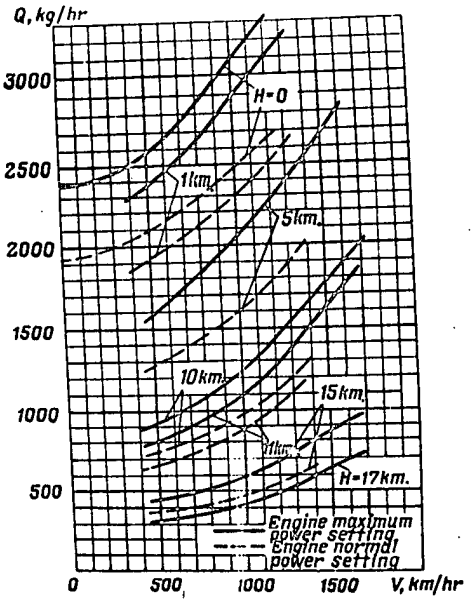

Fig. 123. Per Hour Fuel Consumptions of Engine, Type РД-9Б

Declassified in Part - Sanitized Copy Approved for Release 2011/12/13 : CIA-RDP80T00246A062100050001-6

Declassified in Part - Sanitized Copy Approved for Release 2011/12/13 : CIA-RDP80T00246A062100050001-6

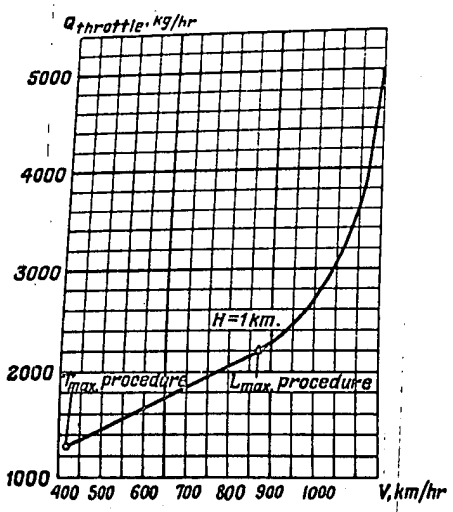

Fig. 124. Per Hour Throttle Fuel Flows in Level Flight without Drop Tanks

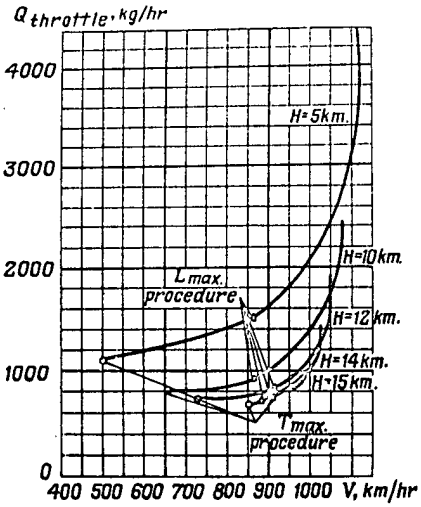

Fig. 125. Per Hour Throttle Fuel Flows in Level Flight without Drop Tanks

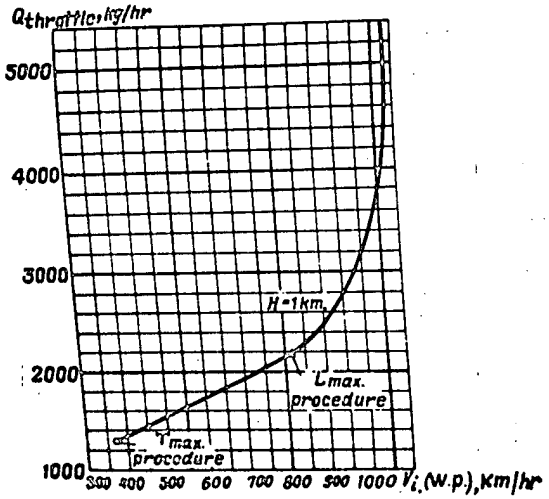

Fig. 126. Per Hour Throttle Fuel Flows in Level Flight without Drop Tanks

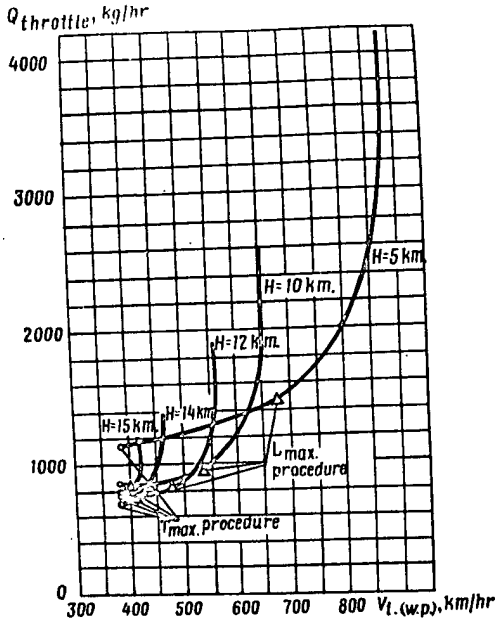

Fig. 127. Per Hour Throttle Fuel Flows in Level Flight without Drop Tanks

Declassified in Part - Sanitized Copy Approved for Release 2011/12/13 : CIA-RDP80T00246A062100050001-6

Declassified in Part - Sanitized Copy Approved for Release 2011/12/13 : CIA-RDP80T00246A062100050001-6

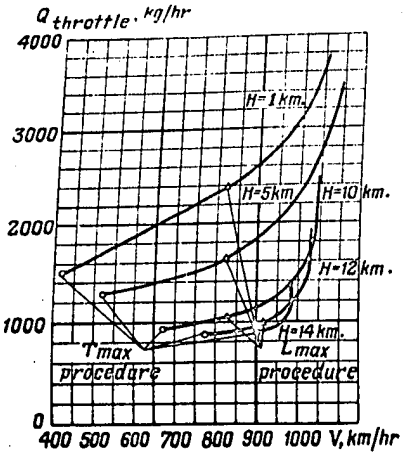

Fig. 128. Per Hour Throttle Fuel Flows in Level Flight with Drop Tanks, 2x760 lit.

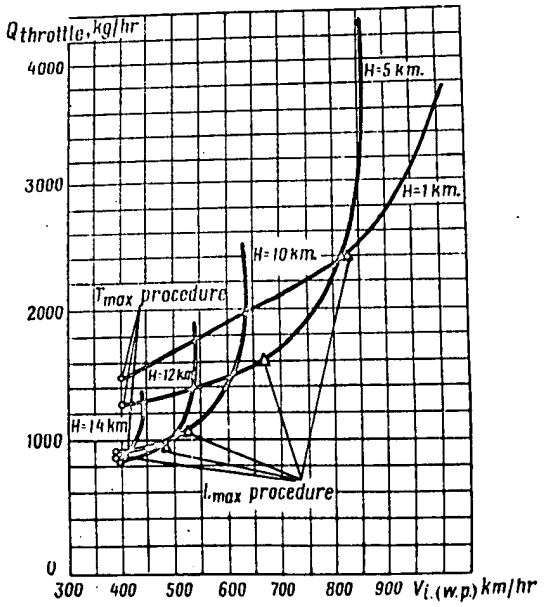

Fig. 129. Per Hour Throttle Fuel Flows in Level Flight with Drop Tanks, 2x760 lit.

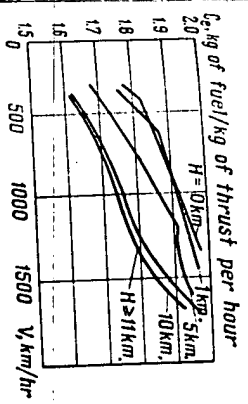

Fig. 130. Specific Fuel Consumptions of РД-95 Engine with Afterburning

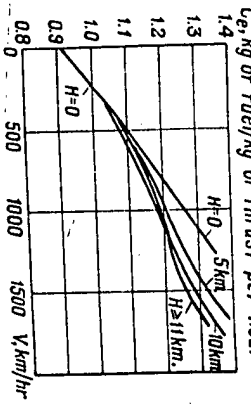

Fig. 131. Specific Fuel Consumptions of РД-95 Engine at Engine Maximum Power Setting

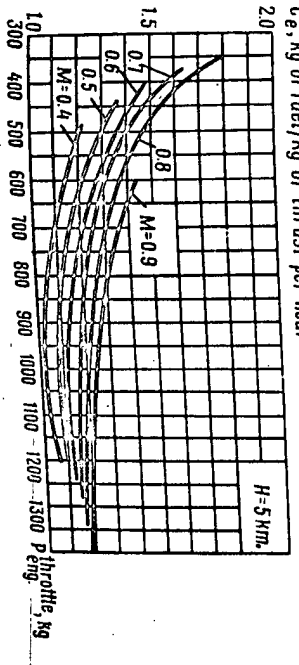

Fig. 132. Specific Fuel Consumptions of РД-95 Engine in Throttle Conditions

Declassified in Part - Sanitized Copy Approved for Release 2011/12/13 : CIA-RDP80T00246A062100050001-6

Declassified in Part - Sanitized Copy Approved for Release 2011/12/13 : CIA-RDP80T00246A062100050001-6

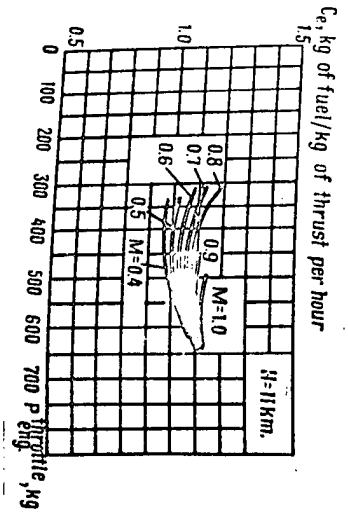

Fig. 134. Specific Fuel Consumptions of PD-9B Engine in Throttle Conditions

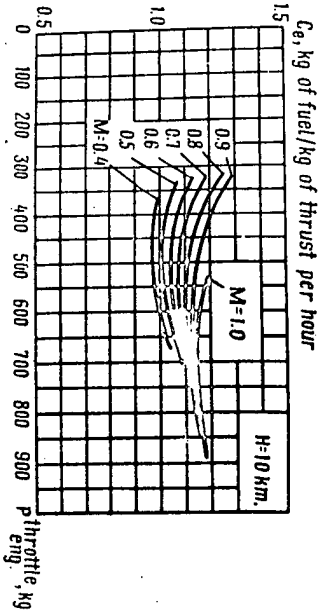

Fig. 133. Specific Fuel Consumptions of PD-9B Engine in Throttle Conditions

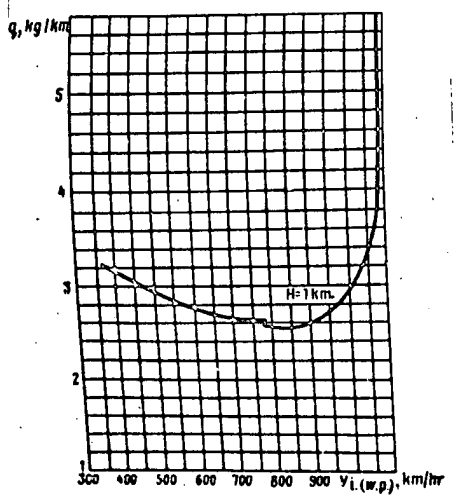

Fig. 135. Per Km. Fuel Consumption in Level Flight without Drop Tanks

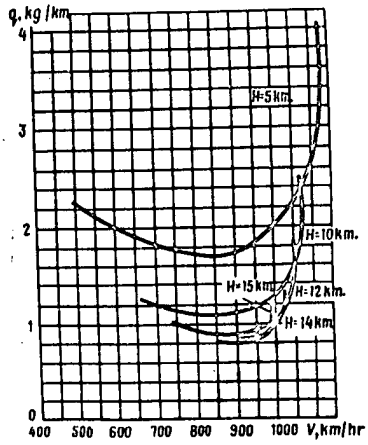

Fig. 136. Per Km. Fuel Consumption in Level Flight without Drop Tanks

Declassified in Part - Sanitized Copy Approved for Release 2011/12/13 : CIA-RDP80T00246A062100050001-6

Declassified in Part - Sanitized Copy Approved for Release 2011/12/13 : CIA-RDP80T00246A062100050001-6

Chapter VII

WEIGHT AND BALANCE DATA

Given below are weight and balance data for different configurations of the aircraft, model МиГ-19С , powered by two engines, type РД-9Б.

Fig.141 pictures the mean aerodynamic chord (MAC) location with indication of the position of balancing axes x and y.

Figs 142 - 144 present in-flight travel of the aircraft C.G. position (in per cent of MAC, along axis x) due to consumption of fuel and ammunition, at different a/c loadings.

Table 16 lists the weights of aircraft detachable parts and separate units incorporated in them. Table 17 contains a summary of the a/c C.G. position variants without special suspended loads. Table 19 presents summaries of overload variants of the aircraft C.G. positions.

Table 19 lists complete weight and balance data of the МиГ-19С aircraft for normal load conditions.

The aircraft C.G. position is estimated relative to coordinate axes x and y (Fig.145).

Axis x is the aircraft longitudinal axis and is found in the reference line plane.

Axis y is normal to axis x and passes in the vertical plane of frame No.15 centre line.

The intersection of axes x and y is the origin of the C.G. position coordinates of the aircraft and of separate items of its equipment.

The coordinates of units located at the aircraft tail along axis x and up of axis y have the plus sign, whereas those of the aircraft nose and down have the minus sign.

The aircraft C.G. positions presented in Tables 17 and 19 and Figs 142 - 144 are given in per cent of MAC relative to the MAC L.E. point.

Declassified in Part - Sanitized Copy Approved for Release 2011/12/13 : CIA-RDP80T00246A062100050001-6

Declassified in Part - Sanitized Copy Approved for Release 2011/12/13 : CIA-RDP80T00246A062100050001-6

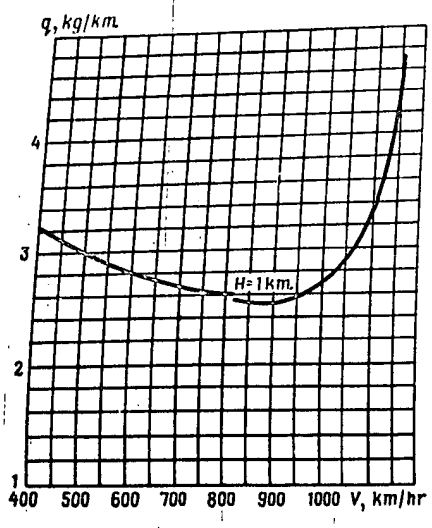

Fig. 137. Per Km. Fuel Consumption in Level Flight without Drop Tanks

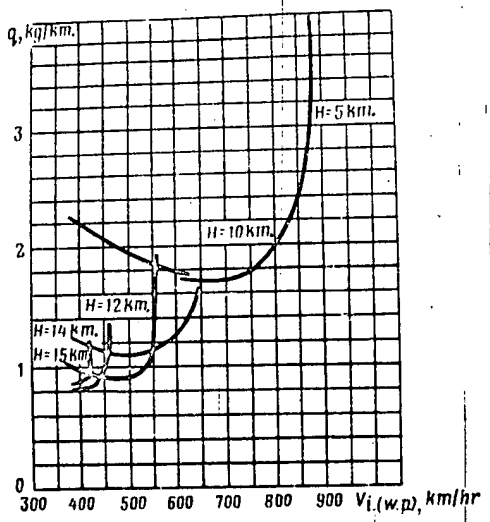

Fig. 138. Per Km. Fuel Consumption in Level Flight without Drop Tanks

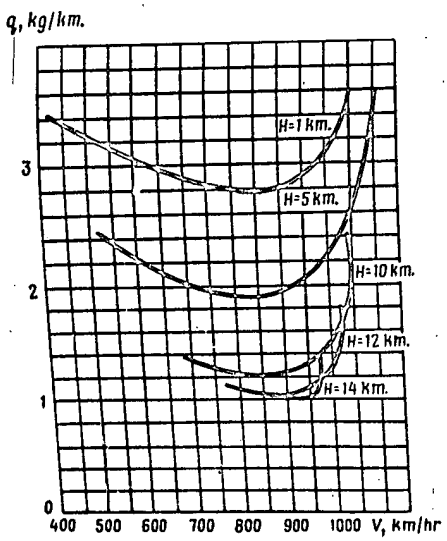

Fig. 139. Per Km. Fuel Consumption in Level Flight with Drop Tanks, 2x760 lit.

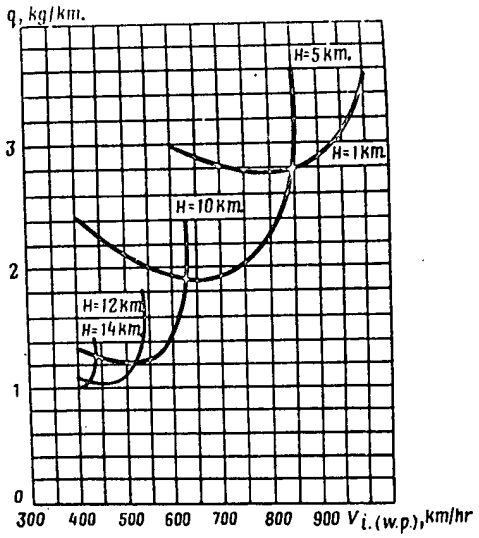

Fig. 140. Per Km. Fuel Consumption in Level Flight with Drop Tanks, 2x760 lit.

Declassified in Part - Sanitized Copy Approved for Release 2011/12/13 : CIA-RDP80T00246A062100050001-6

The coordinates of the aircraft C.G. position relative to axes x and y in per cent of MAC are determined in the following way:

(a) coordinate of the aircraft C.G. position in the direction of axis x, in per cent of MAC:

$$\frac{a + x_{c.g.}}{b_A} \times 100,$$

where: a = 0.770 m. – distance between MAC L.E. point and balancing axis y (See location of C.G. in Fig.141);

$x_{c.g.}$ – distance of the aircraft C.G. position from the coordinates origin, with the pertaining sign;

b_A = 3.023 m. – mean aerodynamic chord (MAC)

(b) coordinate of the aircraft C.G. position in the direction of axis y, in per cent of MAC:

$$\frac{b + y_{c.g.}}{b_A} \times 100,$$

where: b = 0.147 m. – distance between MAC and balancing axis x in the plane of axis y;

$y_{c.g.}$ – distance of the aircraft C.G. position from the coordinates origin, with the pertaining sign.

Given below is an example on recalculation of the aircraft C.G. position with respect to axes x and y for a new aircraft weight (which was changed due to removal or installation of an equipment item).

Example. Removed from the aircraft is the fuselage cannon with ammunition which was substituted by test instruments weighing 50 kg.

Using Table 19, draw up the following summary table (recalculate following methods illustrated in the example given below):

Description	P_x, kg-m	X, m.	P, kg	y, m.	P_y, kg-m
Aircraft with normal load	3114	0.412	7560	-0.035	-264
Removed from aircraft:					
1. Fuselage H-30 cannon	175	-2.55	-68.5	-0.50	34
2. Gas discharge tube	25	-3.53	-7.0	-0.50	4
3. Cannon attachment tube	21	-2.47	-8.5	-0.47	4
4. Ammunition for H-30 cannon, 60 rounds...	127	-2.27	-56.0	-0.39	22
Installed in aircraft:					
5. Test instruments...	-127	-2.55	50.0	-0.50	-25
To summarize:					
I. Aircraft with cannon, attachment units and ammunition removed and test instruments installed (landing gear extended)	3335	0.446	7470	-0.030	-225
II. Aircraft with cannon, attachment units and ammunition removed and test instruments installed (landing gear retracted).....	3090	0.414	7470	0.002	14
Aircraft equipped as indicated under Item I	3335	0.446	7470	-0.030	-225
Landing gear retraction	-245	-	0	-	239

Declassified in Part - Sanitized Copy Approved for Release 2011/12/13 : CIA-RDP80T00246A062100050001-6
Declassified in Part - Sanitized Copy Approved for Release 2011/12/13 : CIA-RDP80T00246A062100050001-6

The aircraft C.G. position relative to the wing MAC is determined as follows:

Landing gear down:

C.G. position relative to axis x:

$$\frac{a + x_{c.g.}}{b_A} \times 100 = \frac{0.770 + 0.446}{3.023} \times 100 = 40.2\% \text{ MAC};$$

C.G. position relative to axis y:

$$\frac{b + y_{c.g.}}{b_A} \times 100 = \frac{0.147 - 0.030}{3.023} \times 100 = 3.87\% \text{ MAC};$$

Landing gear up:

C.G. position relative to axis x:

$$\frac{a + x_{c.g.}}{b_A} \times 100 = \frac{0.770 + 0.414}{3.023} \times 100 = 39.2\% \text{ MAC};$$

C.G. position relative to axis y:

$$\frac{b + y_{c.g.}}{b_A} \times 100 = \frac{0.147 + 0.002}{3.023} \times 100 = 4.93\% \text{ MAC}.$$

Table 16

Weight of Aircraft Detachable Parts and Units Incorporated in Them

1. Fuselage nose section with controls, equipment, hydraulic system, armaments, canopy, ejection seat, landing gear nose leg, fuel system (without fuel) and armour	1744.3 kg
2. Fuselage tail section with vertical empennage, horizontal empennage, controls, equipment, hydraulic system and fuel system (without fuel)	769.5 kg
3. РД-9Б engines with afterburner, ejector and engine-mounted units (two engines)	1504.1 kg
4. Outer wings (2 wings) with controls, equipment, landing gear and two Н-30 cannon, without ammunition, hydraulic system included...	1371.8 kg
5. Canopy sliding section	40.2 kg
6. Ejection seat with armour	65.5 kg

Table 17

Engines

Variant No.	Load	Aircraft weight, kg	C.G. position along axis x, per cent of MAC		C.G. position along axis y, per cent of MAC	
			L.G. down	L.G. up	L.G. down	L.G. up
I - II	13	7560	39.2	38.0	3.71	4.70
III - IV	05	6652	39.6	38.4	3.37	4.56
V - VI	71	6018	42.1	40.8	3.84	5.16
VII - VIII	31	5878	43.5	42.1	4.24	5.60
IX - X	30	6507	38.6	37.3	3.77	5.00
XI - XII	14	5561	46.1	44.5	4.86	6.36

Declassified in Part - Sanitized Copy Approved for Release 2011/12/13 : CIA-RDP80T00246A062100050001-6
Declassified in Part - Sanitized Copy Approved for Release 2011/12/13 : CIA-RDP80T00246A062100050001-6

Declassified in Part - Sanitized Copy Approved for Release 2011/12/13 : CIA-RDP80T00246A062100050001-6

Table 17

Summary of C.G. Position Variants of МиГ-19С Aircraft with Two РД-9Б Engines
(without special suspended loads)

Variant No.	Description	Empty weight, kg	Load, kg												Aircraft weight, kg	C.G. position along axis x, per cent of MAC		C.G. position along axis y, per cent of MAC	
			Fuel, γ = 0.83					Pilot with parachute	Ammunition	Oil in system	De-icing fluid	Oxygen	Starting gas	Load		L.G. down	L.G. up	L.G. down	L.G. up
			Tank 1, v=1485 lit.	Tank 2, v=330 lit.	Tank 3, v = 180 lit.	Tank 4, v=175 lit.	Total fuel, lit.												
I - II	A/c with normal load	5447	1230	275	150	145	1800	100	187	14.5	5	2	4.5	2113	7560	39.2	38.0	3.71	4.70
III - IV	A/c with 50% of fuel stock	5447	755	70	38	37	900	100	187	10	3	2	3	1205	6652	39.6	38.4	3.37	4.56
V - VI	A/c with 20% of fuel and 50% of ammunition	5447	360	-	-	-	360	100	93	10	3	2	3	571	6018	42.1	40.8	3.84	5.16
VII - VIII	A/c with 7% of fuel	5447	126	-	-	-	126	100	187	10	3	2	3	431	5878	43.5	42.1	4.24	5.60
IX - X	Maximum forward C.G. position	5447	755	-	-	-	755	100	187	10	3	2	3	1060	6507	38.6	37.3	3.77	5.00
XI - XII	Maximum rearward C.G. position	5447	-	-	-	-	-	100	-	14	-	-	-	114	5561	45.1	44.5	4.86	6.36

Declassified in Part - Sanitized Copy Approved for Release 2011/12/13 : CIA-RDP80T00246A062100050001-6

Declassified in Part - Sanitized Copy Approved for Release 2011/12/13 : CIA-RDP80T00246A062100050001-6

Table 18

Summary of C.G. Position Overload Variants of МиГ-19С Aircraft with Two РД-9Б Engines
(with drop tanks and rockets on beam)

Variant No.	Description	Aircraft empty weight, kg	Load, kg																C.G. position along axis x, per cent of MAC		C.G. position along axis y, per cent of MAC	
			Fuel, γ = 0.83						Drop tanks, v=2x760 lit.	Pilot with parachute	Overload: 16 rockets on beam	Ammunition	Oil	De-icing fluid	Oxygen	Starting gas	Load	Aircraft weight, kg				
			Tank 1, v=1485 lit.	Tank 2, v=330 lit.	Tank 3, v=180 lit.	Tank 4, v=175 lit.	Drop tanks, v=2x600 lit.	Total fuel, lit.											L.G. down	L.G. up	L.G. down	L.G. up
I - II	Aircraft with drop tanks, v = 2x760 lit., primed with 600 lit. of fuel each	5447	1230	275	150	145	996	2796	106	100	-	187	14.5	5	2	4.5	3215	8662	42.5	41.5	0.60	1.55
III - IV	Aircraft with overload of 16 rockets on beam and with 600 lit. of fuel in each 760-lit. capacity tank . . .	5447	1230	275	150	145	996	2796	106	100	170	187	14.5	5	2	4.5	3385	8832	43.1	42.1	0.33	1.19
V - VI	Aircraft with 50% of fuel, with 16 rockets on beam and ammunition	5447	755	70	38	37	-	900	106	100	170	187	10	3	2	3	1481	6928	40.8	39.6	2.61	3.74
VII - VIII	Aircraft with 20% of fuel and 50% of ammunition	5447	360	-	-	-	-	360	106	100	170	93	10	3	2	3	847	6294	43.4	42.1	2.98	4.24
IX - X	Maximum forward C.G. position	5447	755	-	-	-	-	755	106	100	109	187	10	3	2	3	1275	6722	39.6	38.3	3.21	4.40
XI - XII	Maximum rearward C.G. position	5447	-	-	-	-	-	-	106	100	170	-	14	-	-	-	390	5837	47.1	45.6	3.91	5.26

Declassified in Part - Sanitized Copy Approved for Release 2011/12/13 : CIA-RDP80T00246A062100050001-6

Declassified in Part - Sanitized Copy Approved for Release 2011/12/13 : CIA-RDP80T00246A062100050001-6

Table 16 (continued)

7. N-30 cannon (3 cannon)	205.5 kg
8. Main landing gear struts with wheels (two struts)	217.6 kg
9. Nose landing gear strut with wheel (one strut)	65.2 kg
10. Horizontal empennage (with beam), 2 units	145.7 kg
11. Vertical empennage (without fin fillets) with tail warning station, type SYRENA-2 (SIPENA-2)	94.2 kg
12. Rudder with loads	19.0 kg

Declassified in Part - Sanitized Copy Approved for Release 2011/12/13 : CIA-RDP80T00246A062100050001-6

Declassified in Part - Sanitized Copy Approved for Release 2011/12/13 : CIA-RDP80T00246A062100050001-6

Table 19

Weight and Balance Summary Data of МиГ-19С
Aircraft with Normal Load

Description	$P_{x_{c.g.}}$ kg-m	$X_{c.g.}$ m.	P kg	$y_{c.g.}$ m.	$P_{y_{c.g.}}$ kg-m
1	2	3	4	5	6
Aircraft with normal load, landing gear DOWN	3114	0.412	7560	-0.035	-264
Aircraft empty weight	3701	0.681	5447	-0.007	-38
Normal load	-587	-0.28	2113	-0.11	-226
NORMAL LOAD	-587	-0.28	2113	-0.11	-226
Pilot with parachute	-251	-2.51	100	0.35	35
Ammunition for wing H-30 cannon, 70x2 rounds	13	0.10	131	-0.17	-22
Ammunition for fuselage H-30 cannon, 60 rounds	-127	-2.27	56	-0.39	-22
Fuel in:					
Tank 1	-1218	-0.99	1230	0.028	0
Tank 2	186	0.676	275	-0.47	-129
Tank 3	341	2.27	150	-0.459	-69
Tank 4	489	3.377	145	-0.431	-62
Oil in system	14	0.95	14.5	0.31	5
Starting gas	-2	-0.40	4.5	0.56	3
De-icing fluid	-25	-4.98	5	-	-
Oxygen	-7	-3.40	2	0.18	-
AIRCRAFT EMPTY WEIGHT	3701	0.681	5447	-0.007	-37
Airframe	2522	0.90	2811	-0.06	-158
Power units	2984	1.79	1669	0.04	61
Equipment	-986	-1.81	545	0.10	54
Armaments	-605	-1.78	340	-0.12	-41
Armour	-214	-2.61	82	0.57	47
AIRFRAME	2522	0.90	2811	-0.06	-158

1	2	3	4	5	6
Fuselage	534	0.57	938	-0.01	-8
Canopy	-141	-2.28	62	0.69	43
Pilot's seat	-121	-2.33	52	0.33	17
Wing	768	0.95	806	-0.15	-122
Empennage	1314	5.39	244	0.68	166
Controls	194	1.26	154	0.25	38
Landing gear	-73	-0.21	356	0.88	-312
Pneudraulic system	93	0.49	190	0.13	24
Air-speed tube in fuselage	-46	-5.16	9	-0.42	-4
FUSELAGE	534	0.57	938,0	-0.01	-8
Fuselage nose section	-628	-1.05	598.1	-	-
Bird air brake	-5	-0.57	8.3	-0.70	-6
Fuselage tail section	1118	3.60	310.0	0.02	6
Air brakes	49	2.26	21.6	0.36	-8
CANOPY	-141	-2.28	62.0	0.69	43
Windshield without transparent screen	-28	-3.11	8.9	0.75	7
Canopy sliding section, δ = 10 mm	-87	-2.17	40.2	0.71	28
Tracks (rails) with locks	-11	-2.17	4.9	0.58	3
Canopy emergency jettison system	-7	-2.10	3.5	0.62	2
Canopy pressurization system	-5	-1.88	2.9	0.81	2
Right flight curtains	-	-2.40	0.1	0.60	-
Canopy parts	-1	-2.17	0.6	0.70	-
Canopy antidim system	-2	-2.00	0.9	0.81	1
PILOT'S EJECTION SEAT	121	-2.33	52.0	0.33	17
Ejection seat	-92	-2.37	38.8	0.35	14
Ejection gun in duralumin case	-17	-2.17	8.0	0.30	2
Seat tracks & guide rails	-9	-2.20	3.9	0.25	1

Declassified in Part - Sanitized Copy Approved for Release 2011/12/13 : CIA-RDP80T00246A062100050001-6

Declassified in Part - Sanitized Copy Approved for Release 2011/12/13 : CIA-RDP80T00246A062100050001-6

1	2	3	4	5	6
Attachment fittings ..	-3	-2.20	1.3	0.25	-
WING	768	0.95	806.0	-0.15	-122
Frame	548	0.795	689.0	-0.15	-103
Flap	64	1.52	42.2	-0.13	-5
Aileron without load ..	84	3.34	25.3	-0.27	-7
Aileron load	54	3.27	16.5	-0.24	-4
Wing attachment fittings	-1	-0.06	14.7	-0.06	-1
Wing fillets	-	-0.02	6.0	-0.06	-
Fences	19	1.58	12.2	-0.14	-2
Miscellaneous	-	-	0.1	-	-
EMPENNAGE	1314	5.39	244.0	0.68	166
Fin	369	5.33	69.2	1.13	79
Rudder without balancing load	87	6.52	13.4	1.23	17
Rudder bottom load ...	18	6.73	2.6	1.58	4
Rudder top load	22	7.22	3.0	2.09	6
Fin fillets	28	3.93	7.0	0.81	6
Stabilizer	415	5.56	74.5	0.34	25
Stabilizer beams with bearings	232	4.49	51.5	0.40	21
Stabilizer balancing loads	127	6.44	19.7	0.34	7
Stabilizer attachment fittings	13	4.92	2.6	0.37	1
Various parts	3	5.55	0.5	0.40	-
CONTROLS	194	1.26	154.0	0.25	38
Controls in cockpit ..	-58	-2.53	23.0	0.29	7
Controls in fuselage nose section	-2	-0.24	8.0	0.64	5
Controls in fuselage tail section	18	2.70	6.5	0.56	4
Booster	29	3.87	7.6	0.66	5
Booster attachment fittings	7	3.87	1.8	0.66	1

1	2	3	4	5	6
Rudder controls in fin	6	5.30	1.2	0.52	1
ACII-4 electric actuator	45	3.91	11.6	0.90	12
Electric actuator attachment fittings..	-	4.25	0.1	0.86	-
ДР-5 loading mechanism	5	3.21	1.6	0.72	1
Trimming effect electric mechanism of APУ-2 automatic boost unit	2	3.31	0.6	0.75	-
Control units attachment fittings	5	3.20	1.6	0.73	1
Stabilizer actuating bell crank	14	2.95	4.7	0.59	3
Bell cranks attachment fitting	10	3.24	3.0	0.68	2
Bell cranks attachment fitting with loads...	17	4.15	4.2	0.43	2
Aileron controls in wing	12	4.15	3.0	0.43	1
Aileron booster	14	2.63	5.3	0.67	4
Aileron attachment fittings	33	1.24	26.5	-0.17	-4
Flaps actuating jacks..	-5	-1.44	3.2	-0.09	-
Jack attachment fitting	-7	-1.44	4.9	-0.09	-
Limit switch for flap...	8	0.90	8.6	-0.14	-1
Aileron trim tab controls	-	0.90	0.2	-0.14	-
Air brakes actuating jacks	1	0.88	0.7	-0.10	-
Interceptor with controls	4	2.55	1.5	-0.22	-
Jack of third air brake.	20	2.51	8.1	-0.30	-2
LANDING GEAR (DOWN) ...	18	1.36	13.5	-0.16	-2
	-2	-0.60	3.0	-0.70	-2
	-73	-0.21	356.0	-0.88	-312

Declassified in Part - Sanitized Copy Approved for Release 2011/12/13 : CIA-RDP80T00246A062100050001-6

Declassified in Part - Sanitized Copy Approved for Release 2011/12/13 : CIA-RDP80T00246A062100050001-6

1	2	3	4	5	6
Nose strut without retracting mechanism	-123	-3.53	34.9	-0.85	-30
Retracting mechanism	-27	-3.48	7.8	-0.28	-2
Nose wheel,500x180 KT ..	-103	-3.40	30.3	-1.28	-39
Main strut with axle and standard fittings	67	0.67	99.6	-0.70	-70
Retracting mechanism..	10	0.36	27.2	-0.18	-5
Main wheel KT-37, 660x200B	118	1.00	118,0	-1.24	-146
Landing gear emergency release system	-5	-1.93	2.6	-0.14	-
Nose L.G. doors	-23	3.83	5.9	-0.55	-3
Main L.G. doors with locks and actuating jacks	7	0.23	28.7	-0.56	-16
Tail bumper shock absorber	6	5.51	1.0	-0.74	-1
PNEUMATIC SYSTEM ...	93	0.49	190.0	0.13	24
Pump 435 BM	11	0.79	13.0	0.43	6
Main system hydraulic tank	5	1.56	3.3	0.42	1
Additional antidim parts	2	1.56	1.4	0.45	1
Boost system hydraulic tank	1	0.15	3.9	0.43	2
Boost system hydraulic accumulator	8	1.48	5.1	-0.41	-2
Main system hydraulic accumulator	1	0.14	5.3	0.38	2
Landing gear valve, type PA-46/3	2	0.69	2.9	0.37	1
Flaps valve, type PA-46/2	3	0.99	2.9	0.41	1
Flaps emergency bottle	-6	-3.57	1.8	-0.22	-
Pneumatic control units, types ПУ-7 and ПУ-8	-5	-3.54	1.4	-0.03	-
Filter, type ФГ-100-1	3	1.18	2.5	0.28	1
Low pressure reducer..	1	1.03	0.6	0.45	-
Reverse flow divider, type ГА-57	-	0.22	2.0	0.31	1
Safety valve	2	1.11	1.9	0.24	-
Emergency braking valve	-2	-3.19	0.5	0.34	-
Reducer, type КР-14А	-1	-3.22	0.5	0.19	-
Switch, type УП-22 ..	-1	3.03	0.3	0.15	-
Header	1	1.33	0.5	0.44	-
Header	-	1.14	0.1	0.42	-
Valve, type 665000-Б	-	1.18	0.2	0.68	-
Valve, type 652200А (two valves)	-1	-2.87	0.4	0.28	-
Electric valve, type ЭК-48-МАИ	-1	-3.47	0.4	0.20	-
Air reducer	-3	-2.64	1.0	0.24	-
Ground charging valve (of suction pump)..	-	0.61	0.2	-0.28	-
Ground charging valve (of delivery pump)..	-	0.71	0.2	-0.28	-
Split valve	1	1.20	0.5	0.30	-
Split valve	1	1.08	0.6	0.20	-
Reducing valve	1	1.08	1.2	0.35	-
Attachment units	-	0.07	3.6	0.29	1
Hydraulic mixture in booster system tank	7	0.15	5.5	0.43	2
Hydraulic mixture in fuselage nose section	-1	-0.13	4.8	-0.18	-1
Dust filter	-	1.40	0.1	0.40	-
Hydraulic mixture in engine compartment	10	1.08	8.8	0.43	4

Declassified in Part - Sanitized Copy Approved for Release 2011/12/13 : CIA-RDP80T00246A062100050001-6

Declassified in Part - Sanitized Copy Approved for Release 2011/12/13 : CIA-RDP80T00246A062100050001-6

1	2	3	4	5	6
Pipeline in fuselage nose section	-13	-0.53	24.4	-0.10	-2
Pipeline attachment fittings	-1	-0.57	1.4	-0.10	-
Valves and T-connections.....	-3	-0.57	5.7	-0.09	-
Valve, type ГА-13/4 ..	5	2.54	1.9	0.53	1
Valve, type ГА-74/5	4	3.21	1.3	0.51	1
Valve, type ГА-37 ...	5	2.73	2.0	0.50	1
Split valves (6 valves)	4	2.00	2.4	0.34	1
Electric valve, type ЭК-48	2	2.63	0.9	0.30	-
Drag parachute doors actuating jack.....	1	4.75	0.2	0.41	-
Drag parachute cable disconnect jack....	1	5.16	0.2	0.37	-
Split valves	-	1.35	0.3	0.57	-
Selector jack	1	2.64	0.3	0.54	-
Flow meters, type ГА-148 (two meters)..	3	2.80	1.0	0.52	1
Flow meters, type ГА-173-00-3 (six meters)	10	4.80	2.0	0.60	1
Slide-type selector switch	3	3.21	1.1	0.48	1
Altitude supply valve	1	3.37	0.4	0.55	-
Split valves	1	3.21	0.3	0.48	-
Attachment fittings..	1	2.26	0.8	0.52	-
Pipeline in fuselage tail section.....	22	3.43	6.4	0.46	3
Pipeline attachment fittings	1	3.42	0.3	0.43	-
Valves and T-connections	3	3.42	1.0	0.46	-
Hydraulic mixture in fuselage tail section	13	3.60	3.6	0.42	1
Air bottle, 2x4 lit.	-3	-0.34	10.0	-0.07	-1
Air bottle, 1x2 lit.	-4	-1.42	2.7	-0.09	-
Valve, type ГА-74/3	-1	-0.69	1.3	-0.08	-
Emergency valve and УП-30 switch	-1	-0.50	1.3	-0.11	-
Hydraulic lock	-	-0.39	0.4	-0.12	-
Emergency valve	-	-0.45	0.2	-0.08	-
Sequence valve	-	0.32	0.4	-0.15	-
Slide-type selector switch	-1	-0.80	1.1	-0.11	-
Safety valve	-	-0.99	0.3	-0.11	-
Return valve (two valves)	-	-0.73	0.2	-0.11	-
Emergency system valves mounting parts	-	-0.58	0.4	-0.09	-
Hydraulic lock	-1	-3.51	0.4	-0.25	-
Header	-	-0.35	0.3	-0.07	-
Network valve	-	-0.65	0.2	-0.11	-
Charging union	-	-0.71	0.1	-0.11	-
Attachment fittings...	-1	-0.35	2.9	-0.10	-
Pipeline in wing.....	-4	-0.26	15.5	-0.11	-2
Pipeline attachment fittings	-	-0.15	2.3	-0.11	-
Valves and T-connections	-	-0.15	1.4	-0.11	-
Hydraulic mixture in wing	6	0.51	11.3	-0.14	-2
Air	-	-0.23	2.0	-0.06	-
BOOST CONTROL	64	4.35	14.7	0.82	12
Slide valve, type ГА-21 (4 valves)	34	4.76	7.2	1.00	7
Slide valve attachment fittings	4	4.76	0.8	1.00	1

Declassified in Part - Sanitized Copy Approved for Release 2011/12/13 : CIA-RDP80T00246A062100050001-6

Declassified in Part - Sanitized Copy Approved for Release 2011/12/13 : CIA-RDP80T00246A062100050001-6

1	2	3	4	5	6
Pipeline	16	3.85	4.2	0.46	2
Pipeline attachment fittings	2	3.85	0.4	0.46	-
Hydraulic mixture	4	4.00	1.0	0.50	1
Valves and T-connections	4	3.85	1.1	0.46	1
POWER PLANT	2934	1.79	1669	0.04	61
Engine, type РД-9Б, with diffuser.....	1900	1.545	1230.0	0.06	74
Ejector	54	5.416	10.0	0	-
Afterburner	833	4.336	192.0	0	-
Engine nose bullet with sealings	4	0.40	11.1	0	0
Booster pump	4	0.59	6.2	0.43	3
Afterburner attachment fittings	5	5.18	1.0	0.32	-
Guide track mounting parts	5	5.06	1.0	0.32	-
Engine main mounting parts	11	1.416	7.6	0.20	2
Engine controls	-14	-1.58	8.6	0.33	3
Afterburner shutters controls	64	4.35	14.7	0.82	12
Gasoline tank	-1	-0.42	2.9	0.50	1
Gasoline system pump	-	-0.19	2.9	0.67	2
Gasoline system pipeline with attachment fittings	1	0.41	3.0	0.37	1
Breather mount	2	1.20	1.8	0	0
Oil transmitters.....	-	0.40	0.8	0.43	-
Tachometer transmitters, type ДТ-3 ...	1	0.38	3.2	0.37	1
Thermocouple, type ТХ-1 (2 pieces)	3	2.65	1.9	0.22	-
Rubber hose	3	1.61	1.6	-0.15	-
Connector sealing [illegible]	-	0.03	2.3	0.63	2

1	2	3	4	5	6
Pipeline fittings and engine additional fittings	2	1.61	1.2	-0.15	-
Fuel tank 1.....	-33	-0.87	38.3	0.11	4
Negative G chamber with 495-A pump ...	-16	-0.77	20.8	-0.56	-12
Attachment fittings of tank 1	-2	-0.86	2.1	-0.40	-1
Fuel flow gauge transmitter, type РТС-16	-	-0.33	0.5	0.22	-
Tank 2, v = 330 lit.	9	0.68	12.8	-0.47	-6
Attachment fittings of tank 2	1	0.68	0.8	-0.50	-
Tank 3, v = 180 lit.	29	2.27	12.7	-0.40	-5
Attachment fittings of tank 3	3	2.27	1.3	-0.40	-1
Tank 4, v = 175 lit.	47	3.41	13.7	-0.43	-6
Attachment fittings of tank 4	5	3.41	1.4	-0.43	-1
Filler neck	10	3.49	2.8	0.06	-
Pump, type ПНВ-2, for tank 2	2	0.40	4.3	-0.59	-3
Pump, type ПШР-1-5, for tank 3	4	1.65	2.7	-0.60	-2
Attachment fittings of pumps	1	1.65	0.5	-0.60	-
Pump, type ПШР-1-5, for tank 4	11	3.85	2.7	-0.58	-2
Pump attachment fittings	3	3.89	0.8	-0.58	-
Pressure warning unit, type СД-3 (3 units)	1	0.39	1.2	-0.60	-1
Shut-off valves	2	0.41	4.0	0.93	2
Electric filters, type Ф-14А (3 pieces)	2	1.60	1.5	-0.50	-1

Declassified in Part - Sanitized Copy Approved for Release 2011/12/13 : CIA-RDP80T00246A062100050001-6

Declassified in Part - Sanitized Copy Approved for Release 2011/12/13 : CIA-RDP80T00246A062100050001-6

1	2	3	4	5	6
Electric filter, type Ф-37 (1 piece)	-	-0.16	1.1	0.47	-1
Filters mounting parts	-	0.30	0.7	-0.45	-
Thyratron interrupter	-1	-0.75	1.1	0.40	-
Drop tank pressurization system	1	0.36	2.4	0.32	1
Valves	3	0.70	4.3	0.23	1
Branch pipes	-	0.13	0.6	-0.09	-
Pipeline in fuselage nose section	2	0.25	7.8	0.16	1
Attachment units and fittings	4	0.80	5.3	0.20	1
Pipeline in fuselage tail section	11	2.72	4.2	-0.13	-1
Pipeline in wing (two filters)	5	0.84	5.2	-0.10	-1
Fire-fighting system	-	0.11	9.0	-0.67	-6
EQUIPMENT	-986	-1.81	545.0	0.10	54
Electric equipment	-287	-1.34	214.0	0.26	56
Navigating equipment	-273	-2.57	106.0	-0.13	-14
Communication equipment	-172	-3.49	49.3	0.41	20
Radar equipment	-142	-2.37	60.0	0.21	13
Altitude equipment	- 82	-1.61	51.0	-0.16	-8
Auxiliary equipment	64	1.96	32.6	-0.15	-5
Convertors	-88	-3.30	26.5	-0.30	-8
ПУ-2 control unit power line	-6	-1.00	6.0	-0.03	-
ELECTRIC EQUIPMENT	-287	-1.34	214.0	0.26	56
Storage battery, type 12 СЦ-28	-100	-3.63	27.6	-0.38	10
Storage battery contactor	-13	-3.63	4.0	0.38	2
Storage battery attachment fittings	-7	-3.63	2.0	0.30	1
Generator, type ГСР-СТ-6000 (2)	11	0.27	40.0	0.43	17
Starboard power unit	-5	-0.57	9.2	0.30	3
Port side power unit	-3	-0.57	5.8	0.30	2
Mounting parts of РКР-К box	-1	-0.96	0.6	-0.25	-
Mounting parts of БС 6000	-	0.01	1.0	0.52	1
Mounting parts of converter relay box	-2	-2.56	0.9	-0.58	-1
Mounting parts of button-and-switch control panel	-1	-3.23	0.3	0.56	-
РП-6 and РП-2 relay mount	-1	-2.37	0.4	-0.64	-
Landing lamp mount	-12	-3.24	3.6	-0.56	-2
Taxi lamp mount	-3	-3.74	0.8	-0.59	-
Mach indicator mount	-3	-3.09	1.1	0.46	1
РПА-200А box mount	-2	-1.00	2.1	-0.36	-1
Armament relay box mount	-5	3.59	1.3	0.31	-
Ф-14А filter mount	-3	-3.64	0.7	0.25	-
Transformer	-	-0.20	2.2	0.35	1
Attachment fittings	-	-1.20	0.1	0.25	-
Ultra-violet illumination lamp fittings (2)	-1	-2.92	0.4	0.50	-
Resistor box, type ПОЮ-30М	-	-2.15	0.2	0.22	-
Mount of РПА-200А and ТП-400 units	-8	-4.00	2.0	0.20	-
СДУ unit mount	-1	-3.40	0.3	0.50	-
ПКС-600 starting panel mount	6	0.66	9.4	0.51	3
2ЭМ-2-АЗС unit mount	-	-0.51	0.7	0.31	-
РП-2 warning relay	-	2.00	0.2	-	-
АРУ box	-9	-3.29	2.8	0.10	-
Virus	-87	-1.66	52.3	0.19	10

Declassified in Part - Sanitized Copy Approved for Release 2011/12/13 : CIA-RDP80T00246A062100050001-6

Declassified in Part - Sanitized Copy Approved for Release 2011/12/13 : CIA-RDP80T00246A062100050001-6

1	2	3	4	5	6
Protection	-3	-1.39	1.8	0.10	-
Connectors	-25	-2.57	9.8	0.26	3
Attachment fittings	-2	-1.38	1.5	0.10	-
Right-hand console	-21	-2.74	7.7	0.29	2
Left-hand console	-18	-2.76	6.6	0.33	2
Trim tab relays mount	2	3.35	0.5	0.63	-
Junction box for thermo-couples	1	2.96	0.3	0.11	-
Wires	13	4.20	3.2	0.27	1
Protection	5	4.20	1.3	0.27	-
Connectors	5	3.34	1.4	0.27	-
Attachment fittings	2	4.20	0.4	0.27	-
Electric wiring in right wing	3	0.76	4.0	-0.16	-1
Electric wiring in left wing	3	0.90	3.0	-0.16	-
Electric wiring in special beam	-	0.90	0.5	-0.10	-
NAVIGATING EQUIPMENT	-273	-2.57	106.0	-0.13	-14
Instrument panel	-47	-3.09	15.3	0.40	6
APK-5 automatic radio compass	-94	-2.68	35.0	-0.34	-12
MPI-48 marker receiver	-19	-2.72	7.0	-0.43	-3
TGK-1 gyrocompass	-40	-2.00	20.2	0.10	2
PB-2 radio altimeter	-41	-2.16	19.0	-0.37	-7
Air-speed tube in fuse-lage	-7	-6.12	1.2	-0.41	-
Wires to instrument panel	-9	-3.00	3.0	0.19	1
TP-156 Pitot tube	-2	-4.30	0.5	0.45	-
Wires to TP-156 Pitot tube	-4	-3.00	1.3	0.20	-
NAP-13 converter for [illegible] horizon	-9	-2.58	3.5	-0.34	-1
APK-5 RADIO COMPASS	-94	-2.68	35.0	-0.34	-12

1	2	3	4	5	6
Receiver	-59	-2.67	22.0	-0.40	-9
APAKC frame	-15	-3.02	4.9	-0.57	-3
Change-over switch	-	-2.74	0.1	0.30	-
Control panel	-5	-2.66	2.0	0.33	1
Dehydrator	-1	-2.92	0.4	-0.46	-
Instrument attachment fittings	-6	-2.68	2.2	-0.31	-1
Cables with fittings	-8	-2.42	3.4	-0.12	-
MPI-48 MARKER RECEI-VER	-19	-2.72	7.0	-0.43	-3
Receiver	-5	2.93	1.7	-0.48	-1
Antenna with radome	-9	-2.64	3.5	-0.62	-2
Ring	-2	-2.29	0.8	0.43	-
Instrument attachment fittings	-1	-2.84	0.3	0.40	-
Cables	-2	-2.84	0.7	-0.40	-
PB-2 RADIO COMPASS	-41	-2.16	19.0	-0.37	-7
Converter	-10	-2.66	3.8	-0.20	-1
Receiver-transmitter	-22	-2.62	8.4	-0.45	-4
Receiving-transmit-ting antenna	2	1.30	1.6	-0.22	-
634-1B audio frequen-cy filter	-2	-2.50	0.9	-0.42	-
Instrument attachment fittings	-4	2.55	1.5	-0.46	-1
Cables	-5	-1.83	2.8	-0.27	-1
TGK-1 GYROCOMPASS	-40	-2.00	20.2	0.10	2
Corrector switch	-4	1.97	2.2	-0.30	-1
Panel compass	-1	-2.38	0.5	0.40	-
Junction box	-2	-3.44	0.6	0.44	-
Gyro unit	-11	-3.36	3.4	0.36	1
Amplifier, type Y-6	-8	-3.21	2.5	0.09	-
Correction assembly	-3	-3.30	1.0	0.53	1
Variable inductor	9	5.60	1.5	0.67	1

Declassified in Part - Sanitized Copy Approved for Release 2011/12/13 : CIA-RDP80T00246A062100050001-6

Declassified in Part - Sanitized Copy Approved for Release 2011/12/13 : CIA-RDP80T00246A062100050001-6

1	2	3	4	5	6
Wiring	-8	-2.40	3.3	0.32	1
Attachment fittings ..	-2	-3.40	0.8	0.36	-
ПТ-70 unit	-10	-2.63	4.2	-0.30	-1
COMMUNICATION EQUIPMENT PCMУ-4 RADIO SET	-172	-3.49	49.3	0.41	20
Receiver-transmitter	-127	-4.01	31.6	0.40	13
Rectifier	-28	-3.73	7.2	0.41	3
Aerial mount	3	5.00	0.5	0.80	1
КИ-2И panel	-3	-2.96	0.9	0.26	-
Instrument attachment fittings	-5	-3.85	1.3	0.24	-
Cables	-12	-1.58	7.8	0.40	3
RADAR EQUIPMENT	-142	-2.37	60.0	0.21	13
СРД-1 radar ranging unit	-120	-3.33	36.0	0.03	1
СРО-1 IFF transponder	-54	-3.00	18.0	0.06	1
СИРЕНА-2 tail attack warning unit	32	5.34	6.0	1.83	11
СРД-1 RADAR RANGING UNIT	-120	-3.33	36.0	-	-
Antenna	-2	-4.54	0.5	0.41	-
Receiver-transmitter..	-41	-4.01	10.3	0.07	1
Supply and range unit	-39	-2.94	13.3	-0.29	-4
Voltage stabilizer....	-12	-3.68	3.3	0.24	1
Special panel	-2	-2.64	0.6	0.43	-
Waveguide	-3	-4.20	0.8	0.20	-
Selector switch	-1	-2.11	0.4	0.17	-
Attachment fittings ..	-4	-2.98	1.5	0.20	-
Wires	-16	-3.00	5.3	0.29	2
СРО-1 IFF TRANSPONDER	-54	-3.00	18.0	0.06	1
Receiver-transmitter...	-45	-3.77	12.0	0.03	1

1	2	3	4	5	6
Destructor button	-	-2.94	0.1	0.33	-
Selector switch	-	-3.01	0.1	0.33	-
Control panel	-2	-2.43	1.0	0.18	-
Antenna mount	2	2.03	1.0	0.67	-
Instrument panel	-1	-4.25	0.2	0.19	-
Inertia switch	-2	-3.90	0.6	0.34	-
Cables and connectors..	-5	-2.50	2.1	0.08	-
Attachment fittings ...	-2	-2.75	0.9	0.12	-
СИРЕНА-2 TAIL WARNING UNIT	32	5.34	6.0	1.83	11
Unit No.2	25	6.30	4.0	1.94	8
Unit No.1	2	7.62	0.3	2.19	1
Unit No.3	-	1.50	0.3	0.53	-
Cables	2	1.80	0.9	0.60	1
Attachment fittings....	3	5.00	0.5	2.50	1
ALTITUDE EQUIPMENT.....	-88	-1.61	51.0	-0.16	-8
Oxygen equipment.....	-66	-2.28	29.0	-0.14	-4
Cockpit supply	-16	-0.73	22.0	-0.18	-4
OXYGEN EQUIPMENT	-66	-2.28	29.0	-0.14	-4
Oxygen bottles 2x4 lit.	-30	-2.39	12.6	-0.40	-5
Oxygen bottles 2x2 lit.	-7	-1.11	6.3	-0.16	-1
Common connector.....	-1	-2.46	0.4	0.13	-
Inboard hoses junction	-2	-2.46	0.8	0.13	-
КР-26 regulator	-1	-2.16	0.4	0.07	-
КП-30 apparatus	-6	-2.38	2.6	0.40	1
Hoses and fittings....	-13	-3.13	4.1	0.20	1
Attachment fittings...	-6	-3.34	1.8	-0.22	-
COCKPIT SUPPLY	-16	-0.73	22.0	-0.18	-4
Supply valve	-1	-2.54	0.4	0.17	-
Return valve	1	1.61	0.9	0.33	-
Electric distributor..	1	0.45	1.3	0.61	1
ТК-477 unit	-1	-0.49	3.0	-0.35	-1
ВВР air reducing valve	-2	-0.49	3.8	-0.33	-1
РД2П and ИК units..	-4	-2.39	1.7	-0.21	-

Declassified in Part - Sanitized Copy Approved for Release 2011/12/13 : CIA-RDP80T00246A062100050001-6

Declassified in Part - Sanitized Copy Approved for Release 2011/12/13 : CIA-RDP80T00246A062100050001-6

1	2	3	4	5	6
Wiring	-8	-2.40	3.3	0.32	1
Attachment fittings ..	-2	-3.40	0.8	0.36	-
ПТ-70 unit	-10	-2.63	4.2	-0.30	-1
COMMUNICATION EQUIPMENT РСИУ-4 RADIO SET	-172	-3.49	49.3	0.41	20
Receiver-transmitter	-127	-4.01	31.6	0.40	13
Rectifier	-28	-3.73	7.2	0.41	3
Aerial mount	3	5.00	0.5	0.80	1
КИ-2И panel	-3	-2.96	0.9	0.26	-
Instrument attachment fittings	-5	-3.85	1.3	0.24	-
Cables	-12	-1.58	7.8	0.40	3
RADAR EQUIPMENT	-142	-2.37	60.0	0.21	13
СРД-1 radar ranging unit	-120	-3.33	36.0	0.03	1
СРО-1 IFF transponder	-54	-3.00	18.0	0.06	1
СИРЕНА-2 tail attack warning unit	32	5.34	6.0	1.83	11
СРД-1 RADAR RANGING UNIT	-120	-3.33	36.0	-	-
Antenna	-2	-4.54	0.5	0.41	-
Receiver-transmitter..	-41	-4.01	10.3	0.07	1
Supply and range unit	-39	-2.94	13.3	-0.29	-4
Voltage stabilizer....	-12	-3.68	3.3	0.24	1
Special panel	-2	-2.64	0.6	0.43	-
Waveguide	-3	-4.20	0.8	0.20	-
Selector switch	-1	-2.11	0.4	0.17	-
Attachment fittings ..	-4	-2.98	1.9	0.20	-
Wires	-16	-3.00	5.3	0.29	2
СРО-1 IFF TRANSPONDER	-54	-3.00	18.0	0.06	1
Receiver-transmitter...	-43	-3.77	12.0	0.03	1

1	2	3	4	5	6
Destructor button	-	-2.94	0.1	0.33	-
Selector switch	-	-3.01	0.1	0.33	-
Control panel	-2	-2.43	1.0	0.18	-
Antenna mount	2	2.03	1.0	0.67	-
Instrument panel	-1	-4.25	0.2	0.19	-
Inertia switch	-2	-3.90	0.6	0.34	-
Cables and connectors..	-5	-2.50	2.1	0.08	-
Attachment fittings ...	-2	-2.75	0.9	0.12	-
СИРЕНА-2 TAIL WARNING UNIT	32	5.34	6.0	1.83	11
Unit No.2	25	6.30	4.0	1.94	8
Unit No.1	2	7.62	0.3	2.19	1
Unit No.3	-	1.50	0.3	0.53	-
Cables	2	1.80	0.9	0.60	1
Attachment fittings....	3	5.00	0.5	2.50	1
ALTITUDE EQUIPMENT.....	-88	-1.61	51.0	-0.16	-8
Oxygen equipment.....	-66	-2.28	29.0	-0.14	-4
Cockpit supply	-16	-0.73	22.0	-0.18	-4
OXYGEN EQUIPMENT	-66	-2.28	29.0	-0.14	-4
Oxygen bottle 2x4 lit.	-30	-2.39	12.6	-0.40	-5
Oxygen bottle 2x2 lit.	-7	-1.11	6.3	-0.16	-1
Common connector.....	-1	-2.46	0.4	0.13	-
Inboard hoses junction	-2	-2.46	0.8	0.13	-
KP-26 regulator	-1	-2.16	0.4	0.07	-
КП-30 apparatus	-6	-2.38	2.6	0.40	1
Hoses and fittings....	-13	-3.13	4.1	0.20	1
Attachment fittings...	-6	-3.34	1.8	-0.22	-
COCKPIT SUPPLY	-16	-0.73	22.0	-0.18	-4
Supply valve	-1	-2.54	0.4	0.17	-
Return valve	1	1.61	0.9	0.33	-
Electric distributor..	1	0.45	1.3	0.61	1
ТК-477 unit	-1	-0.49	3.0	-0.35	-1
ВВР air reducing valve	-2	-0.49	3.8	-0.39	-1
РД2П and ИК units..	-4	-2.39	1.7	-0.21	-

Declassified in Part - Sanitized Copy Approved for Release 2011/12/13 : CIA-RDP80T00246A062100050001-6

Declassified in Part - Sanitized Copy Approved for Release 2011/12/13 : CIA-RDP80T00246A062100050001-6

1	2	3	4	5	6
Transmitter	-1	-2.25	0.4	-0.03	-
Windshield antidim system	-1	-3.13	0.3	0.61	-
Cockpit heating system	-1	-3.26	0.4	-0.08	-
Wiring and fittings....	-4	-0.65	7.3	-0.25	-2
Attachment units	-3	-1.20	2.5	-0.40	-1
AUXILIARY EQUIPMENT....	64	1.96	32.6	-0.15	-5
Signal flare launcher	14	4.59	3.0	0.76	2
Map holder	-	-2.74	0.1	0.20	-
De-icer	-24	-4.90	4.8	-	-
MMK-1 anti-G suit....	-4	-2.35	1.5	0.13	-
Drop tank locks	12	1.42	8.6	-0.30	-3
Drag parachute	66	4.52	14.6	-0.29	-4
CONVERTERS	-88	-3.30	26.5	-0.30	-8
PO-750 converter.....			14.0		
PO-500 converter	-88	-3.30	11.5	-0.30	-8
Attachment fittings...			1.0		
ARMAMENT	-605	-1.78	340.0	-0.12	-41
Armaments	-466	-1.64	284.0	-0.12	-61
ASP-5N-B3 sight	-139	-2.48	56.0	0.36	20
ARMAMENT	-466	-1.64	284.0	-0.21	-61
N-30 cannon	-175	-2.55	68.5	-0.50	-34
Gas-discharge tube....	-25	-3.53	7.0	-0.50	-4
Front attachment unit	-15	-2.67	5.7	0.50	-3
Rear attachment unit..	-4	-1.90	2.0	-0.50	-1
Third-point attachment unit	-2	-3.46	0.6	-0.50	-
Ammunition box and feed chute	-22	-2.27	9.8	-0.39	-4
Case ejection chute...	-1	-2.28	0.4	-0.54	-
Link chute	-5	-2.16	2.4	-0.30	-1
N-30 cannon	-178	-1.30	137.0	-0.07	-10
Front attachment unit	-15	-1.42	10.8	-0.07	-1
Rear attachment unit	-2	-0.59	3.8	-0.02	-

1	2	3	4	5	6
Third-point attachment unit	-3	-2.15	1.3	-0.07	-
Shell chute	-5	-1.00	5.4	-0.06	-
Link chute head pieces	-1	-0.97	1.2	-0.03	-
Link catcher bag	-4	-1.08	3.8	-0.35	-1
Link chute with head piece	-2	-1.00	1.6	-0.20	-
Charging unit	-6	-1.46	4.1	-0.09	-
PM-2 time-piece unit	-4	-4.05	1.1	0.39	-
AKS-5 cinecamera unit	-7	-4.70	1.5	0.40	1
AKS-5 cinecamera mount	-3	-4.70	0.7	0.40	-
Wiring	-2	-3.00	0.4	0.30	-
Nose guide tracks.....	15	0.99	15.0	-0.22	-3
ASP-5N-B3 SIGHT	-139	-2.48	56.0	0.36	20
Unit No.1	-33	-3.04	10.9	0.70	8
Unit No.2	-12	-2.03	6.1	0.23	1
Unit No.3	-10	-2.04	4.7	0.17	1
Unit No.4	-8	-2.05	3.9	0.43	2
Units Nos 5 and 9	-23	-2.06	11.0	0.26	3
Unit No.6	-12	-4.30	2.7	0.19	1
Unit No.7	-3	-2.58	1.1	0.43	-
Unit No.8	-7	-2.05	3.3	0.43	1
Fire control relay	-3	-3.19	0.8	0.30	-
Sight head bracket.....	-7	-3.17	2.1	0.70	1
ZS-14 A filter	-1	-1.98	0.7	0.30	-
Set of cables	-16	-2.50	6.5	0.20	1
Attachment fittings....	-4	-2.00	2.2	0.25	1
GUNNER	-214	-2.61	82.0	0.57	47
Armour in front of pilot, δ = 10 mm ...	-107	-3.47	30.8	0.30	9
Armoured glass panel with frame, δ = 64 mm	-52	-3.17	16.5	0.81	13
Armoured back plate, δ = 16 mm	-30	-2.13	14.3	0.56	8
Armoured head rest, δ = 25 mm	-29	-2.30	12.5	0.02	11

Declassified in Part - Sanitized Copy Approved for Release 2011/12/13 : CIA-RDP80T00246A062100050001-6

Declassified in Part - Sanitized Copy Approved for Release 2011/12/13 : CIA-RDP80T00246A062100050001-6

1	2	3	4	5	6
Ejection gun armour ...	-9	-1.97	4.7	0.75	4
Plate on frame No.31...	13	4.30	3.0	0.60	2
Miscellaneous	-	-	0.2	-	-

Summary of МИГ-19С Aircraft Inertia Moments
(landing gear UP)

Variant No.	Description	G, kg	J_pA, kg-m/sec^2	J_pB, kg-m/sec^2	J_pC, kg-m/sec^2	α
I	Aircraft with normal load	7560	889	4697	4017	-1°02'
II	Aircraft with 50 per cent of fuel	6652	867	4443	3754	-1°47'
III	Extreme forward C.G. position.....	6472	860	4367	3671	-2°02'
IV	Aircraft without fuel	5748	849	4199	3499	-1°46'

Notes: 1. The tubular inertia moments are calculated with respect to the aircraft main axes.
2. Absence of ammunition decreases the inertia moments: J_pA - by 134 kg-m/sec^2; J_pB - by 157 kg-m/sec^2; J_pC - by 55 kg-m/sec^2.

The graph of inertia moments of the aircraft without special suspended loads is presented in Fig.146.

Auxiliary graphs for determining aircraft flight performances are given in Appendix 1 (Figs 147 - 153).

Appendix 2 presents the aircraft levelling diagram (Fig.154) and parameters of the boost units (Fig.155).

Appendix 3 gives characteristics of the RV-I4ЦС and RV-I3Ц boosters (Figs 156 and 157).

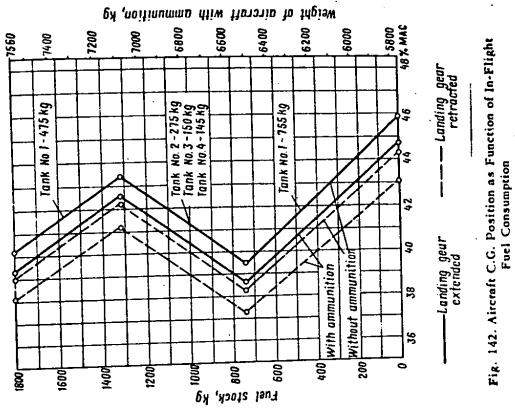
Weight of aircraft with ammunition, kg
Fuel stock, kg
Tank No 1 - 475 kg
Tank No 2 - 275 kg
Tank No 3 - 150 kg
Tank No 4 - 145 kg
Tank No 1 - 755 kg
with ammunition
Without ammunition
Landing gear extended
Landing gear retracted
%MAC

Fig. 142. Aircraft C.G. Position as Function of In-Flight Fuel Consumption

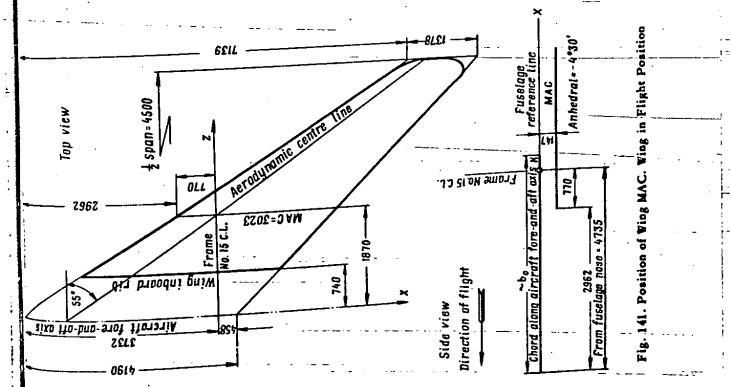

Fig. 141. Position of Wing MAC. Wing in Flight Position

Declassified in Part - Sanitized Copy Approved for Release 2011/12/13 : CIA-RDP80T00246A062100050001-6

Declassified in Part - Sanitized Copy Approved for Release 2011/12/13 : CIA-RDP80T00246A062100050001-6

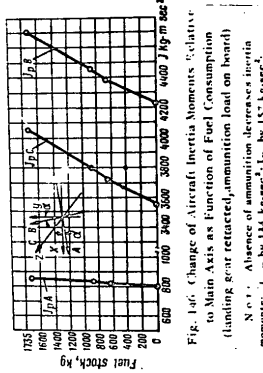

Fig. 1a6. Change of Aircraft Inertia Moments Relative to Main Axis as Function of Fuel Consumption (landing gear retracted, ammunition load on board)

Note: Absence of ammunition decreases inertia moments: I_A by 144 kg·sec²; I_B by 157 kg·sec²; I_C by 55 kg·sec².

APPENDIX 1

Auxiliary Graphs and Formulas Used in Evaluation of MiG-19C Aircraft Flight Performance Characteristics

1. Graphs and Formulas Used to Convert V, Mach Number and H

To convert the IAS into TAS and Mach number and vice versa, the following formulas are used:

V – aircraft true air speed (TAS), km/hr

$$V = \frac{V_i}{\sqrt{\Delta}} = (V_{i.(w.p.)} + \delta V_{instr.} + \delta V_{compr.} + \delta V_a + \delta V_{shock} + \delta V_{lag}) \times \frac{1}{\sqrt{\Delta}} = 72.2M\sqrt{T} ;$$

V_i – indicated air speed (IAS), km/hr,

$$V_i = V\sqrt{\Delta} = V_{i.(sea\ level)} + \delta V_{compr.} = 44.4\ M\sqrt{p}$$

(p in mm of Hg);

$V_{i.3}$ (sea level) – indicated air speed at sea level;

$V_{i.3}$ (sea level) $= V_{i.} - \delta V_{compr.} = V_{i.(w.p.)o.} + (\delta V_a + \delta V_{shock} + \delta V_{lag})$;

$V'_{i.3}$ (sea level) – indicated air speed at sea level without shock stall correction,

$V_{i.3}$ (sea level) $= V_{i.(w.p.)o.} + \delta V_a + \delta V_{lag}$;

$V_{i.(w.p.)}$ – IAS by the wide pointer of the airspeed indicator;

V_{narrow} – airspeed by the narrow pointer of the airspeed indicator;

Declassified in Part - Sanitized Copy Approved for Release 2011/12/13 : CIA-RDP80T00246A062100050001-6

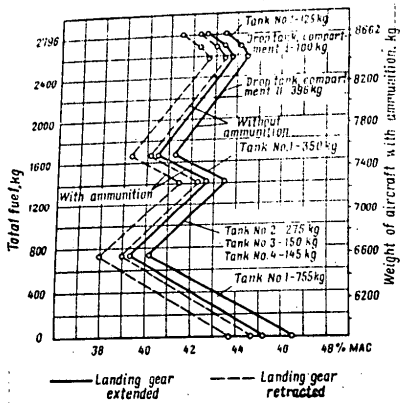

Fig. 143. Aircraft C.G. Position as Function of In-Flight Fuel Consumption (with drop tanks of 2x760 lit. capacity, primed with 600 lit. of fuel each)

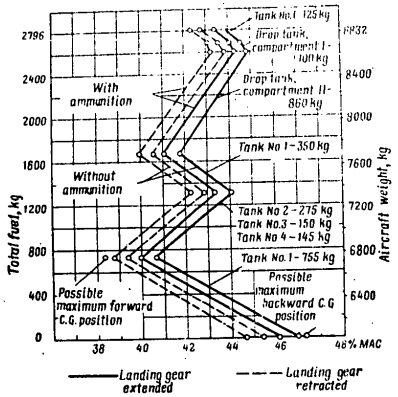

Fig. 144. Aircraft C.G. Position as Function of In Flight Fuel Consumption (with drop tanks of 2x760 lit capacity primed with 600 lit. of fuel each and 16 rockets carried on rack)

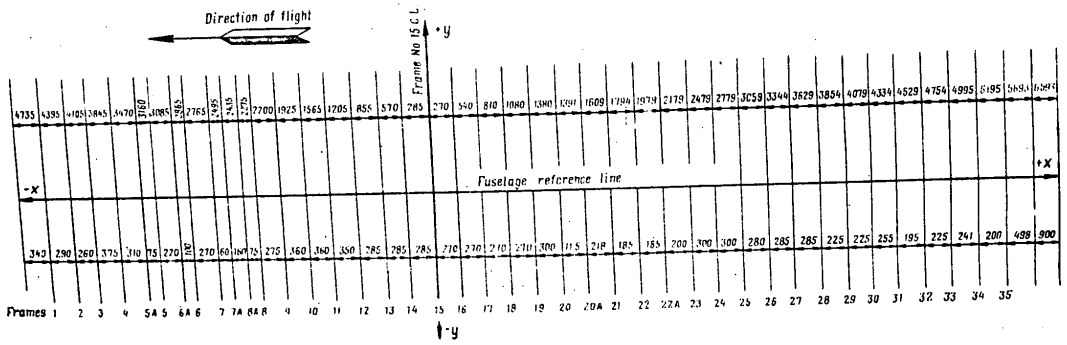

Fig. 145. Relative Positions of Fuselage Frames and Centring Axes x and y

Declassified in Part - Sanitized Copy Approved for Release 2011/12/13 : CIA-RDP80T00246A062100050001-6

Declassified in Part - Sanitized Copy Approved for Release 2011/12/13 : CIA-RDP80T00246A062100050001-6

$$V_{narrow} = \frac{V_{i.(w.p.)} + \delta V_{compr.}}{\sqrt{\Delta}} = V - (\delta V_{instr.} + \delta V_a + \delta V_{shock} + \delta V_{lag}) \frac{1}{\sqrt{\Delta}} ;$$

$V_{i.(w.p.)c.}$ - corrected IAS;

$V_{i.(w.p.)c.} = V_{i.(w.p.)} + \delta V_{instr.}$;

$V_{r.}$ - recorded speed,

$$V_{recorder} = V_{i.(w.p.)c.};$$

M - true Mach number;

$$M = \frac{V}{a} = M_{ind.} + \delta M_{instr.} + \delta M_a + \delta M_{shock} + \delta M_{lag} = \frac{V_{i.}}{44.4\sqrt{p}};$$

$M_{ind.}$ - indicated Mach number;

H - pressure altitude of flight,

$$H = H_{ind.} + \delta H_{instr.} + \delta H_a + \delta H_{shock} + \delta H_{lag};$$

$H_{ind.}$ - indicated altitude of flight;

$H_{act.}$ - actual altitude of flight (terrain clearance altitude, along the vertical),

$$H_{act.} = H + \delta H_{gr/s.l.}$$

$\delta V_{instr.}$ - instrument error correction to the airspeed indicator (by the airspeed indicator wide pointer);

$\delta M_{instr.}$ - instrument error correction to the Mach number indicator,

$$\delta M_{instr.} \approx \frac{\delta V_{instr.}}{a\sqrt{\Delta}} ;$$

$\delta H_{instr.}$ - instrument error correction to the altimeter;

δV_a - aerodynamic correction to the airspeed indicator for distortion of static pressure at the installation place of the airspeed tube and airspeed tube coefficient at small Mach numbers (by the wide pointer of the airspeed indicator).

δM_a - aerodynamic correction to the Mach number indicator,

$$\delta M_a \approx \frac{\delta V_a}{a\sqrt{\Delta}} ;$$

Note: Here and above the relations between δM and δV and δH are approximate.

$$\delta H_a \approx \frac{a^2 \delta M_a}{9.81} \times (M_{ind.} + \frac{\delta M_a}{2}) ;$$

Note: Here and in two formulas below the "a" value is given in m/sec.

δV_{shock} - shock corrections for distortion of static pressure at the airspeed tube installation place due to shock wave effect (by the airspeed indicator wide pointer).

δM_{shock} - shock correction to the Mach number indicator ;

$$\delta M_{shock} \approx \frac{\delta V_{shock}}{a\sqrt{\Delta}} ;$$

δH_{shock} - shock correction to the altimeter, m.,

$$\delta H_{shock} \approx \frac{a^2 \delta M_{shock}}{9.81} \times (M_{ind.} + \frac{\delta M_{shock}}{2}) ;$$

$\delta V_{compr.}$ - compressibility error correction (by the airspeed indicator wide pointer);

δV_{lag} - correction for time lag in instrument indication (by the airspeed indicator wide pointer);

δM_{lag} - correction for time lag in instrument indications (of the Mach number indicator),

$$\delta M_{lag} \approx \frac{\delta V_{lag}}{a\sqrt{\Delta}};$$

δH_{lag} - correction for time lag in the altimeter indications;

$\delta H_{ground/s.l.}$ - local elevation (depression) of terrain relative to the sea level;

a - speed of sound in still atmosphere, km/hr,

$$a = 72.2\sqrt{T} ;$$

Declassified in Part - Sanitized Copy Approved for Release 2011/12/13 : CIA-RDP80T00246A062100050001-6

Declassified in Part - Sanitized Copy Approved for Release 2011/12/13 : CIA-RDP80T00246A062100050001-6

q - impact pressure in flight;

$$q = \frac{\rho v^2}{2} ;$$

ρ - air density in still atmosphere;

$\Delta \frac{\rho_H}{\rho_{H=0}}$ - relative air density at the given altitude,

$$\Delta = \frac{\rho_H}{\rho_{H=0}} = 0.379 \frac{p}{T} ;$$

Note: Here the p value is given in mm of Hg.

p - pressure in still atmosphere;

$T^{o}_{abs.}$ - temperature in still atmosphere,

$$T = 273 + t^{o}C;$$

$t_{meas.}$ - "measured temperature", indication of the temperature gauge with stagnation attachment tube (B - nozzle stagnation coefficient),

$$t_{meas.}{}^{o}C = t^{o}C + (273 + t^{o}C)\, BM^2.$$

The above relations are universal and are applicable both for actual and standard conditions. Speed values obtained in flight are put down with "act" (actual) index while speeds reduced to the standard atmosphere conditions are marked with "st" (standard) index (for example, $V_{act.}$ or $V_{st.}$).

For simplification purposes, in the given book the speeds reduced to the standard atmosphere conditions have no "st" index.

For each pressure altitude of flight (the pressure altitude will be determined by pressure p taken from the Standard Atmosphere Tables) the relation between the indicated air speed, indicated speed by the airspeed indicator wide pointer (calibrated airspeed), Mach number and impact pressure does not depend on changes in the ambient air temperature, i.e. at any temperature only one value of $V_{i.}$ (calibrated), M or q corresponds to certain values of $V_{i.(w.p.)}$ (See the formulas). Corrections will be introduced into the formulas with their own signs.

The airspeed tube, type ПВД-3А, is installed in the МиГ-19С aircraft fuselage nose part.

The altitude, airspeed and Mach number indicating instruments during acrobatic maneuvres performed at high vertical speeds (dive, Nesterov's loop, etc.) are erratic due to the delay in the transmission of the static pressure from the airspeed tube to the instruments. This error is compensated by introduction of corrections δV_{lag}, δM_{lag} and δH_{lag}.

Presented in Fig.147 is the graph for determining V by the indicated airspeed (calibrated) and indicated altitude. The TAS graph makes possible to find:

(a) TAS by known $V_{i.(w.p.)}$ and $H_{ind.}$ or

(b) $V_{i.(w.p.)}$ by known TAS and $H_{ind.}$

The graph is valid at any air temperature of flight.

Fig.148 presents the graph of the summary (aerodynamic and shock) correction to the altimeter plotted according to the above formula and with the use of Fig.150 for the δM value.

It will be seen that the δH correction value is positive, i.e. the МиГ-19С aircraft altimeter reads a lower-than-actual altitude, and introduction of the correction provides for flight safety at low altitudes.

Fig.149 shows the graph of corrections for the air compressibility ($\delta V_{compr.}$).

Fig.150 presents the summary aerodynamic-and-shock correction $\delta M = \delta M_a + \delta M_{shock}$.

The drop tanks and rockets in practice do not change the summary aerodynamic-and-shock correction δM.

2. Table and Graph of Maximum Airspeed as Function of Ambient Air Temperature

Fig.151 presents the maximum indicated (by the wide pointer) airspeed in level flight at 10,000-m. altitude as function of the ambient air temperature measured with the temperature gauge provided with full stagnation attachment tube.

The graph is used for checking the V_{max} values by the results of flight at any free air temperature

$$t_{meas.}{}^{o}C = t_{act.}{}^{o}C + (273 + t_{act.}{}^{o}C)\, 0.19\, M^2,$$

where: $t^{o}_{meas.}$ - indication of the temperature gauge with stagnation attachment tube in a steady flight;

Declassified in Part - Sanitized Copy Approved for Release 2011/12/13 : CIA-RDP80T00246A062100050001-6

Declassified in Part - Sanitized Copy Approved for Release 2011/12/13 : CIA-RDP80T00246A062100050001-6

$t^{o}_{act.}$ - actual temperature of the air at the flight altitude.

The temperature gauge installation diagram is shown in Fig.152.

The free air temperature gauge in the МиГ-19С aircraft is installed on the pilot's cockpit canopy.

Temperature gauges are not used without attachment tubes since their indications depend on their shape and location on the aircraft, and special tests are required to obtain the relations of $t^{o}_{meas.}$ and $t^{o}_{act.}$

Temperature gauges in common use are slow in the reaction to temperature changes (due to their high inertness): therefore during the tests the $t^{o}_{meas.}$ value will be gauged during 3 minutes of flight at constant speed.

The graph presented in Fig.151 will be used as follows:

Let us assume that a temperature indication $t^{o}_{meas.} = +20^{o}C$ and a speed value by the airspeed indicator wide pointer were put down by the pilot in a level flight at H = 10,000 m. with the engines operating with afterburning.

Having set off the $t^{o}_{meas.} = +20^{o}C$ value on the graph horizontal axis, draw a vertical line through this point till it intersects the curve representing the 10,000-m. altitude, and then plot a horizontal line from the intersection point to the vertical scale (speed scale) of the graph.

The speed value nearest to that obtained in the graph ($V_{i.(w.p.)}$ = 951 km/hr) should be observed by the pilot on the airspeed indicator dial in flight.

The graph should be used as indicated by the arrows.

Given below is the Table presenting the airspeed as function of the free air temperature.

The Table gives the lower limit of airspeed values which may be obtained during the measurements as a result of possible variations (within specified limits) of the engines thrust and aircraft drag.

The Table contains some explanations.

Maximum Indicated Airspeeds as Function of Free Air Temperature

(to be used during acceptance trials)

Level flight maximum airspeeds of production МиГ-19С aircraft powered with РД-9Б engines will be evaluated with the aid of the Tables.

(1) Engines operating with afterburners ON, $H_{ind.}$ = 10,000 m.

$t^{o}_{meas.}$ C	10	20	25	30	40	45
$V_{i.(w.p.)}$, km/hr	970	951	930 x/	908	850	815
$V_{i.(w.p.)}$, km/hr (lower limit)	938	912	888	862	797	760

(2) Engines operating at normal power setting, $H_{ind.}$ = 10,000 m.

$t^{o}_{meas.}$ C	-30	-20	-8	0	10	20
$V_{i.(w.p.)}$, km/hr	652	650	646 x/	640	630	618
$V_{i.(w.p.)}$, km/hr (lower limit)	627	625	621	615	605	593

x/ Maximum airspeeds at standard free air temperature.

Note: Table of airspeeds at engines maximum power setting is not given here due to poor accuracy of airspeed and altitude measurements in these power conditions since the shock correction in this case is not stable.

The graphs of $V_{i.(w.p.)} = f(t^{o}_{meas.})$ use the data of maximum $H_{act.}$ values as function of free air temperatures as the basis for the graphical presentation of the function.

The stagnation coefficient of the alcohol temperature gauge with attachment tube is assumed to be 0.95.

The tabular maximum IAS values at standard temperature correspond to Mach 1.33 for the engines operating in power augmentation conditions (with afterburner ON) and Mach 0.999 for the engines at normal power setting.

Declassified in Part - Sanitized Copy Approved for Release 2011/12/13 : CIA-RDP80T00246A062100050001-6

Declassified in Part - Sanitized Copy Approved for Release 2011/12/13 : CIA-RDP80T00246A062100050001-6

The lower limit of the maximum IAS was evaluated with due account for the following tolerances:

- airspeed measurement error .....10 km/hr
- altitude measurement error .....100 m.
- temperature measurement error .....2°
- tolerated engine thrust variation.....2 per cent
- tolerated aircraft drag variation.....2 per cent.

At thrust air temperature ratios equal to $h_t = -1.3$ for the engine operating with the afterburner ON and $h_t = -2.0$ at engine normal power setting, the values of the tolerated variations of the engine thrust and aircraft drag will correspond to the variation of the measured temperatures by 6.5°C with afterburning and 3.8°C at nominal setting, respectively.

The airspeed measuring error at normal power setting is assumed to be 25 km/hr, due account being taken for decreased accuracy of airspeed and altitude measurements due to shock effects.

Employ for the airspeed and altitude measurements special self-recording devices and alcohol temperature gauges (with attached stagnation tube) for air temperature measurements.

For greater accuracy of air temperature measurements, the regular straight-and-level flight should be maintained during not less than 3 minutes.

If the level flight altitude is other than 10,000 m., increase (decrease) the required airspeed by 10 km/hr for afterburning conditions and by 5 km/hr for normal power setting conditions for every 100 m. of altitude difference.

If the aircraft weight on the level flight leg is other than 6800 kg, the required airspeed in afterburning conditions should be increased (decreased) by 1 km/hr for every 100 kg of weight variation. During flight at normal power setting the weight correction will not be introduced.

3. Co-Ordinate Axes System and Designation of Values

Some special values given in Article 4, Chapter IV ("Aircraft Control") and Chapter V ("Aerodynamic Characteristics") are explained by the axes system diagram (Fig.153) and the list of designations given below.

The so-called "semidependent axes system" (Fig.153)

shows the vectors and corresponding signs of the angles, pressures and moments used in Chapter V ("Aerodynamic Characteristics") as well as the vectors and signs of angles and angular speeds used in Article 4, Chapter IV ("Aircraft Control").

Note: Coefficient c_x is given in the Tables and graphs in its absolute value (the minus sign is omitted for reasons of convenience). During manoeuvres and aerobatics the values will be measured in the so-called "dependent axes system", according to which the x axis coincides with the aircraft fore-and-aft axis.

Some positive values (with sign "+") for some values are given below in addition to the axes system diagram.

Angles (sign "+")

Slip angle β ..... right wing slip (right wing ahead)
Bank angle γ ..... right wing bank
Stabilizer setting angle φ relative to wing..... stabilizer leading edge UP

Pressures (sign "+")

On stabilizer control handle,
$P_{elevator}$ .....push
On ailerons control handle,
$P_{aileron}$ .....push to the left
On pedals, P_{pedal} .....push the right pedal

Travel of Controls (sign "+")

Stabilizer control handle, x_e .....forward travel
Ailerons control handle, $x_{aileron}$ .....left travel
Pedals, x_{pedal} .....forward travel of right pedal

Declassified in Part - Sanitized Copy Approved for Release 2011/12/13 : CIA-RDP80T00246A062100050001-6

Declassified in Part - Sanitized Copy Approved for Release 2011/12/13 : CIA-RDP80T00246A062100050001-6

Overloads (sign "+")

n_y - inertia force is directed downwards (the pilot is pulled down into the seat);

n_x - inertia force is directed forward (flight speed is decreased, the pilot is drawn forward);

n_z - inertia force is directed towards the right wing (the pilot is pressed to the starboard).

Distance (sign "+")

C.G. position relative to wing MAC in height, Y_g ..... C.G. below MAC

In the graphs of the aerodynamic performances, coefficient m_z is related to the wing mean aerodynamic chord MAC (b_A = 3.023 m.). Coefficients m_x and m_y are related to span l = 9.0 m.

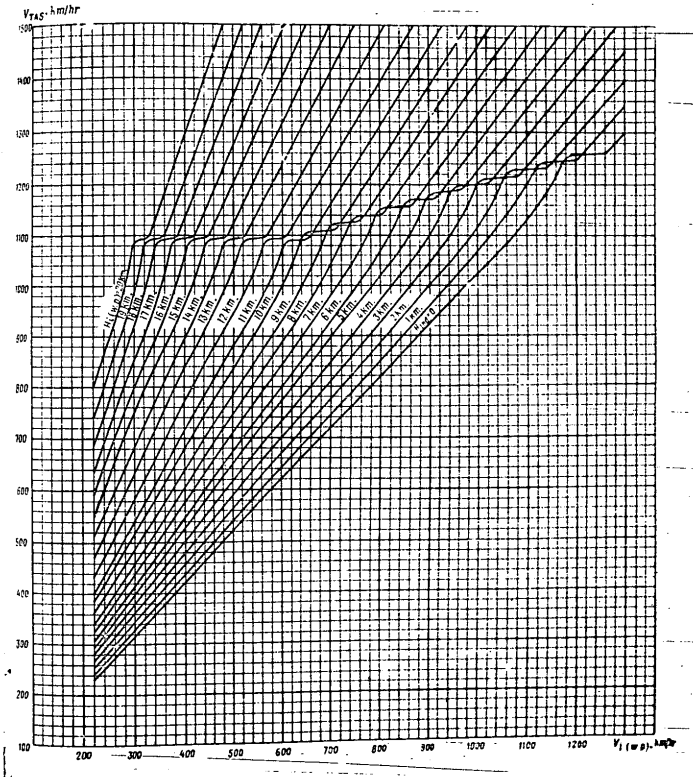

Fig. 147. IAS – TAS and TAS – IAS Conversion Graph

Declassified in Part - Sanitized Copy Approved for Release 2011/12/13 : CIA-RDP80T00246A062100050001-6

Declassified in Part - Sanitized Copy Approved for Release 2011/12/13 : CIA-RDP80T00246A062100050001-6

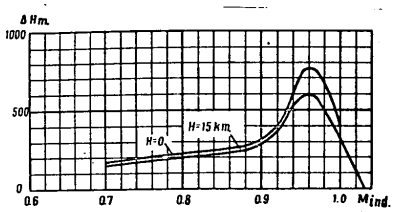

Fig. 148. Summary Aerodynamic and Shock Corrections for Altimeter

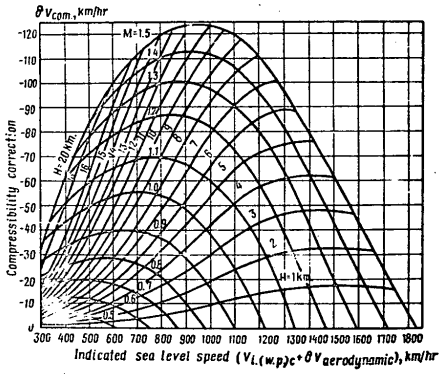
δVcom., km/hr
M=1.5
H=20 km.
H=1 km.
Compressibility correction
300 400 500 600 700 800 900 1000 1100 1200 1300 1400 1500 1600 1700 1800
Indicated sea level speed (Vi.(w.p)c+δVaerodynamic), km/hr

Fig. 149. Graph of Corrections for Air Compressibility

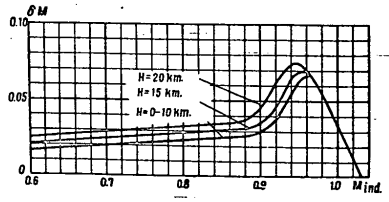

Fig. 150. Summary Aerodynamic and Shock Corrections for Airspeed Tube Installed in Fuselage Nose Section

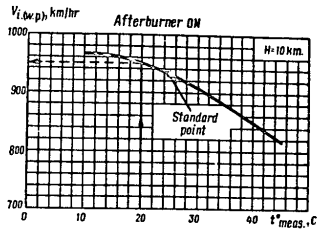

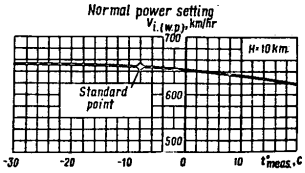

Fig. 151 Maximum IAS of Level Flight as Function of Air Temperature Measured with Aid of Temperature Gauge Provided with Full Stagnation Extension Tube

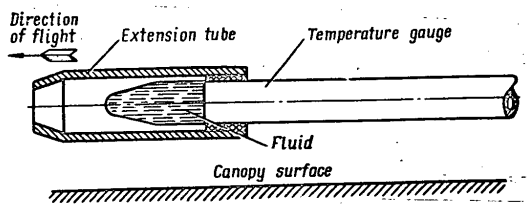

Fig. 152. Temperature Gauge Installation Diagram

Declassified in Part - Sanitized Copy Approved for Release 2011/12/13 : CIA-RDP80T00246A062100050001-6

Declassified in Part - Sanitized Copy Approved for Release 2011/12/13 : CIA-RDP80T00246A062100050001-6

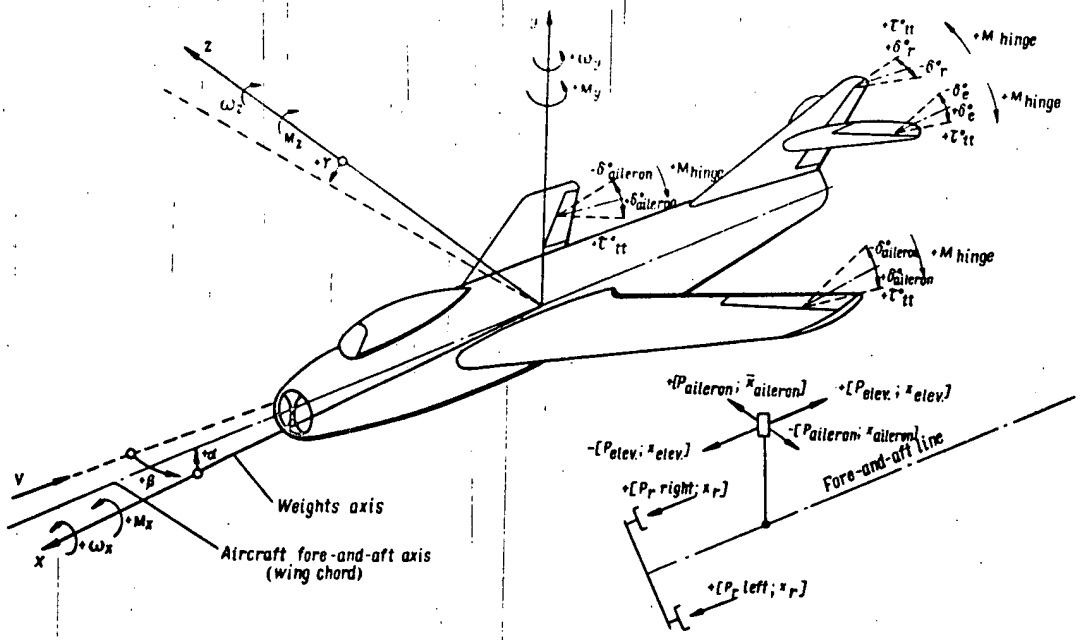

Fig. 153. Semidependent Axes System Diagram. Conventional Designations and Control Force Vectors

Table II

STABILIZER CONTROL HANDLE PRESSURES (kg) WITH TRIMMING EFFECT MECHANISM NEUTRAL

Table position	Handle in extreme position					
	Booster				OFF	
	ON					
	backward (pull)		forward (push)		backward (pull)	forward (push)
Greater arm	11^{+2}_{-1}		5^{+2}		11^{+2}_{-1}	5^{+2}
Smaller arm	39^{+4}_{-2}		16^{+3}_{-1}		39^{+4}_{-2}	16^{+3}_{-1}

Table III

AILERONS CONTROL HANDLE PRESSURES, kg

Booster	Handle in extreme position			
	Left		Right	
ON	$6.5^{+0.5}$			
OFF	8^{+2}			

Table IV

PEDAL PRESSURES, kg

Left pedal	
Forward (push)	Backward (pull)
up to 2.5	up to 2.5

2. The balance stress vector should pass through point T of the control stick (or point H of the pedals) normal to the control stick axis.

3. Carry out the measurements for the extreme positions assumed from the neutral position.

Declassified in Part - Sanitized Copy Approved for Release 2011/12/13 : CIA-RDP80T00246A062100050001-6

Declassified in Part - Sanitized Copy Approved for Release 2011/12/13 : CIA-RDP80T00246A062100050001-6

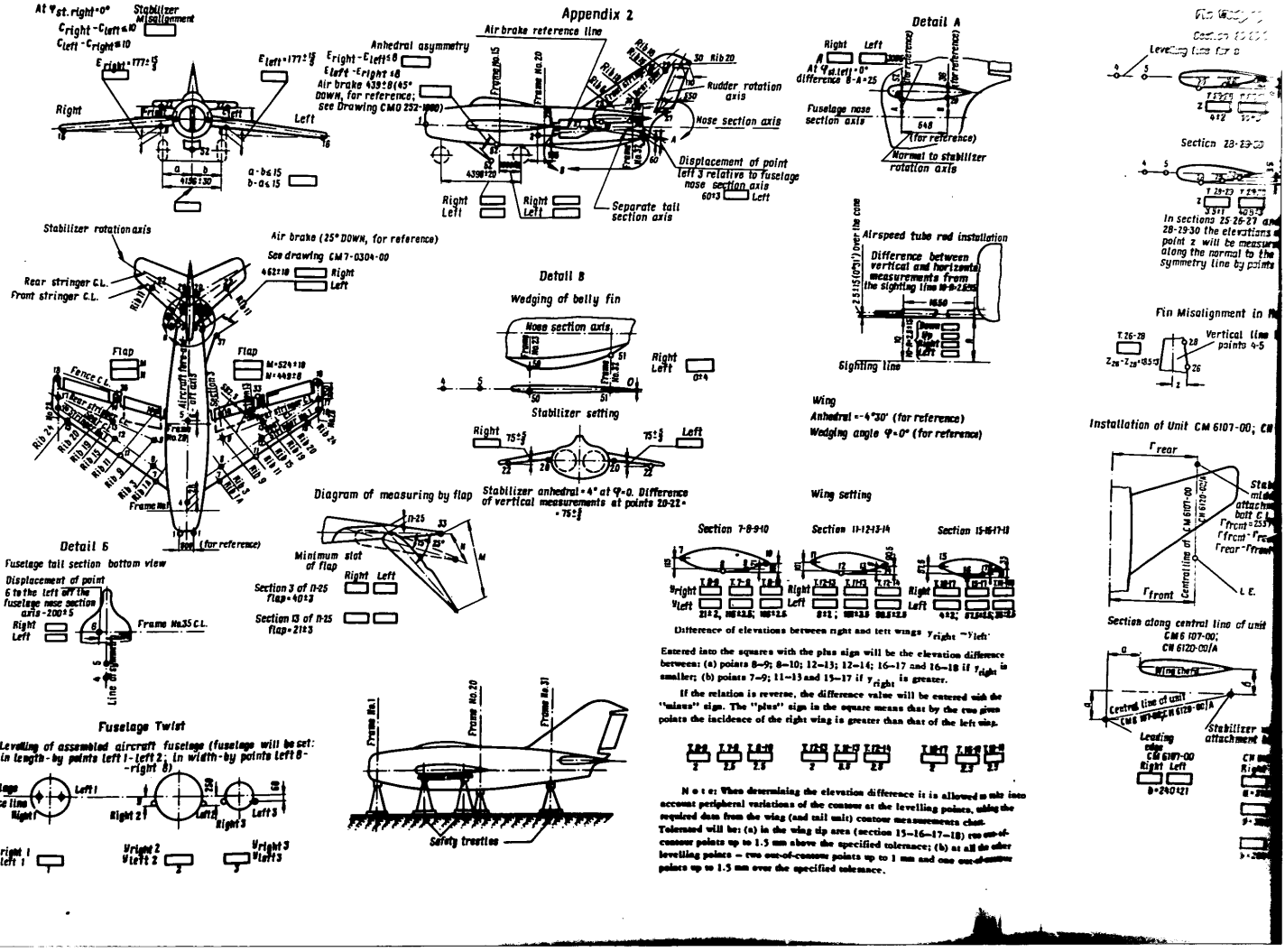
Appendix 2
Detail A
Detail B
Detail 6
Fuselage Twist
Stabilizer setting
Wing setting
Airspeed tube rod installation
Sighting line
Air brake reference line
Anhedral asymmetry
Rudder rotation axis
Nose section axis
Displacement of point Left 3 relative to fuselage nose section axis
Separate tail section axis
Fuselage nose section axis
Normal to stabilizer rotation axis
Stabilizer rotation axis
Air brake (25° DOWN, for reference)
See drawing CM 7-0304-00
Rear stringer C.L.
Front stringer C.L.
Flap
Wedging of belly fin
Nose section axis
Diagram of measuring by flap
Stabilizer anhedral +4° at φ=0. Difference of vertical measurements at points 20-22
Minimum slot of flap
Section 3 of fl-25 flap=40±3
Section 13 of fl-25 flap=21±3
Fuselage tail section bottom view
Displacement of point 6 to the left off the fuselage nose section axis -200±5
Frame No.35 C.L.
Leveling of assembled aircraft fuselage (fuselage will be set: in length - by points Left 1 - Left 2; in width - by points Left 8 - -right 8)
Fuselage reference line
Safety trestles
Wing
Anhedral +4°30' (for reference)
Wedging angle φ=0° (for reference)
Section 7-8-9-10
Section 11-12-13-14
Section 15-16-17-18
Difference of elevations between right and left wings
Entered into the squares with the plus sign will be the elevation difference between: (a) points 8–9; 8–10; 12–13; 12–14; 16–17 and 16–18 if is smaller; (b) points 7–9; 11–13 and 15–17 if is greater.
If the relation is reverse, the difference value will be entered with the "minus" sign. The "plus" sign in the square means that by the two given points the incidence of the right wing is greater than that of the left wing.
Note: When determining the elevation difference it is allowed to take into account peripheral variations of the contour at the levelling points, using the required data from the wing (and tail unit) contour measurements chart. Tolerance will be: (a) in the wing tip area (section 15–16–17–18) two out-of-contour points up to 1.5 mm above the specified tolerance; (b) at all the other levelling points – two out-of-contour points up to 1 mm and one out-of-contour points up to 1.5 mm over the specified tolerance.
Section along central line of unit CM 6 107-00; CM 6120-00/A
Wing Chord
Central line of unit
Leading edge
Stabilizer attachment
Fin Misalignment in
Vertical line points 4-5
Installation of Unit CM 6107-00; CM
Rear
Front
Central line of CM 6107-00
L.E.

Declassified in Part - Sanitized Copy Approved for Release 2011/12/13 : CIA-RDP80T00246A062100050001-6

Declassified in Part - Sanitized Copy Approved for Release 2011/12/13 : CIA-RDP80T00246A062100050001-6

Fin Wedging

Section 25-26-27

Levelling line for z

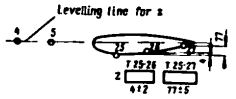

Section 28-29-30

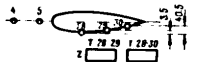

In sections 25-26-27 and 28-29-30 the elevations of point z will be measured along the normal to the symmetry line by points 4 5

Fin Misalignment in Height

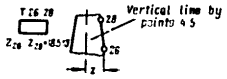

Installation of Unit CM 6107 00, CM 6120 00/A

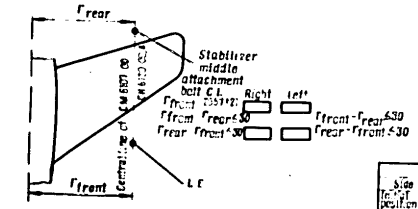

Section along central line of unit CM 6 107 00, CM 6120 00/A

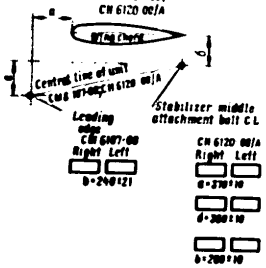

For Levelling of Units

Levelling of units and contour conformity check will be performed in the scope set forth by specifications BTU CM 2-00-01

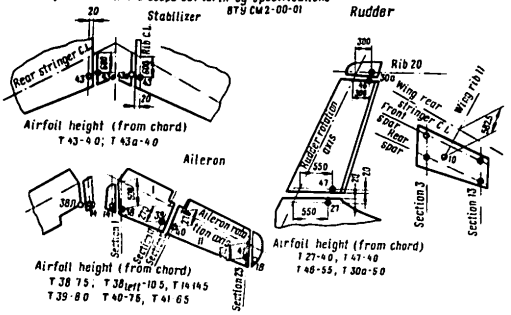

Airfoil height (from chord) T 43-40; T 43a-40

Airfoil height (from chord) T 38 75, T 38 left-105, T 1414 5, T 39-80, T 40-76, T 41 65

Airfoil height (from chord) T 27-40, T 47-40, T 46-55, T 30a-50

Table No 1

Stabilizer						
Variable ratio automatic boost unit set up at greater arm (Trimming effect mechanism neutral, for reference) Booster ON, normal pressure						
Side	Left	Right	Left	Left	Left	Right
Stabilizer LE position	Maximum Down		Down	Up	Maximum Up	
Stabilizer deflection						
Control handle travel from neutral position	Rackward		Rack ward	For ward	Forward	
Values a b and b c are given for reference						

Table No 2

Left stabilizer (Trimming effect mechanism neutral, - for reference) Booster ON, normal pressure						
Indications of variable ratio boost unit	Position of stabilizer LE					
Value	Maximum down		Maximum up			
km/hr	Angle	Δ	Angle	Δ		
450						
600						
750						
900						
Booster OFF						
0						
900						

Scissors

T.E. of stabilizer fillet			Stabilizer	Aileron		Rudder
Side	Right	Left		Right	Left	
Initial position	Left stabilizer setting angle: 0°		Left stabilizer setting angle: 0°	Align points		
Measured points	43-43a	43-43a	Right stabilizer setting angle:			
Scissors H	Normal					
	Actual					

If out-of contour points are found at the measured levelling marks, correct the obtained measurement data by the value of the original step between the wing and aileron, stabilizer and fillet, rudder and tail fairing

Plate

Side	Left plate and aileron	Right plate and aileron
Initial position		
Values measured		

Drawing CM 5120-1000

To be measured by the middle of the plate span

Rudder

Rudder angular movement	Left	Right
Rudder handle movement		
Right point		

Ailerons

Hydraulic system ON

Side	Right	Left	Right	Left
Aileron deflection angle				
Control stick deflection angle	Right		Left	

Hydraulic system OFF

Left aileron trim tab angle		
Switch	Right	Left

Stabilizer Control Handle Diagram

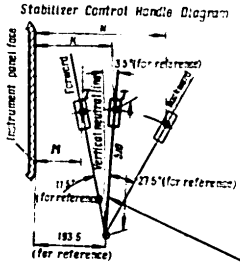

Forward travel of handle equals 8 M
Backward travel of handle equals 6 M
± 725 (for reference)

Note The handle travel length in the direction perpendicular to the handle neutral position and along the reference line are in practice identical (for reference)

Point T is a conventional point of pilot's hand effort application. The position of point T of the handle will be fixed with a special valve

Diagram No 1 of linear measurements of stabilizer angular movements

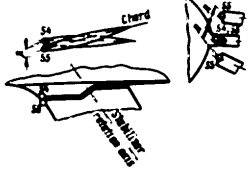

Angles and handle travel datum line (corresponds to stabilizer angle 0°)

Distance A between levelling marks 54 and 55 will be measured (during the control position check) as its projection on the vertical (to avoid influence of the elevator while during the check of extreme positions (See Tables No 1 and No 2) directly between points 54 and 55.

Declassified in Part - Sanitized Copy Approved for Release 2011/12/13 : CIA-RDP80T00246A062100050001-6

Declassified in Part - Sanitized Copy Approved for Release 2011/12/13 : CIA-RDP80T00246A062100050001-6

Fig. 154. Levelling Diagram of МиГ-19С Aircraft

CHECK OF LONGITUDINAL CONTROL NEUTRAL POSITION

The entire check is performed with the booster ON. Levelling marks on the stabilizer and fillet (points 54 and 55) will be plotted on their leading edges along the chord (See Diagram No. 1).

1. CHECK OF STABILIZER SETTING ANGLE WITH LEVELLING MARKS ALIGNED (TO CHECK LEADING EDGE FOR CORRECT POSITION)

LEVEL THE A/C OUT AT POINTS (LEFT 1 – LEFT 2 OF FUSELAGE AND LEFT 8 – RIGHT 8 OF WING).

Set the variable ratio automatic boost unit (APУ) for greater arm (i.e. for greater angular movement of stabilizer). (Trimming effect mechanism neutral for reference).

Align levelling marks 54 and 55 of left stabilizer.

Measure difference b – a by points 19 – 20 of left stabilizer.

$$b - a = 8 \pm 3 \text{ mm} \quad \text{left.}$$

(At this, stabilizer setting angle equals 1°30', L.E. up for reference).

2. CHECK OF STABILIZER POSITION $Д_0$ AT ZERO ANGLE AND CONTROL STICK NEUTRAL POSITION K

Position the aircraft by points left 1 – left 2 and left 8 – right 8. Set the variable ratio automatic boost unit for greater arm. (Trimming effect mechanism neutral for reference).

By pulling the control stick from extreme forward position, set up left stabilizer by points 19 – 20 for b – a = 25 and lock the control stick in this position.

At this, levelling mark 55 on stabilizer should be depressed with respect to levelling mark 54 of fillet.

Measure distance $Д_0$ between levelling marks 54 and 55.

$$Д_0 = 13 \pm 3 \text{ mm} \quad \text{left.}$$

Check distance between control stick point T and instrument panel:

$$K = 225 \pm 3 \text{ mm}.$$

(In this position – control stick backward pressure is up to ±1.5 kg, for reference). Set protractor zero for left stabilizer in this position.

N o t e: Protractor zero for right panel of stabilizer will be set up when points right 19–20 are positioned to obtain b – a = 25.

At this, "scissors" are by points right 54–55.

$$Д_0 = 13 \pm 3 \text{ mm} \quad \text{right.}$$

Point 55 is below point 54.

3. CHECK OF STABILIZER DEFLECTION WITH VARIABLE RATIO AUTOMATIC BOOST UNIT ADJUSTED FOR SMALLER ARM

(Trimming effect mechanism neutral, for reference).

By pulling control stick from extreme forward place position levelling mark 55 of left stabilizer above levelling mark 54 of fillet at distance Д=8 (at this, setting angle equals 0°30', L.E. UP, for reference) and lock control stick in this position. Holding the control stick in this position, switch over the variable ratio automatic boost unit for smaller arm. At this, levelling point 55 should get depressed relative to levelling point 54 on fillet.

Measure distance between levelling marks 55 and 54.

$Д_{left} = 30 \pm 3$ mm (at this, setting angle equals 2°± 20' L.E. DOWN, for reference). (In this position – control stick forward pressure is up to 3 – 6 kg, for reference).

4. CHECK OF TRIMMING EFFECT MECHANISM NEUTRAL POSITION

Set up variable ratio automatic boost unit (APУ) for greater arm.

Set trimming effect mechanism neutral; as soon as the signal lamp lights up, throw the control stick to the extreme forward position by turning the switch on the control stick back (having previously cut out the lamps by turning the switch forward); gradually release it till it is stopped in next to balanced position due to friction. Measure distance between levelling marks 54 and 55 and then repeat the measurement in control stick deflection for extreme backward position. In both cases levelling mark of stabilizer should be elevated relative to levelling mark 54 of fillet.

Return travel of control stick from extreme forward position:

$$Д_1 = 30 \pm 3 \text{ mm}$$

Return travel of control stick from extreme backward position:

$$Д_2 = 6 \pm 3 \text{ mm}$$

Mean value Д will be determined for greater arm of variable ratio automatic boost unit at zero stick pressure:

$$Д = \frac{Д_1 + Д_2}{2} = 8 \pm 3 \text{ mm} \quad \text{left}$$

(at this, setting angle equals 0°30' ± 20'. L.E. UP, for reference. See Also Notes, Item 7, below).

LEVELLING INSTRUCTIONS

1. The levelling should be performed without fuel and military load and pilot although with all the standard equipment items installed.

For levelling, the aircraft is treated under frames Nos 1 and 20; at this, it is not necessary to suspend a load from the aircraft noze (application of a 100-kg load to the horizontal empennage during aircraft maintenance is envisaged).

2. Safety trestles are installed under the wings (at a distance of 3000 mm from the aircraft fore-and-aft line) and under the fuselage at frame No. 31.

3. During levelling operations the fuselage fore-and-aft line will be set up horizontally by the fuselage left side levelling marks 1 and 2.

4. To obtain a levelled lateral position of the aircraft, align two points 8-8 in height.

5. Pressure in the variable ratio automatic boost unit dynamic pressure pipe will be checked by the wide pointer of the airspeed indicator ($V_{i.\ (w.p.)}$ whereas the static pressure line will be checked against the altimeter ($H_{ind.}$, See Table 1).

When setting up the required transmission ratio, introduce values $V_{i.(w.p.)}$ and $H_{ind.}$ accurately, beginning with small values no matter at which value of $V_{i.\ (w.p.)}$ and $H_{ind.}$ the last pulse arm travel of the automatic boost unit takes place.

6. After the levelling diagram is filled in at the Assembly Department, the inspection check-up of the stabilizer angular movement will be carried out by distance Д between levelling points 54 and 55, without bringing the aircraft in the levelled position.

For final check-up of setting angles with a protractor, set the protractor scale zero according to distance $Д_0$ (by points 54 and 55) which corresponds to zero angle of the stabilizer setting.

7. If the pre-acceptance aircraft trimming requires additional adjustment of the controls, enter corrected data into the Diagram for points which underwent adjustment.

Final data on the stabilizer trimming position will be also entered into the aircraft Service Log. For instructions on levelling aircraft in active service see the Maintenance Manual.

8. Control stick pressures and trimming effect mechanism range will be checked according to the data given in Fig. 155.

N o t e s: 1. All the levelling points will be plotted in aircraft construction trusses before levelling according to specifications presented in Supplement No. 1 to Specifications No. 14. It is allowed to plot levelling points by drilling through a depth of 0.5 – 0.8 mm, dia. 2 mm.

Declassified in Part - Sanitized Copy Approved for Release 2011/12/13 : CIA-RDP80T00246A062100050001-6

Declassified in Part - Sanitized Copy Approved for Release 2011/12/13 : CIA-RDP80T00246A062100050001-6

Levelling points on the wing and horizontal empennage will be plotted only at the bottom, and on the fin – at the left side only.

2. Angular movement of the stabilizer, ailerons, rudder and trim tabs will be measured by means of protractors, in degrees normal to the rotation axes, while the travel of the flap, control stick and pedals – with a rule, in mm.

3. When entering data into the squares with differences, such as a – b and b – a, cross out extra designations.

4. Levelling point elevations indicated in the Diagram which represent the wing anhedral correspond to the wing setting angle relative to the aircraft reference line.

5. Elevations of levelling points 13, 14, 15, 16, 17 and 38Л are given by the actual contour of the skin taking into account its 0.5 mm depression relative to the theoretical contour.

6. Longitudinal control to the booster is weight-balanced at control stick neutral position and artificial feel mechanism disconnected (for reference).

7. In-flight trimming position of the stabilizer corresponds to $V_{i.(w.p.)} = 750$ km/hr at H=0 – 7000 m.; at this, the stabilizer setting angle equals 0° and Д = 13 ± 3; variable ratio automatic boost unit arm is in an intermediate position (for reference).

PRESSURES ON CONTROLS

The required measurements will be carried out on each aircraft. More thorough measurements will be performed on every first and twentieth aircraft of each series according to the data indicated in Fig. 155.

Table I

TRIMMING EFFECT MECHANISM WORKING RANGE
Stick setting with mechanism in extreme positions
Booster ON

Switch	Forward (push)		Backward (pull)	
Indications of variable ratio automatic boost unit transmitters				
$V_{i.(w.p.)}$, km/hr	0	900	0	900
$H_{ind.}$	0	0	0	0
Stick travel, mm	forward	forward	backward	backward
Stabilizer L.E. travel Д	94±10	56±10	175±10	100±10

IMPORTANT: To measure the control stick travel, operate the change-over switch to set the trimming effect mechanism to the extreme position; then put the control stick to the neutral position and slowly release it (gently retaining its movement) so that it would stop next to the extreme position due to friction.

Table II

STABILIZER CONTROL HANDLE PRESSURES (kg) WITH TRIMMING EFFECT MECHANISM NEUTRAL

Handle in extreme position		Booster			
		ON		OFF	
		backward (pull)	forward (push)	backward (pull)	forward (push)
Variable ratio automatic boost unit	Greater arm	11^{+2}_{-1}	5^{+2}	11^{+2}_{-1}	5^{+2}
	Smaller arm	39^{+4}_{-2}	16^{+3}_{-1}	39^{+4}_{-2}	16^{+3}_{-1}

Table III

AILERONS CONTROL HANDLE PRESSURES, kg

Booster			
ON		OFF	
Handle in extreme position			
Left	Right	Left	Right
$6.5^{+0.5}$		8^{+2}	

Table IV

PEDAL PRESSURES, kg

Left pedal	
Forward (push)	Backward (pull)
up to 2.5	up to 2.5

IMPORTANT: 1. Under the Levelling Diagram, pressures will be measured with the aid of a spring balance or dynamometer (and on every first and twentieth aircraft of each new series – by means of a special dynamometric device).

2. The balance stress vector should pass through point T of the control stick (or point H of the pedals) normal to the control stick axis.

3. Carry out the measurements for the extreme positions assumed from the neutral position.

Declassified in Part - Sanitized Copy Approved for Release 2011/12/13 : CIA-RDP80T00246A062100050001-6

Declassified in Part - Sanitized Copy Approved for Release 2011/12/13 : CIA-RDP80T00246A062100050001-6

Appendix 2

art 1. Control Stick Pressures from Stabilizer Automatic Unit with Trimming Effect Mechanism Neutral and Booster Friction);
ır reference – for emergency control by АПС-4 stabilizer ic control unit the Chart data are valid).
zimum gradient of pressure change of forward travel.

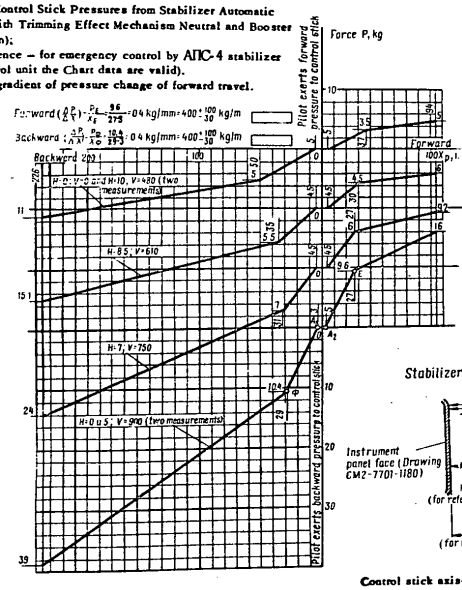
Force P, kg
Pilot exerts forward pressure to control stick
Pilot exerts backward pressure to control stick
Forward
Backward
H=0; V=0 and H=10, V=480 (two measurements)
H=85, V=610
H=7, V=750
H=0 и 5; V=900 (two measurements)

1. Tolerances for zero pressure points position in control stick travel;

(a) for position of zero pressure points A_1 and A_2 (at $V_{i.(w.p.)} = 750 \pm 5$ mm;

(b) for difference between zero pressure points A_1 and $A_2 - \pm 5$ mm.

2. Tolerance for length of lines A_2E and $A_1\Phi$ projections in control stick travel – ±5 mm.

3. Tolerance for pressure change gradient for all chart lines – ±15% (except lines A_2E and $A_1\Phi$ on variable ratio automatic boost unit smaller arm).

Pressure change gradient (or tangent of the chart lines slope angle) is ratio between the pressure increase and increase in control stick movement.

Chart 1. Control Stick Friction Force

Booster	ON		OFF
АПС-4 stabilizer automatic control unit	OFF		ON
Indications of variable + radio automatic boost unit	Friction force, kg		
V_i (w.p.) km/hr	Hind km.	Neutral position	Extreme position backward
0	0		up to 1.0
900	0		up to 1.0

Stabilizer Control Stick Diagram

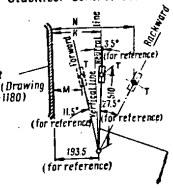

Stick forward travel equals H-M
Stick backward travel equals H-N
K=225 (for reference)

Note: Travels of the control stick in the direction perpendicular to the stick neutral position and along the reference line are practically identical.

Point T is the conventional point of the pilot's hand effort application.

Mark the position of point T on the control stick left side by means of a punch.

Control stick axis-datum line of control stick angular and linear movements (for stabilizer setting angle $\phi = 0°$)

Chart 2. Control Stick Pressure from Ailerons Automatic Control Units (no friction)

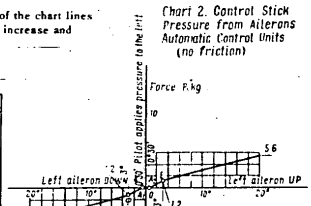

Chart No 2. Aileron Friction Force

Booster	Friction force, kg			
	Normal	Neutral position	Extreme position	
			Right	Left
ON				
OFF				

Sample Plotting of Measuring Points and Representative Force Lines on Chart 1 (for reference)

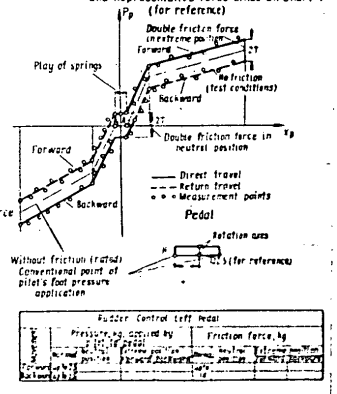

Rudder Control Left Pedal

Pressure, kg, applied by	Friction force, kg

1. Tolerance for zero pressure position of points A_1 and A_2 by aileron angle +0°; −0.5°.

2. Tolerance for position of points E and Φ by aileron angle +1°; −0.5°.

3. Tolerance for pressure change gradient for all chart lines ±15° per cent. The pressure change gradient (or tangent of chart lines slope angle) is a ratio between the pressure increase and increase in control stick movement.

Declassified in Part - Sanitized Copy Approved for Release 2011/12/13 : CIA-RDP80T00246A062100050001-6

Declassified in Part - Sanitized Copy Approved for Release 2011/12/13 : CIA-RDP80T00246A062100050001-6

Fig. 155. Characteristics of Automatic Boost Units of Aircraft, Model МиГ-19С

Sample Plotting of Measuring Points and Representative Force Lines on Chart I

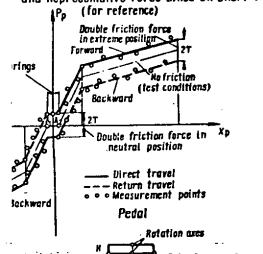

Rudder Control Left Pedal							
ressure, kg, applied by pilot to pedal			Friction force, kg				
Neutral position	Extreme position	Direction	Backward	Forward	Neutral position	Extreme position	Direction

INSTRUCTIONS: Measurements according to the present Diagram will be carried out in their full scope for the first aircraft of each series.

1. The measurements will be performed after carrying out operations under the Levelling Diagram (See Fig. 54) which will include the check of the controls and trimming effect mechanism for neutral position and check of the stabilizer setting angles in all flight procedures ($V_{i.\,(w.p.)}$ and $H_{ind.}$) according to Table II in Fig. 154.

2. Measurements of forces will be carried out with the trimming effect mechanism in neutral position.

3. To determine characteristics of the controls, all the measurements should be carried out in compliance with the instructions given in Fig. 155; fill in the tables and plot, in Indian ink, measurement points and force lines passing through the measurement points on the charts. At this, plotted on the charts will be actual measurement data which include friction force.

4. Measurements of forces will be carried out during the forward and backward travel of the control handle. Forward travel will be estimated from the neutral line (i.e. P=0 kg). Before evaluating the forces by the dynamometer, take up the automatic boost unit plays. To do this, when measuring the stabilizer control handle pressures:

(a) send the control handle to the extreme forward position and then slowly (at a rate not exceeding 100 mm of handle travel per 10 sec.) release it until the neutral position is assumed to have the handle stop in a position stipulated by friction (by this, plays in the automatic boost units are taken up). Then accomplish measurements of pressures during the forward (from the neutral line) travels of the handle and backwards (to the neutral line), thus covering the entire range of the handle travel;

(b) repeat the procedure under Item "a" for the neutral line-to-extreme backward position range of the control handle travel. To measure pressures on the ailerons control handle and pedals employ the same procedure as for stabilizer measurements, taking up play first for left travel range, and then for right travel range.

5. The pressures will be measured with a special dynamometer used in the manufacturer's measurements.

6. All the measurements in booster ON conditions will be accomplished at the working pressure.

7. The pressure in the variable ratio automatic boost unit dynamic pressure pipe will be checked by the IAS indicator (by wide pointer) $V_{i.\,(w.p.)}$ (calibrated) while the pressure in the static tube will be checked by the altimeter pointer ($H_{ind.}$). To do this set the altimeter pointer at an altitude value which would be indicated by the instrument in standard atmospheric conditions at ground barometric pressure at the moment the measurement is taken (this brings the measurements to standard conditions).

To check the pressures:

(a) fasten the rack clamp and set the pointer to indicate altitude H=0;

(b) release the rack clamp and build up a pressure in the observation window which would be equal to the ground pressure at the moment the measurement is taken;

(c) fasten the rack clamp and set up a pressure of 760 mm Hg in the observation window.

The indications of the airspeed indicator and altimeter will be taken corrected for the index errors of the instruments.

When setting up the required transmission ratio, introduce the values of $V_{i.\,(w.p.)}$ and $H_{ind.}$ accurately, beginning with low values, no matter at which value of $V_{i.\,(w.p.)}$ and $H_{ind.}$ the last pulse shift of the variable ratio automatic boost unit arm will take place.

Notes: (1) All the pressure measurements will be taken with control stick and pedals in motion, i.e. with friction forces taken into account.

Friction force at controls starting moment will not be considered.

(2) The stick (or pedal) friction force in any position will be evaluated as half of the control stick pressure difference measured during the control stick forward and backward travel.

(3) Angular movements of the stabilizer, ailerons, rudder and trim tabs will be measured in degrees, perpendicular to rotation axes, with the aid of protractors, whereas deflection of the flap, control stick and pedals will be measured with a ruler (in mm).

(4) Friction forces data indicated in the Diagram are valid only when the measurements are taken at a temperature not lower than +10°C.

(5) The arm of the variable ratio automatic boost unit undergoes linear changes, depending on the impact pressure with due account for compressibility and flight altitude.

The variable ratio automatic boost unit arm changes linearly from 50 to 96 mm in 18 pulses in conditions of $V_{i.\,(w.p.)}$ = 480 – 900 km/hr change and constant altitude H = 0 – 5 km, and in 13 – 39 pulses when climbing from H=5 km. to 10 km. at constant $V_{i.\,(w.p.)}$ equal to 900 km/hr.

Time of maximum change of the boost unit arm (from 50 to 96 mm) does not exceed 4 seconds in no load conditions (for reference).

ADDITIONAL INSTRUCTIONS FOR CHART NO. 1

1. To measure pressures of the longitudinal controls it is necessary to set the variable ratio automatic boost unit into a special position according to special instructions.

Measurements over, return the boost unit into the operating position according to the same instructions. Measure the pressures over ± 100 mm of the control stick travel from the neutral line through every 5 mm, and further on – through every 10 mm.

2. In case of noticeable point scattering repeat the pressure measurements for all conditions of $V_{i.\,(w.p.)}$ and $H_{ind.}$ The data of the repeated measurements will be entered into the spare lines of the Table and Chart.

Declassified in Part - Sanitized Copy Approved for Release 2011/12/13 : CIA-RDP80T00246A062100050001-6

Declassified in Part - Sanitized Copy Approved for Release 2011/12/13 : CIA-RDP80T00246A062100050001-6

APPENDIX 2

МиГ-19С Aircraft Control Power Train Data

Longitudinal Control

1. Characteristics of Booster, Type БУ-14МС

Pressure in hydraulic system, kg/cm^2		Normal pressure		Booster-to-main system transition pressure		Pressure at transition to electric control	
		135		65		50	
1		2		3		4	
Rod pressure, kg	Maximum, at V=0	4500		2200		1700	
Hinge moment of stabilizer normal to rotation axis, kg-m	Maximum, at V=0	485		235		180	
		W	ω	W	ω	W	ω
Rod velocity W, mm/sec. and stabiliser angular speed normal to rotation axis ω deg/sec.	At engine maximum r.p.m. and zero pressure of booster	82	43	53	27.5	45	23.7
	At engine idle r.p.m., H=5000 m.	82	43	53	27.5	45	23.7
	At engine idle r.p.m., H=0	56.7	29.6	56.7	29.6	45	23.7

Declassified in Part - Sanitized Copy Approved for Release 2011/12/13 : CIA-RDP80T00246A062100050001-6

Declassified in Part - Sanitized Copy Approved for Release 2011/12/13 : CIA-RDP80T00246A062100050001-6

1		2		3		4	
	At engines self-rotation: $V_{i.(w.p.)}$ = 550 km/hr	28.6	14.9	28.6	14.9	28.6	14.9
	$V_{i.(w.p.)}$ = 450 km/hr	21.9	11.5	21.9	11.5	21.9	11.5

Note: Values of velocities are given for longitudinal and lateral controls effected separately.
Maximum working travel of БУ-14МС booster rod equals 73-mm.
БУ-14МС booster slide valve travel is 1.5 mm.
Relations between characteristics of БУ-14МС booster are presented in Fig.156.
Maximum capacity of hydraulic pump on РД-9Б engine is 36 lit/min.

50X1-HUM

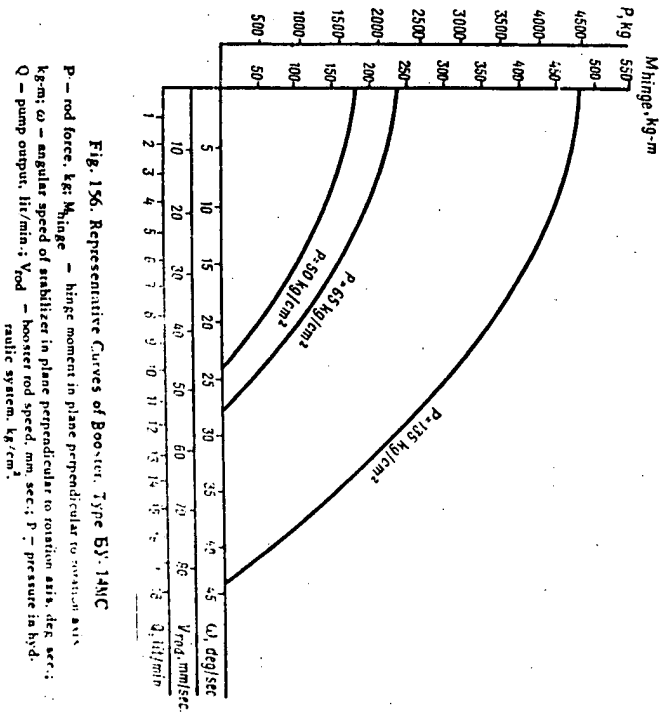

Fig. 156. Representative Curves of Booster, Type БУ-14МС

P – rod force, kg; M_{hinge} – hinge moment in plane perpendicular to rotation axis, kg-m; ω – angular speed of stabilizer in plane perpendicular to rotation axis, deg/sec; Q – pump output, lit/min.; V_{rod} – booster rod speed, mm/sec.; P – pressure in hydraulic system, kg/cm².

50X1-HUM

Declassified in Part - Sanitized Copy Approved for Release 2011/12/13 : CIA-RDP80T00246A062100050001-6

Declassified in Part - Sanitized Copy Approved for Release 2011/12/13 : CIA-RDP80T00246A062100050001-6

50X1-HUM

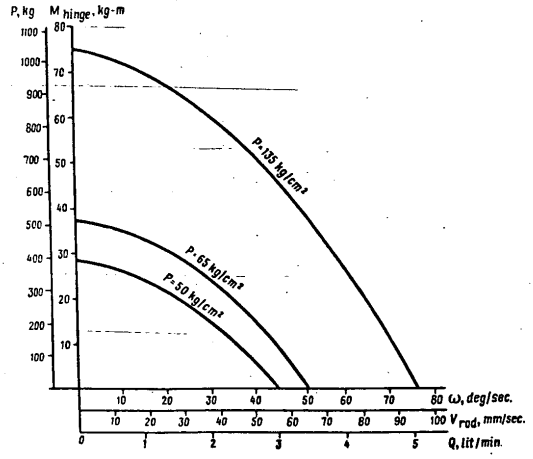

Fig. 157. Representative Curves of Booster, Type BY- 13M

P – rod force, kg; M_{hinge} – hinge moment in plane perpendicular to rotation axis, kg-m; ω – angular speed of aileron, deg/sec.; Q – pump output, lit./min.; V_{rod} – booster rod speed, mm/sec.; p – pressure in hydraulic system, kg/cm².

2. Characteristics of Booster, Type BY-13M

Pressure in hydraulic system, kg/cm²		Normal pressure		Booster-to-main system transition pressure			Pressure at transition to electric control		
1		135		65			50		
		2		3			4		
Rod pressure, kg	Maximum, at V=0	1035		514			390		
Hinge moment of stabilizer normal to rotation axis, kg-m	Maximum, at V=0	75		37			28.5		
		W	ω	W	ω		W	ω	
Rod velocity V,mm/sec. and stabilizer angular speed normal to rotation axis ω, deg/sec.	At engine maximum r.p.m. and zero pressure of booster	94	76.5	64	51.5		56	45	
	At engine idle r.p.m., H=5000 m.	94	76.5	64	51.5		56	45	
	At engine idle r.p.m., H=0	94	76.5	64	51.5		56	45	

50X1-HUM

Declassified in Part - Sanitized Copy Approved for Release 2011/12/13 : CIA-RDP80T00246A062100050001-6

Declassified in Part - Sanitized Copy Approved for Release 2011/12/13 : CIA-RDP80T00246A062100050001-6

1		2		3		4	
	At engines self-rotation: $V_{i.(w.p.)}$ = 550 km/hr	94	76.5	64	51.5	56	45
	$V_{i.(w.p.)}$ = 450 km/hr	84	68	64	51.5	56	45

Note: Values of velocities are given for longitudinal and lateral controls effected separately.
Maximum travel of BU-13M booster rod is 50 mm.
BU-13M booster slide valve travel equals 2 mm.
Relations between characteristics of BU-13M booster are presented in Fig.157.

88

50X1-HUM

50X1-HUM

Declassified in Part - Sanitized Copy Approved for Release 2011/12/13 : CIA-RDP80T00246A062100050001-6

Declassified in Part - Sanitized Copy Approved for Release 2011/12/13 : CIA-RDP80T00246A062100050001-6

50X1-HUM

Page Denied

Declassified in Part - Sanitized Copy Approved for Release 2011/12/13 : CIA-RDP80T00246A062100050001-6